Brain Shape Analysis & Registration

Contributions from the Epidaure group at INRIA

IPAM-MBI 2004

UCLA

Los Angeles

Nicholas Ayache

INRIA - 2004 Route des Lucioles, 06902 Sophia-Antipolis , France

ayache@sophia.inria.fr

http://www-sop.inria.fr/epidaure/personnel/ayache/ayache.html

Brain Shape Analysis

- In this talk :
  - a survey of registration methods developed in our group
  - combined with methods to detect and quantify anatomical or pathological shape variations
- Medical Applications
  - Patient Follow-Up, Image-Guided Neurosurgery,
  - Atlas Construction from Cross-Sections, Atlas Mapping,
  - Brain Asymmetry,Variability of Sulcal Lines, etc.

N. A : Epidaure: a Research Project in Medical Image Analysis, Simulation and Robotics at INRIA, IEEE Trans. on Medical Imaging, 22(10):1185--1201, October 2003.

Overview

- Geometric Registration
- Iconic Registration
- Hybrid Registration
- Shape Statistics
- Perspectives

Geometric Methods

- Extraction of geometric primitives
  - invariant for the chosen group of transformations (typically rigid)

- Registration then consists of
  - matching homologous primitives
  - estimating the transformation T

X. Pennec, N. Ayache and J.P. Thirion : *Landmark-Based Registration Using Features Identified Through Differential Geometry*, Handbook of Medical Imaging, Chapter 31, Academic Press, 2000.

Crest Lines and Extremal Points

- Intersection of 2 or 3 implicit surfaces

$f(x,y,z) = I$ $\quad e_1 = \nabla k_1 . t_1 = 0$ $\quad e_2 = \nabla k_2 . t_2 = 0$

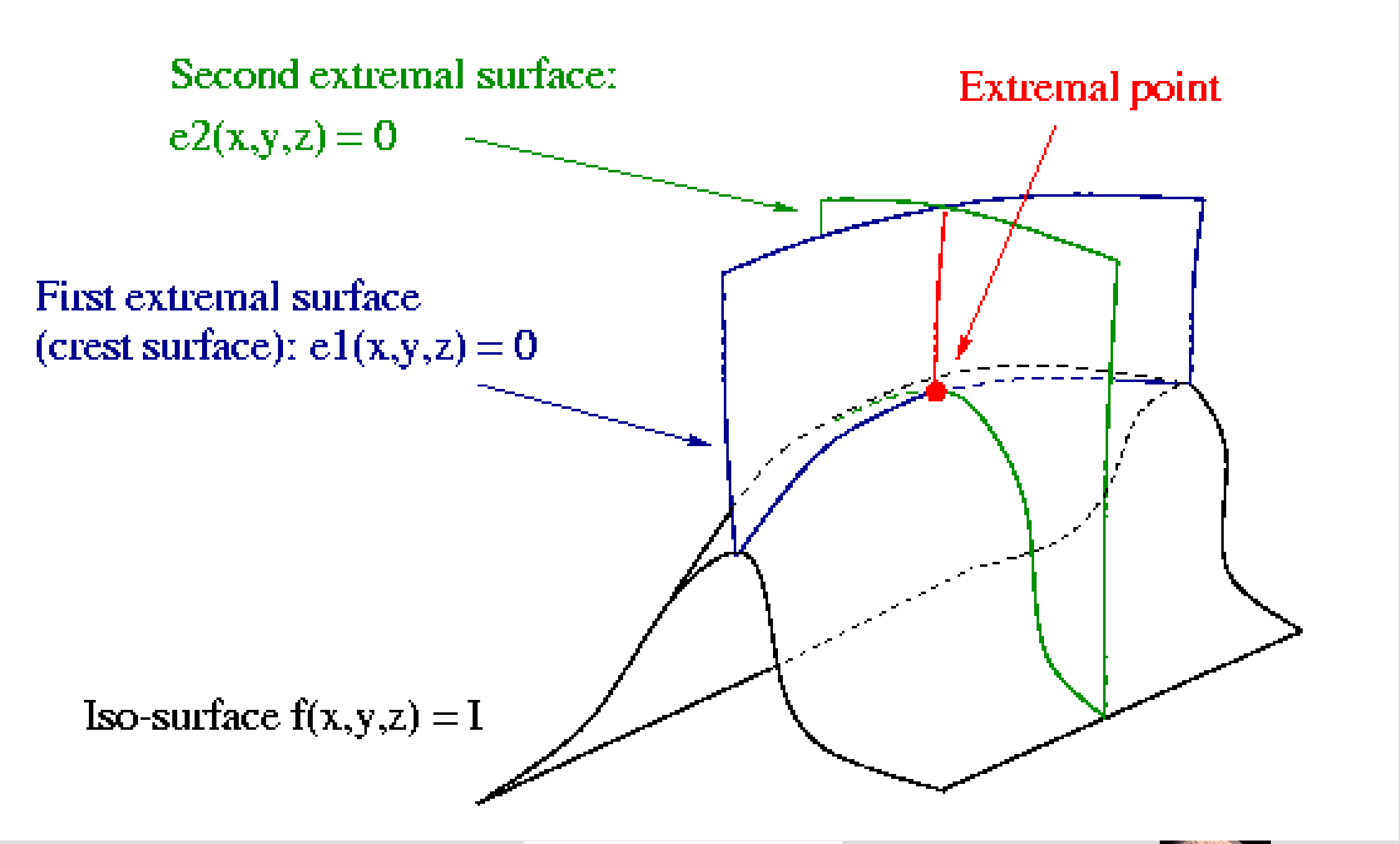

Crest Lines on Cortex (MRI)

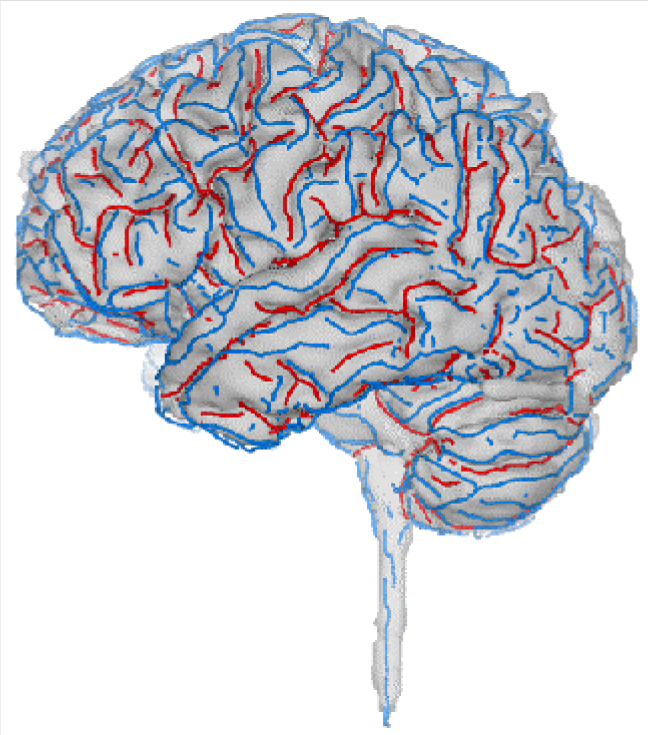

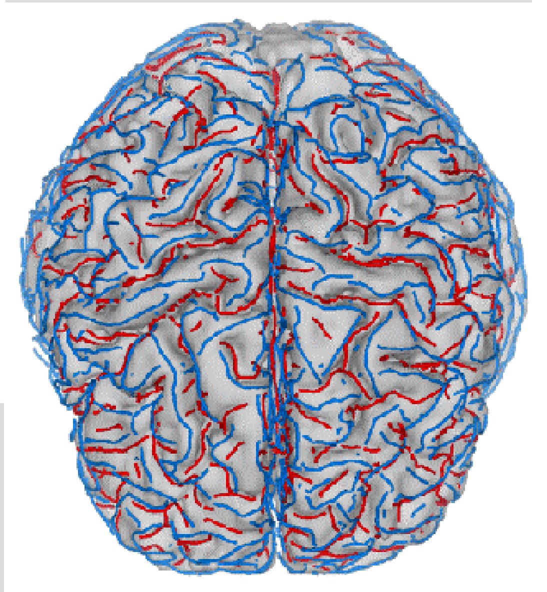

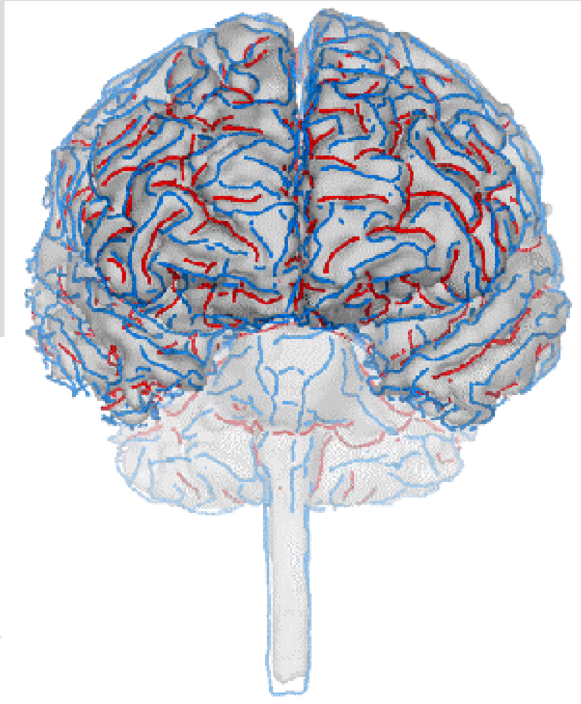

Compact description

Invariant by displacement

Rigid Matching

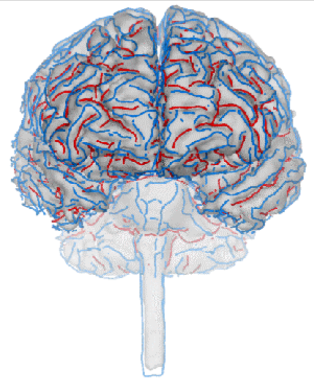

- Adapted algorithms from Computer Vision (Geometric Hashing, Prediction-Verification, ICP) establish correspondences between homologous points and best rigid transformation between 2 images

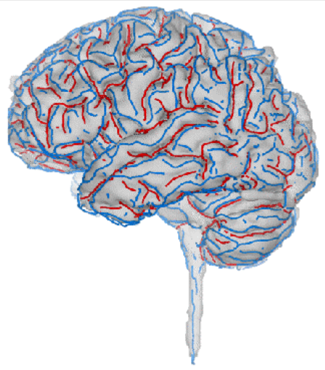

- These algorithms use additional invariants computed along crest lines and on the underlying anatomical surface

Multiple Sclerosis Follow-Up

Original Sequence

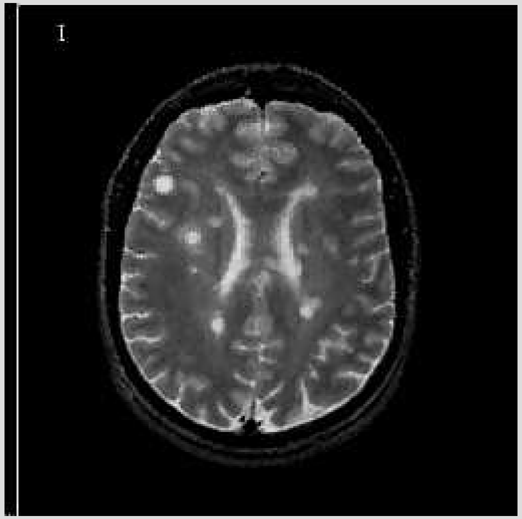

Rigid Registration

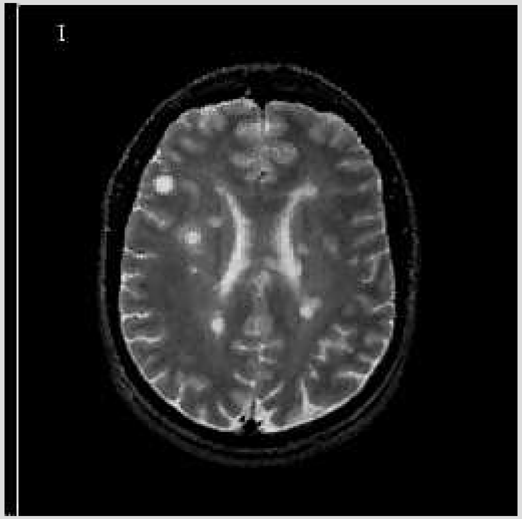

Rigid Registration
+ Intensity Correction

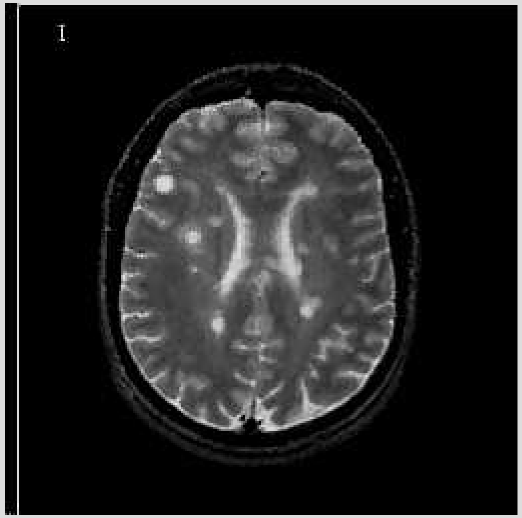

Patient Followed during 18 months (24 acquisitions)

Image acquisition: R. Kikinis

D. Rey, G. Subsol, H. Delingette, N.Ayache : *Automatic Detection and Segmentation of Evolving Processes in 3D Medical Images: Application to Multiple Sclerosis.*
Medical Image Analysis, 6(2):163-179, June 2002.

Geometric Registration

- PROS :
  - Automatic, no initialization required
  - Accuracy and Robustness
- CONS :
  - Requires High Resolution & Low Noise
  - Invariant Landmarks : Rigid, Mono-modal, Single Patient
  - Possible exception : Skull Images

Skull (CT Scan)

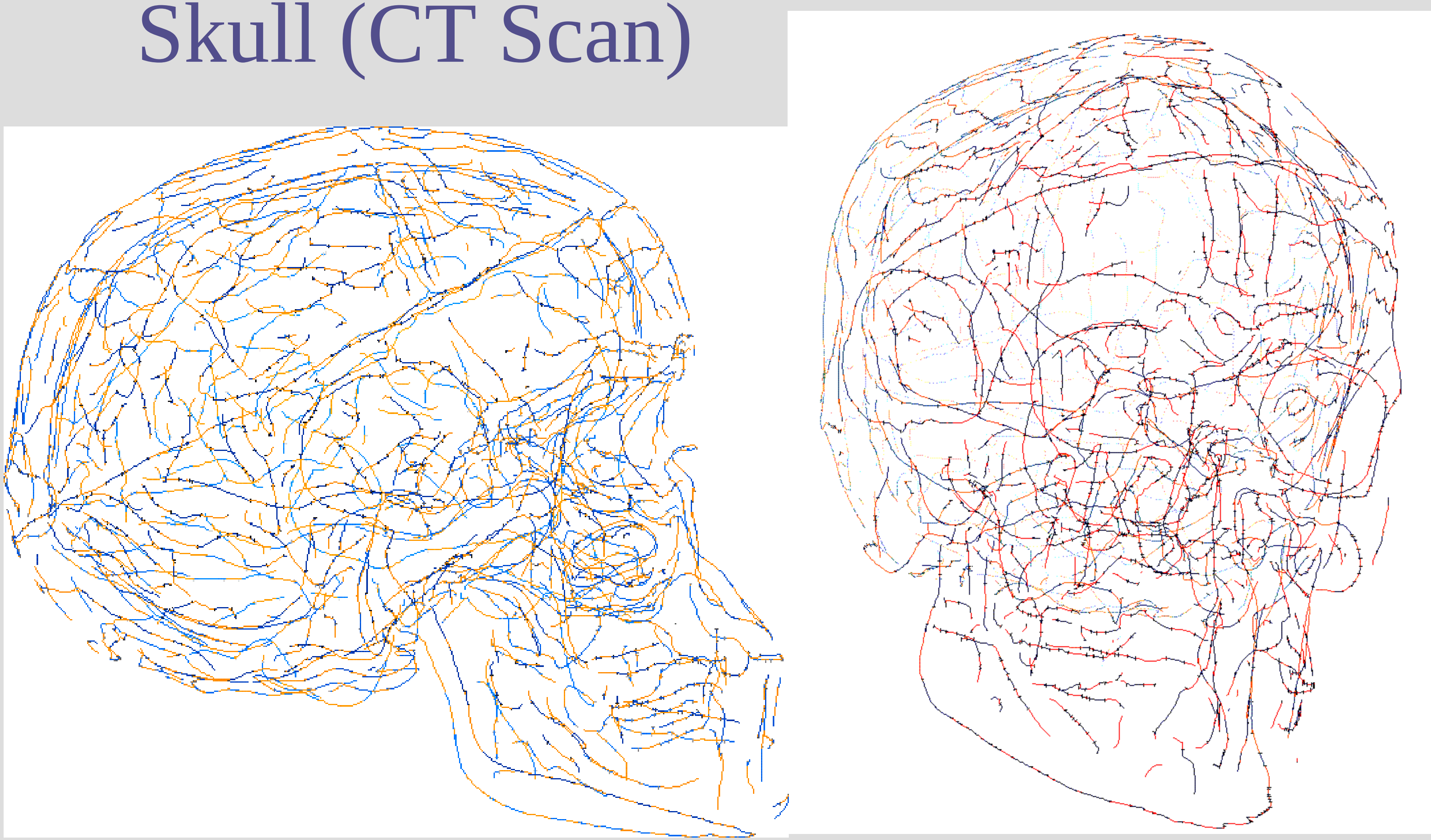

G. Subsol, J.-Ph. Thirion, and N. Ayache. *A General Scheme for Automatically Building 3D Morphometric Anatomical Atlases: application to a Skull Atlas.*

Medical Image Analysis, 2(1):37-60, 1998.

Through Aging or Through Ages

1 month 8 months 4 years

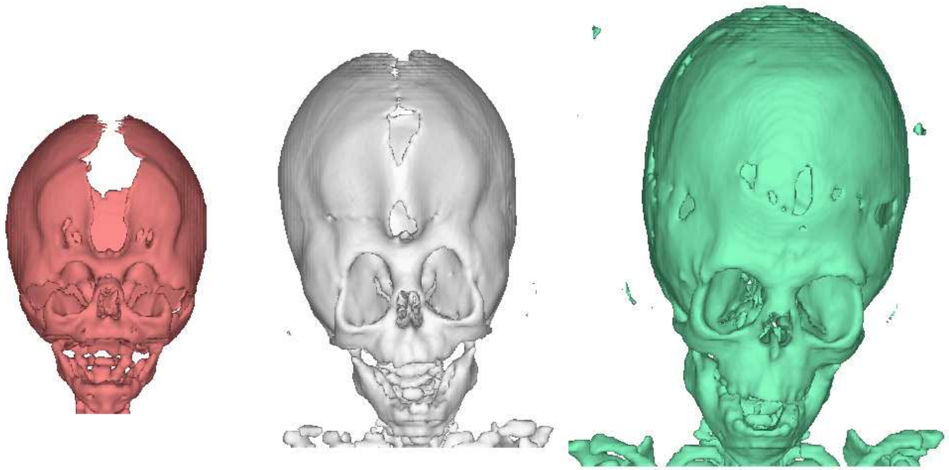

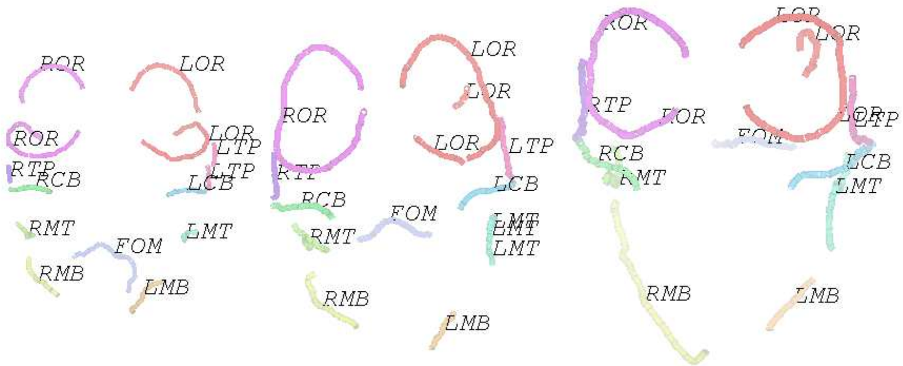

Comtemporary Tautavel

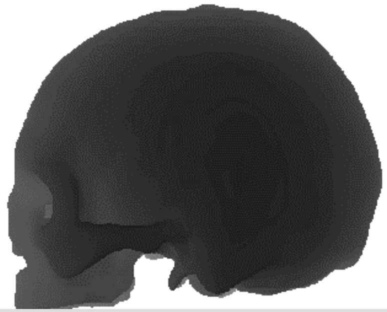

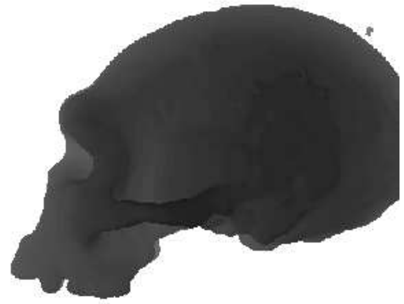

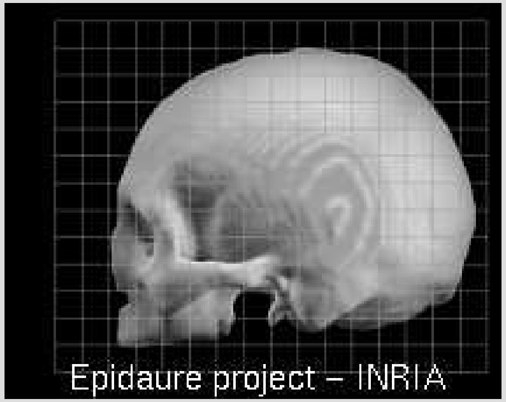

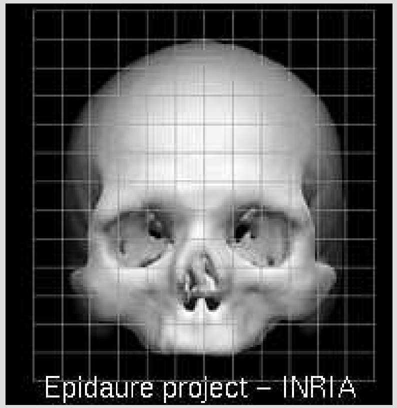

- G. Subsol-Meline-Mafart- De Lumley 2002

•G. Subsol. *Crest Lines for Curve Based Warping* Brain Warping, chapter 13, pages 225-246, Academic Press, 1998.

Content

- Geometric
- Iconic (Monomodal, Multimodal)
- Hybrid
- Rule Based
- Shape Statistics
- Perspectives

Demons Algorithm (Thirion)

- Inspired by the work of Christensen, Miller, et al.
- O(N) Algorithm.
- 2 main iterated stages
  - Image forces which create displacements u_n (normalized optical flow)
  - Regularization of u_n by Gaussian Filtering

J.P. Thirion: Image Matching as a diffusion process: an analogy with Maxwell's demons. Medical Image Analysis 2(3), 242-260, 1998.

Demons Algorithm

- T_0= Identity
- Correction field C_{n+1}

$$C_{n+1} = \frac{I - J \circ T_n}{\|\nabla I\|^2 + (I - J \circ T_n)^2} \nabla I$$

- Regularization : by Gaussian Filtering

Elastic

$$\hat{C}_{n+1} = U_n \circ C_{n+1}$$

$$U_{n+1} = G_\sigma * \hat{C}_{n+1}$$

Fluid

$$\tilde{C}_{n+1} = G_\sigma * C_{n+1}$$

$$U_{n+1} = U_n \circ \tilde{C}_{n+1}$$

- Remark: $\|C_{n+1}\| \leq 1/2$

Interpretation of Demons

- Pennec-Cachier and then Modersitzki put the demons algorithm in a variational framework to show that it minimizes a global energy.
- Modersitzki: Min E under Neumann BC :

$$E = SSD * + \int \left\| \nabla u \right\|^2$$

J. Modersitzki : Numerical Methods for Image Registration, Oxford University Press,2004.

X. Pennec, P. Cachier and N. Ayache : Understanding the Demons Algorithm : 3D non rigid registration by gradient descent, MICCAI 1999, Springer-Verlag.

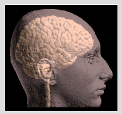

PASHA Algorithm (1/2)

- P. Cachier introduces auxilliary variables (cf. L. Cohen 1996) to formalize the alternate minimization of the Demon’s Algorithm while preserving its efficiency

$$E(C,U) = E_S(I,J,C) + \sigma \int \| C - U \|^2 + \lambda \int \| \nabla U \|^2$$

P. Cachier E. Bardinet, E. Dormont, X. Pennec and N. Ayache: *Iconic Feature Based Nonrigid Registration: the PASHA Algorithm*, Comp. Vision and Image Understanding (CVIU), Special Issue on Non Rigid Registration, 89 (2-3), 272-298, 2003.

PASHA Algorithm (2/2)

$$E(C,U) = E_S(I,J,C) + \sigma \int \| C - U \|^2 + \lambda \int \| \nabla U \|^2$$

- Minimization on C by differentiation of the similarity criterion (gradient descent,1st or 2nd order)
- Minimization on U, explicit solution by Gaussian convolution

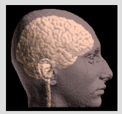

Mixed Elastic/Fluid Regularization

$$E(C,U,\dot{U}) = E_S(I,J,C) + \sigma \int \| C - U \|^2 + \lambda \int \| \nabla U \|^2 + \mu \int \| \nabla \dot{U} \|^2$$

- **Advantage**:
  - regularization still by convolution
  - can handle larger displacements

P. Cachier N. Ayache, *Isotropic Energies, Filters and Splines for Vector Field Regulatization,* J. of Mathematical Imaging and Vision, 20: 251-265, 2004

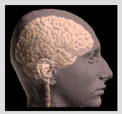

Nice Properties of PASHA

- Alternate minimization of a single positive criterion : Convergence
- Algorithmic Complexity O(N)
- Smooth deformation field:
  - Careful gradient descent $\|C_{n+1}\| \leq 1/2$
  - Eulerian scheme for interpolation
  - Regularization by “low pass” filters

Symmetric energies

- Similarity

$$SSD(I,J,C)=\int (I-J\circ C)^2 \neq SSD(J,I,C^{-1})$$

$$\boxed{E_s^*(I,J,C)=\frac{1}{2}\left[E_s(I,J,C)+E_s(J,I,C^{-1})\right]}$$

$$SSD^*(I,J,C)=\frac{1}{2}\int (1+|\nabla C|)(I-J\circ C)^2$$

- Regularization :

$$E_\nabla(I,J,U)=\int \|\nabla U\|^2 \neq E_\nabla(J,I,U^{-1})$$

$$\boxed{E_{reg}^*(U)=\frac{1}{2}\left[E_{reg}(U)+E_{reg}(U^{-1})\right]}$$

$$E_\nabla^*(U)=\frac{1}{2}\int\left(1+\frac{1}{|\nabla U|}\right)\left(\|\nabla U\|^2\right)$$

[P. Cachier, D. Rey, MICCAI'00]

Quantifying Apparent Brain Variations

- Introduce Differential Operators to the deformation field to detect non-rigid brain variations

- Exemple : Jacobian of deformation field :
  - J = 1 for rigid transformation
  - J > 1 for local expansion
  - J < 1 for local contraction

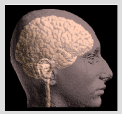

1.Multiple Sclerosis Evolution

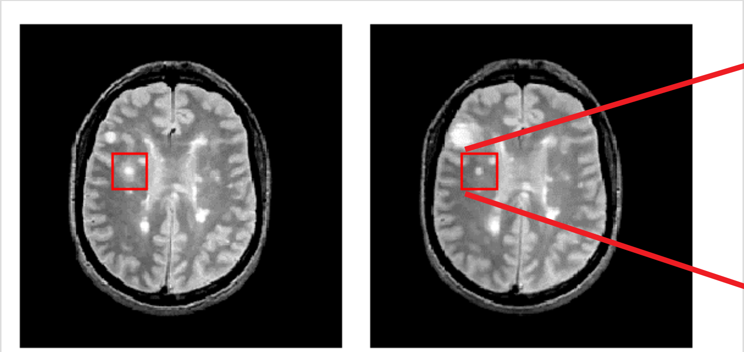

Time i   Time i+1

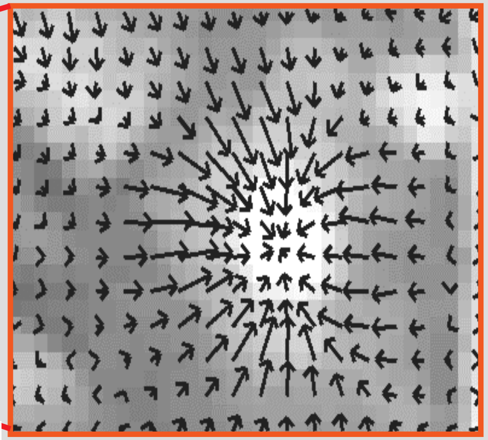

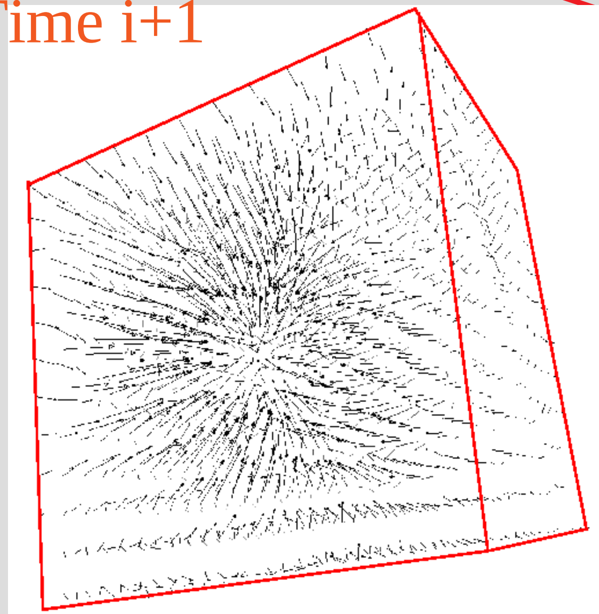

Apparent Deformation Field

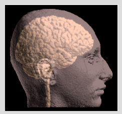

Apparent Residual Deformations

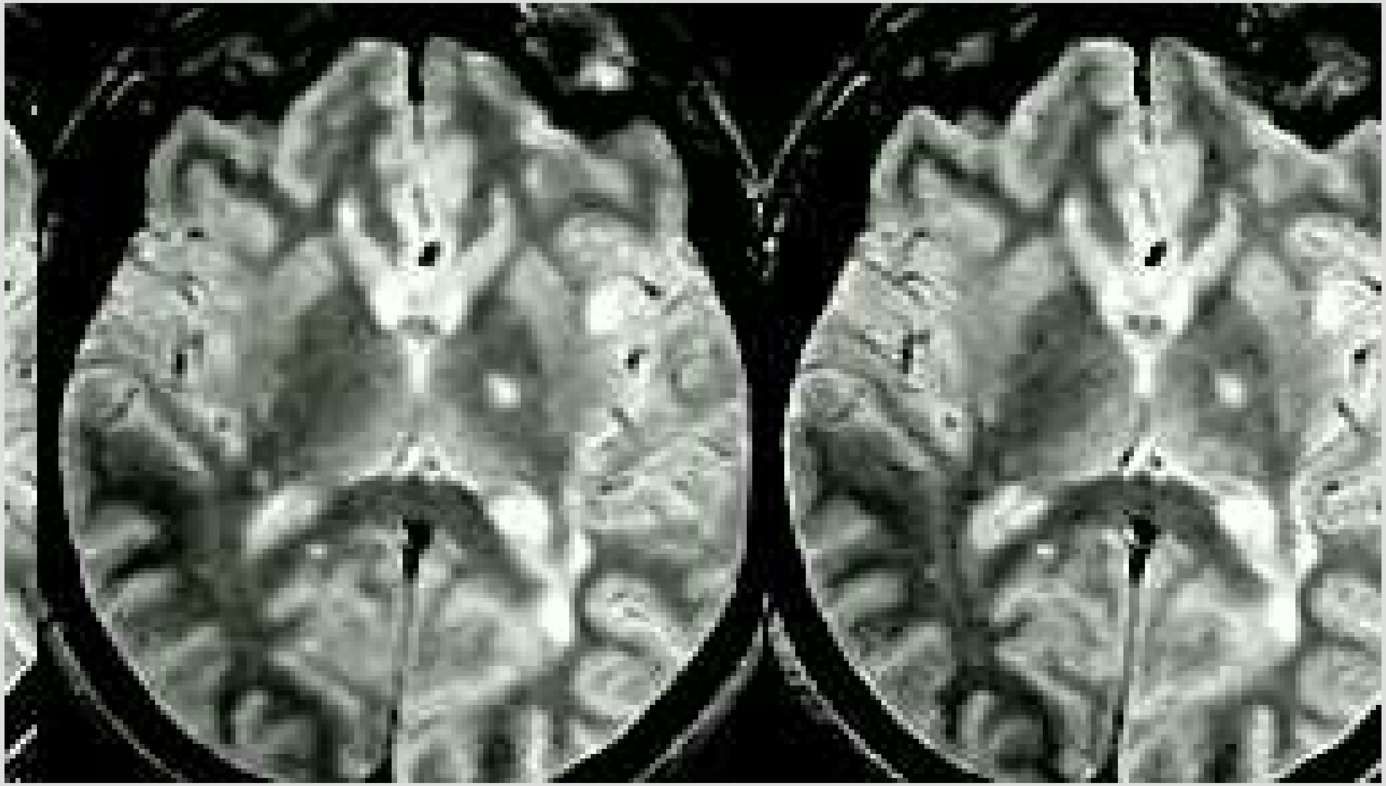

Time i　　　　Aligned Time i+1

Isovalues of Log[Jacobian]

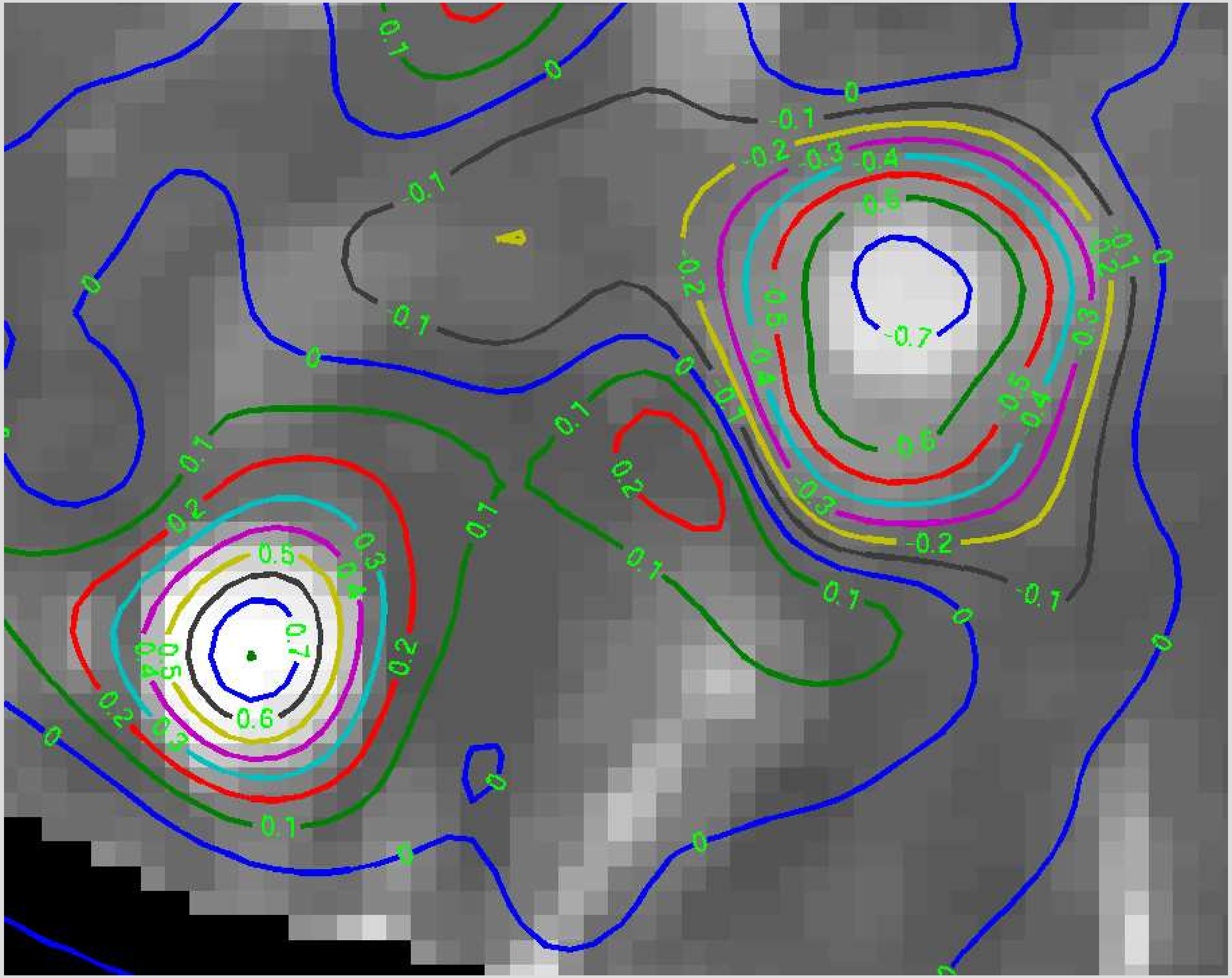

Detection of evolving lesions

Time i Time i+1

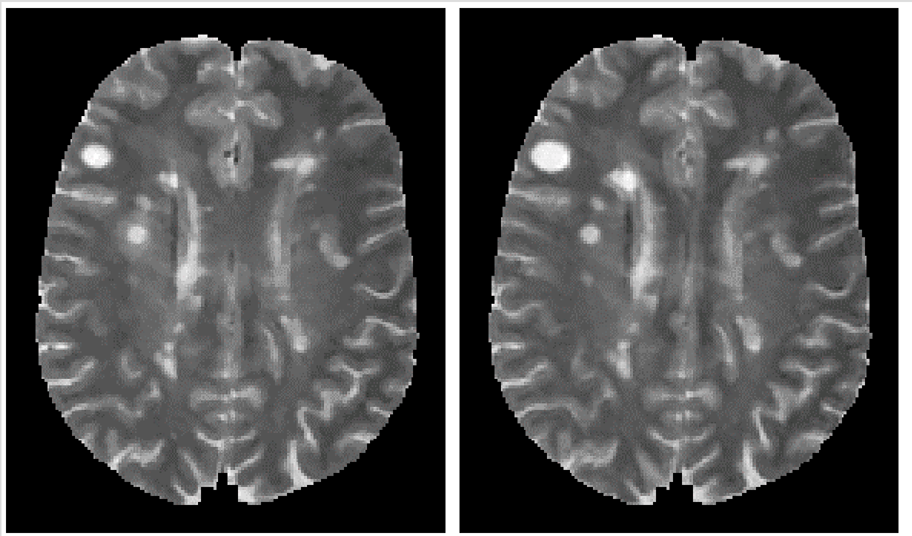

Time i Time i+1

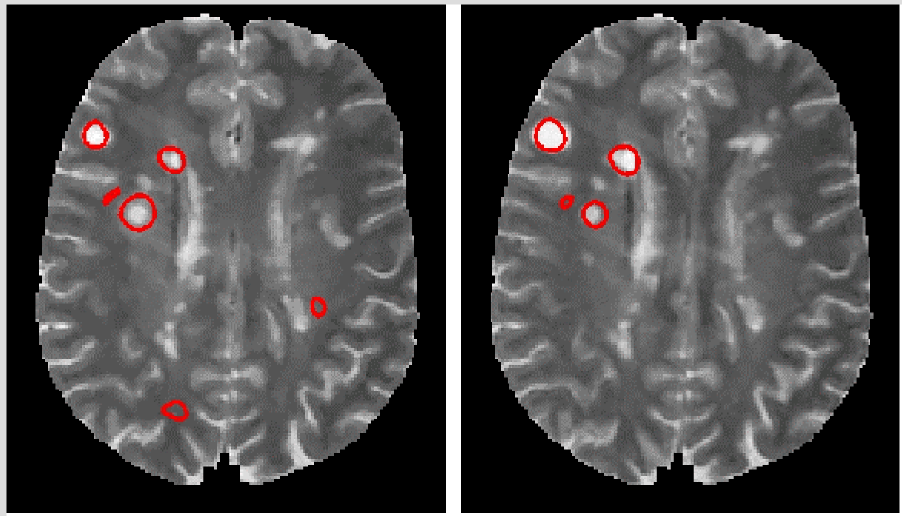

$$\left|\ln(jac)\right| \geq 0{,}4$$

Symmetric Energies (1/2)

axial coronal sagittal

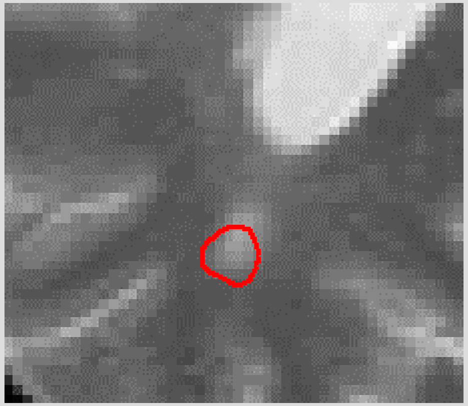

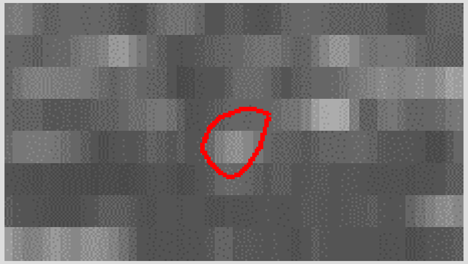

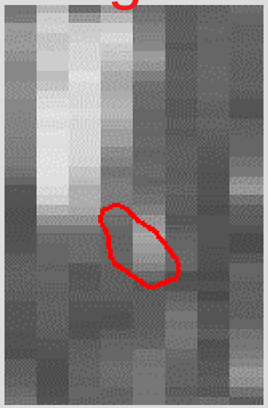

DIRECT T

Time i

log(Jac)= +1

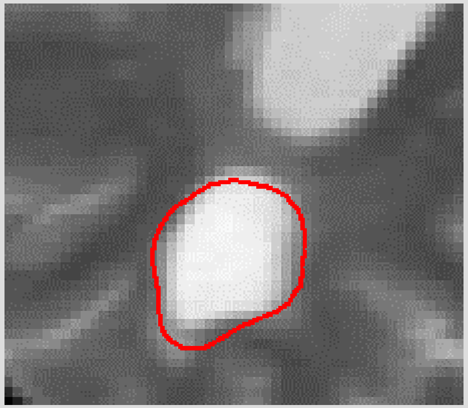

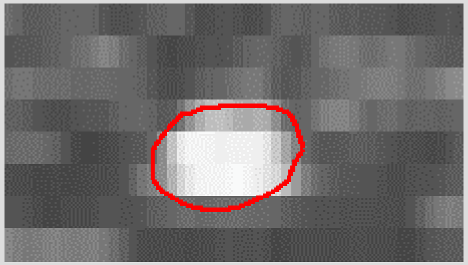

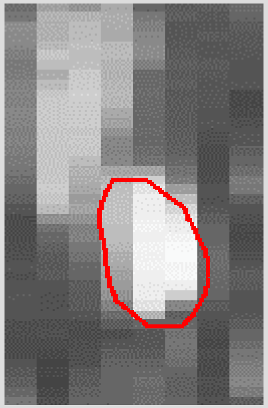

Time i+1

T2- MRI 0.89x0.89x5.5mm

[P. Cachier, D. Rey, MICCAI'00]

Symmetric Energies (2/2)

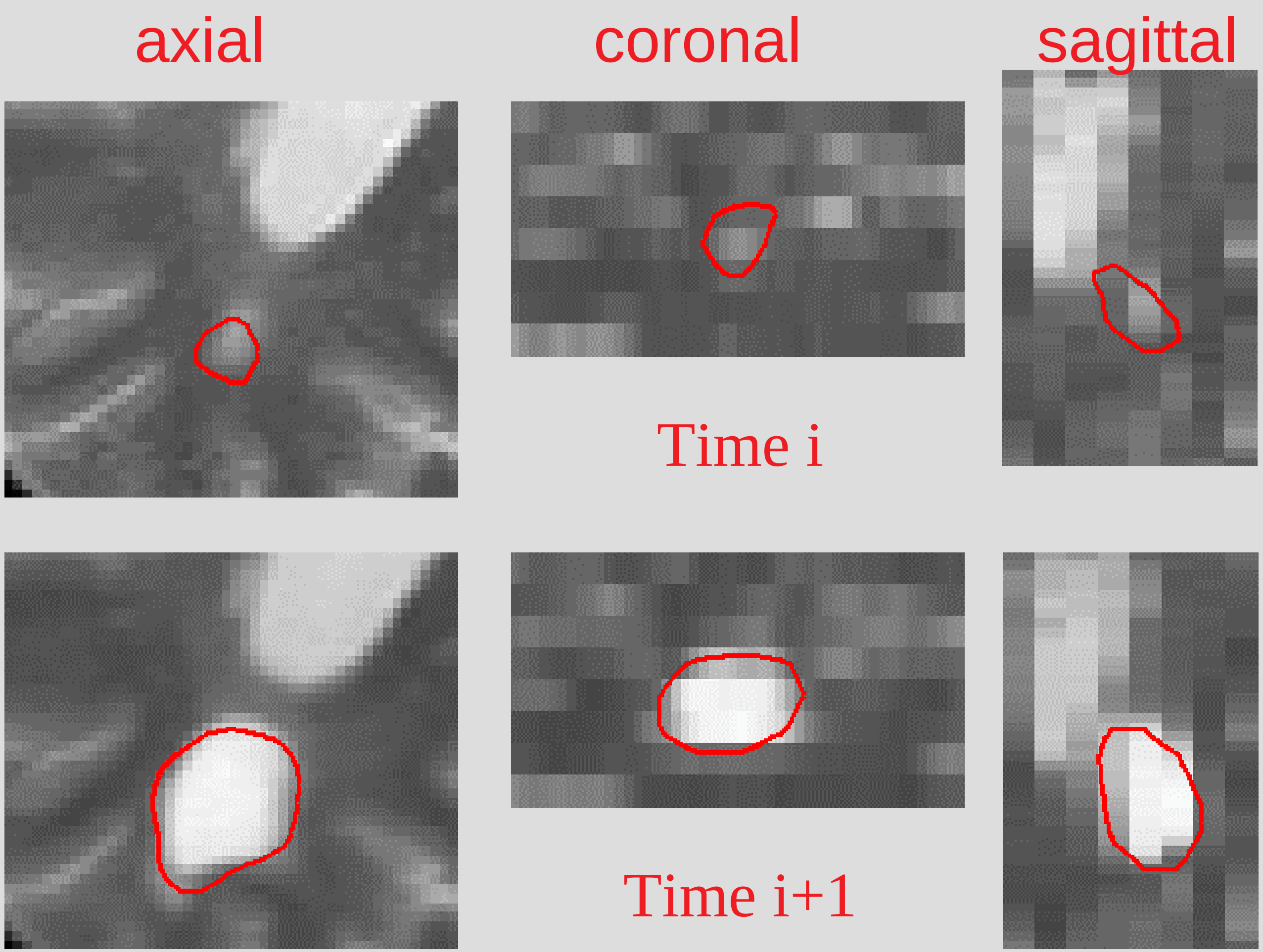

INVERSE T

log(Jac)= -1

T2- MRI 0.89x0.89x5.5mm

[P. Cachier, D. Rey, MICCAI'00]

Temporal Evolution of Lesions

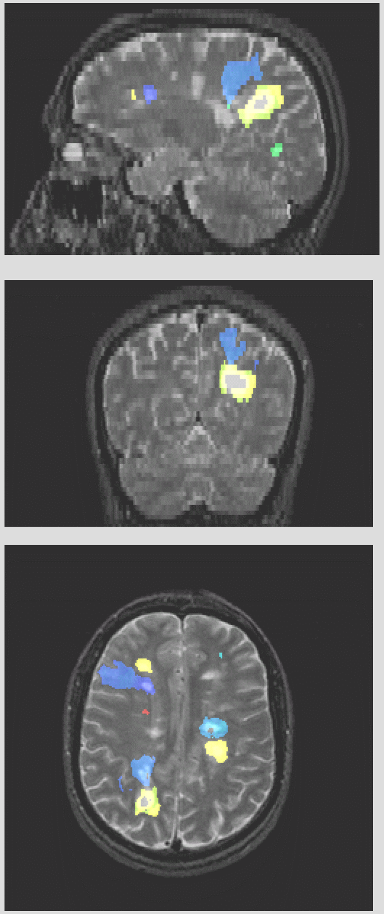

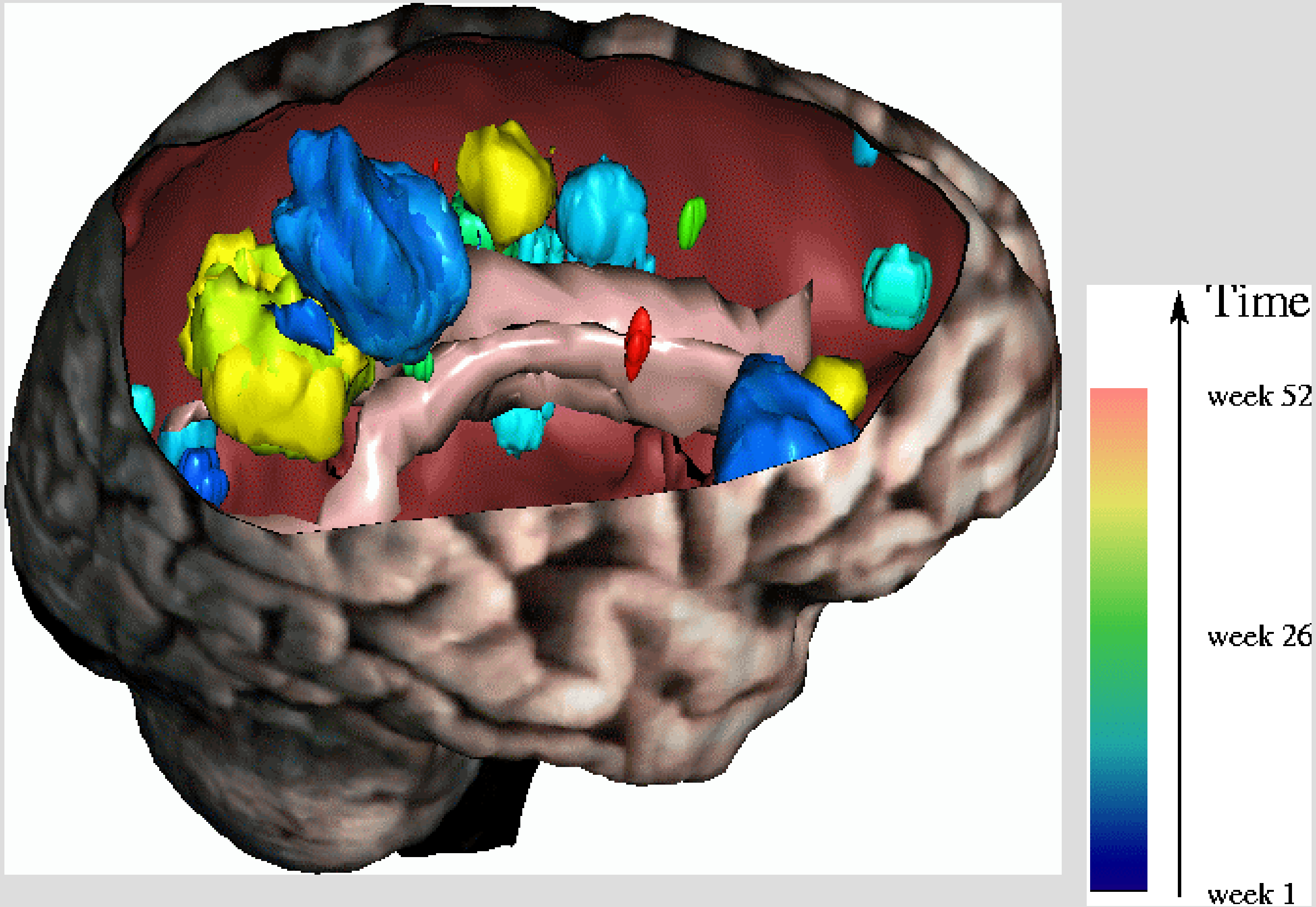

D. Rey, G. Subsol, H. Delingette, N.Ayache : *Automatic Detection and Segmentation of Evolving Processes in 3D Medical Images: Application to Multiple Sclerosis.* Medical Image Analysis, 6(2):163-179, June 2002.

2. Brain Asymmetry

- Local and quantitative measure of cerebral asymmetry

PhD Thesis of S. Prima
Biomorph Project
A. Colchester, G. Gerig,
M. Brady, T. Crow, et al.

Stage 1 : Find Mid-Sagittal Plane

- Find Plane which minimizes SSD criterion between homologous points

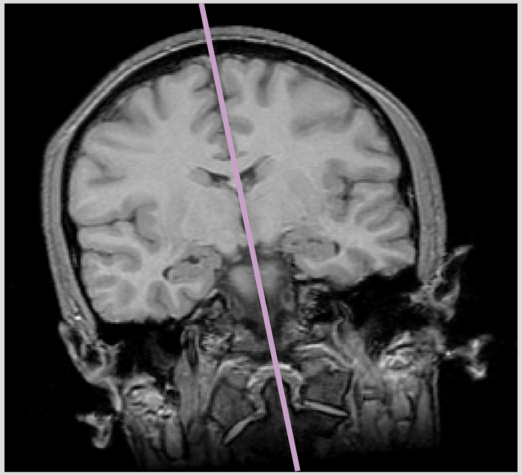

- Rotate image to place MSP in a reference position

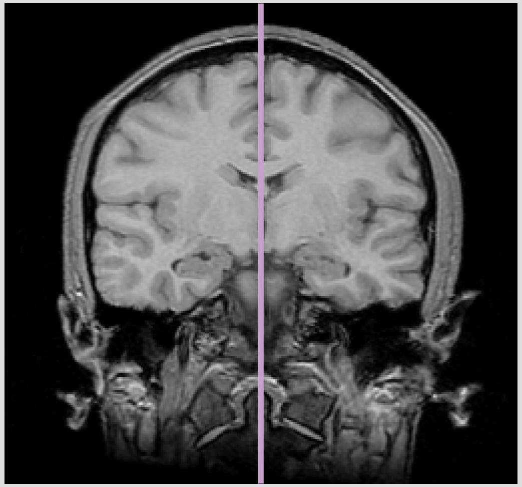

S. Prima, S. Ourselin, N. Ayache : *Computation of the Mid-Sagittal Plane in 3D Brain Images.* IEEE Transaction on Medical Imaging, 21(2):122--138, February 2002.

Mid-Sagittal Plane

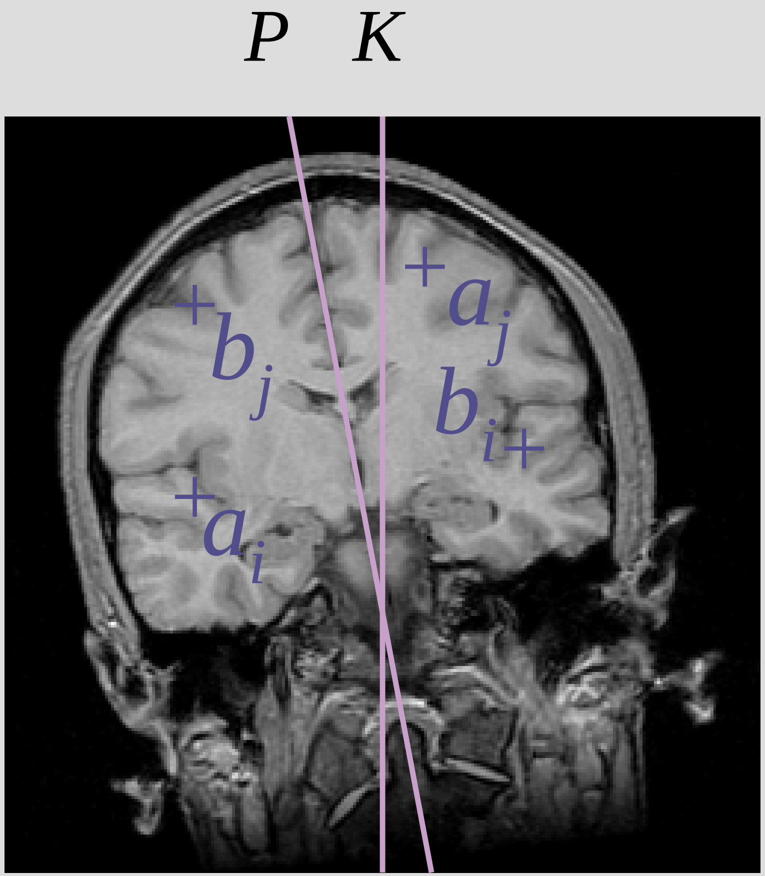

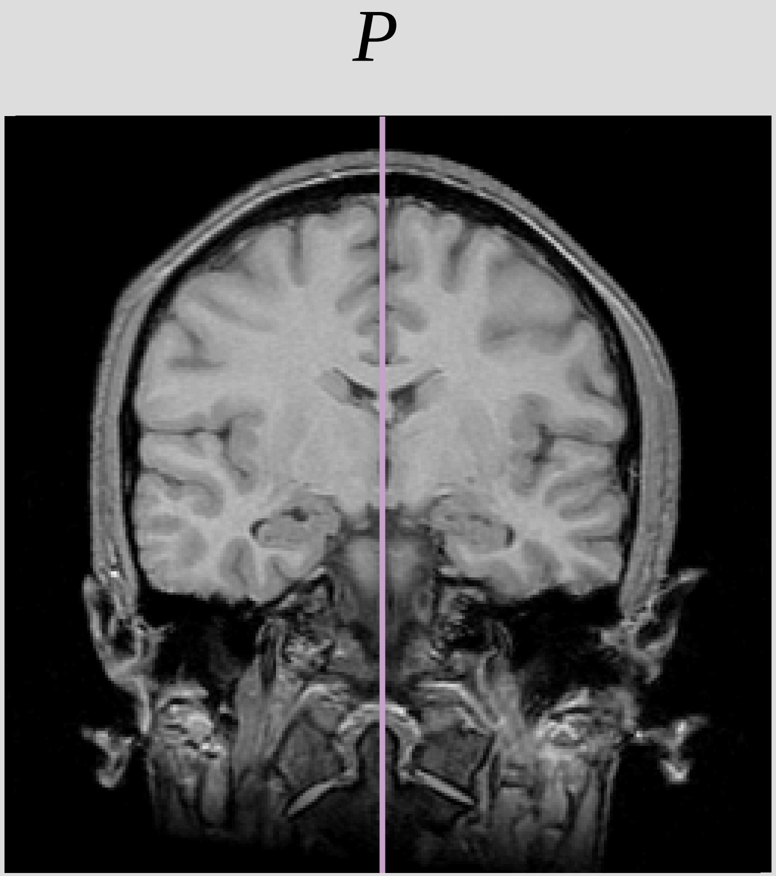

$$R = (S_K \circ S_P)^{1/2}$$

Estimation of coronal mid-sagittal plane

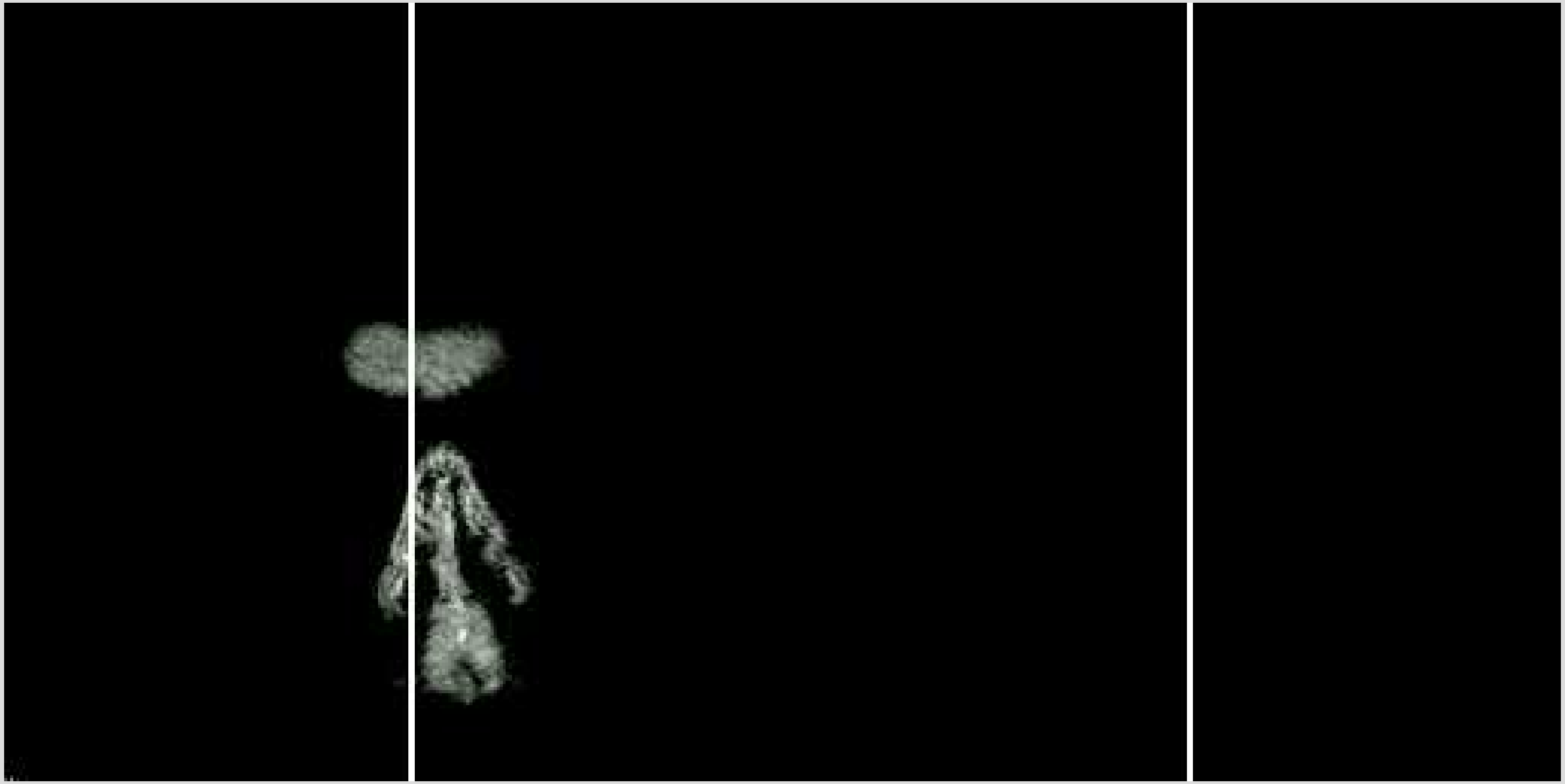

Original

Aligned

S. Prima, S. Ourselin, N. Ayache : *Computation of the Mid-Sagittal Plane in 3D Brain Images.* IEEE Transaction on Medical Imaging, 21(2):122--138, February 2002.

Stage 2 : Quantify Asymmetry

- Compute deformation field F between each hemisphere and its symmetrized version

- Quantify “deviation” from rigid transformations
  - several differential operators including Jacobian
  - good experimental results with ||F||.div(F)

J.-P. Thirion, S. Prima, G. Subsol, and N. Roberts. *Statistical Analysis of Normal and Abnormal Dissymmetry in Volumetric Medical Images*. Medical Image Analysis, 4(2):111--121, June 2000

Asymmetry Field (Synthetic Example)

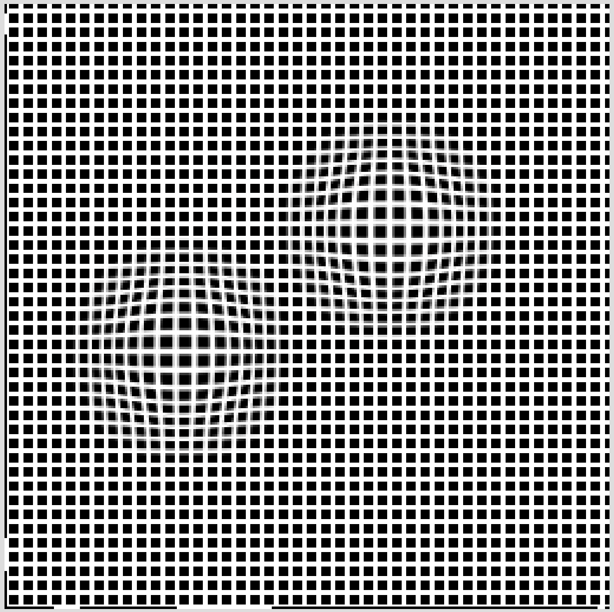

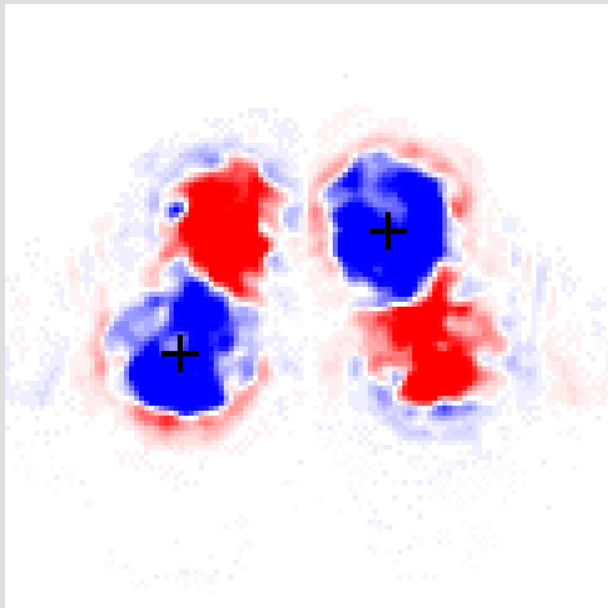

$||F||\mathrm{div}(F)$

Asymmetry Field (Real Example)

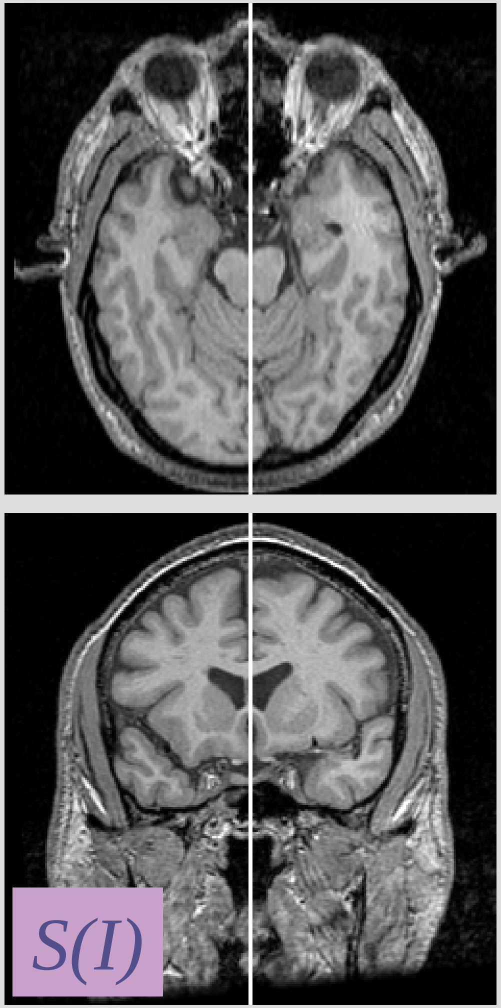

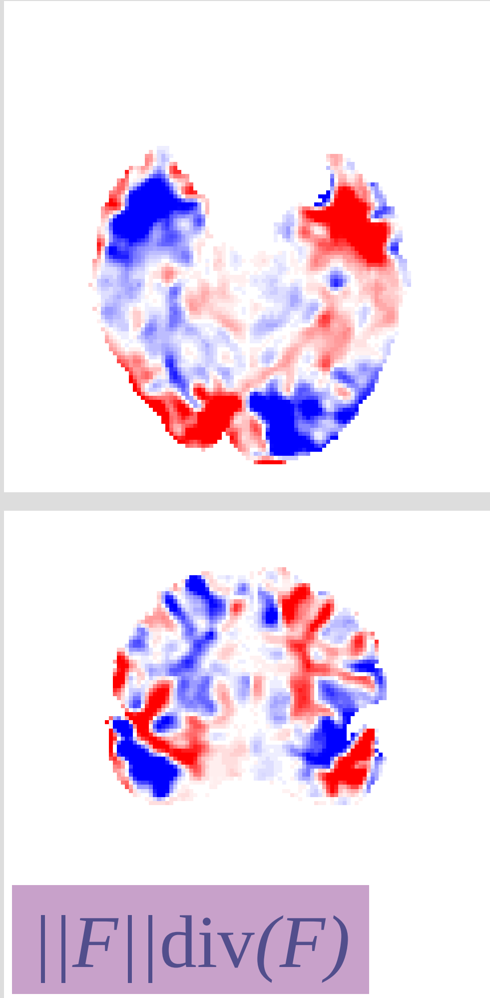

Controls vs. Schizophrenics

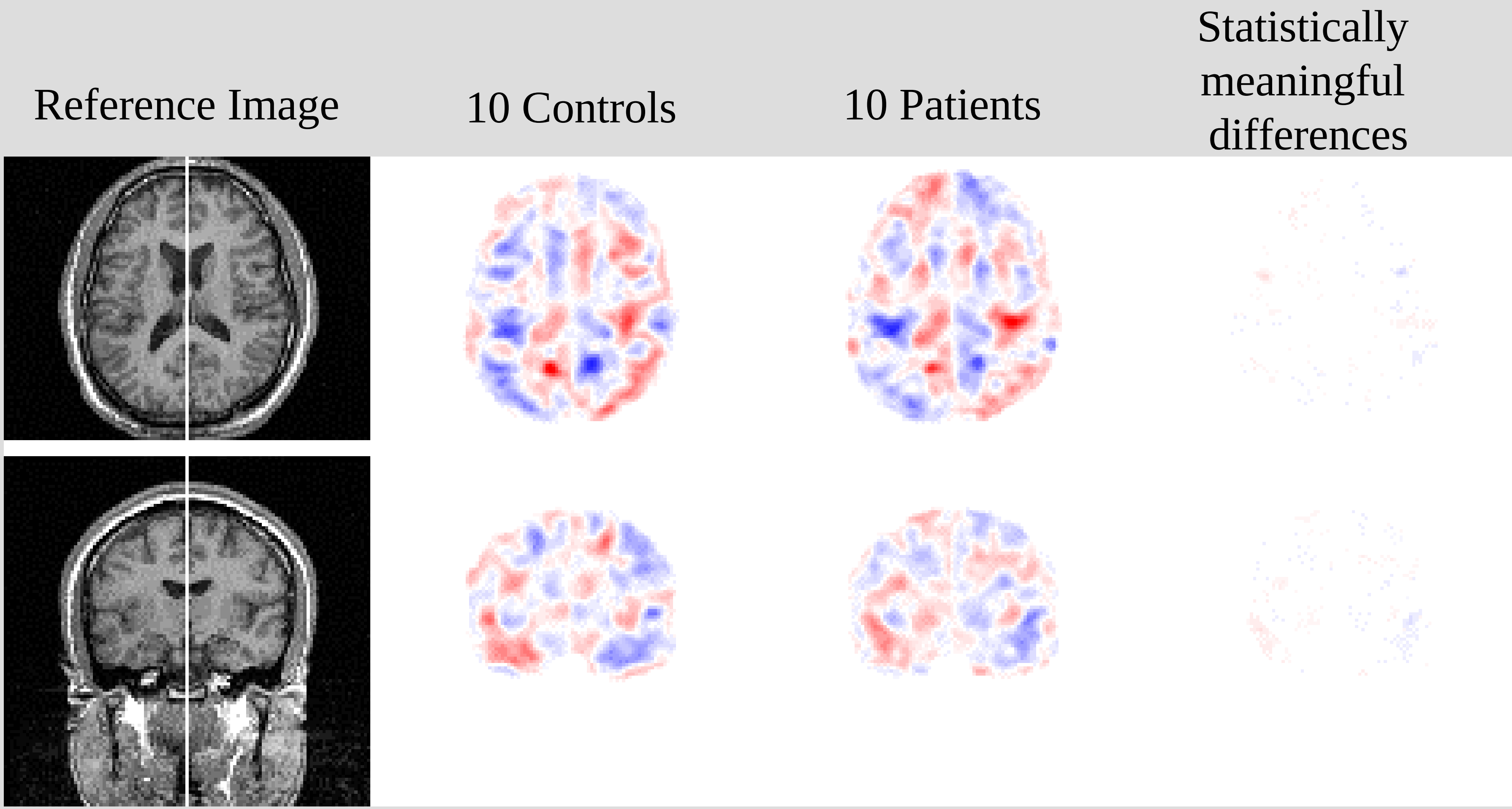

J.-P. Thirion, S. Prima, G. Subsol, and N. Roberts. *Statistical Analysis of Normal and Abnormal Dissymmetry in Volumetric Medical Images*. Medical Image Analysis, 4(2):111--121, June 2000

Content

- Geometric
- Iconic (Monomodal, Multimodal)
- Hybrid
- Shape Statistics
- Perspectives

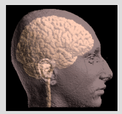

Comparing Multimodal images?

- Which Similarity Criterion?
  - Numerous criterions available:
    - SSD, Correlation, Mutual information,...?
  - Variable costs and performances
  - Which one is optimal?

Maintz & Viergever, Survey of Registration Methods, Medical Image Analysis 1997

A general framework

- A. Roche proposed a unifying maximum likelihood framework
- Based on a physical and statistical modeling of the image acquisition process
- Creates a hierarchy of criteria, introduces new ones (correlation ratio)

A. Roche, G. Malandain and N.Ayache : *Unifying maximum likelihood approaches in medical image registration.* International Journal of Imaging Systems and Technology : Special Issue on 3D Imaging 11(1), 71-80, 2000.

• Following the pioneering work of (Costa et al, 1993), (Viola, 1995), (Leventon & Grimson, 1998), (Bansal et al, 1998)

Maximum Likelihood Formulation

- General dependence model (Roche et al.)

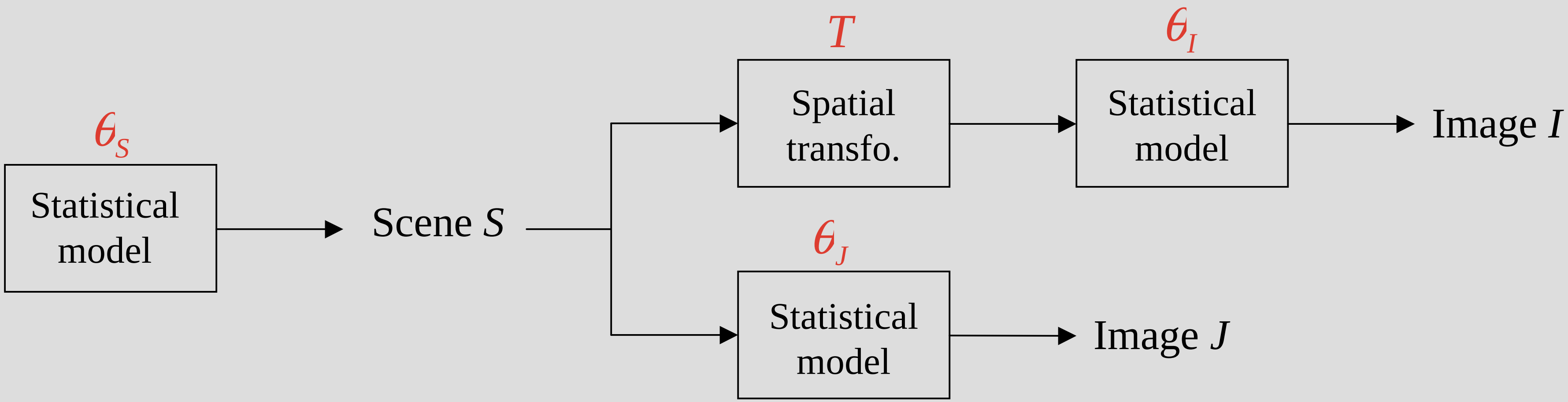

- Maximum Likelihood

$$\max_{T,\theta_I,\theta_J,\theta_S} P(I,J \mid T,\underbrace{\theta_I,\theta_J,\theta_S}_{\text{Auxiliary parameter: } \theta})$$

Optimal Criterion for Intensity Similarity

Identity: Sum of Square Differences

$$ssd^2 = \sum_k (I(x_k) - J(T(x_k)))^2$$

Affine: Correlation Coefficient

$$\rho^2 = \frac{Cov^2(I, J(T))}{Var(I)}$$

Functional: Correlation Ratio

$$\eta^2 = 1 - \frac{Var(E(I / J(T)))}{Var(I)}$$

Statistical: Mutual Information

$$I(I,J) = H(I) + H(J) - H(I,J)$$

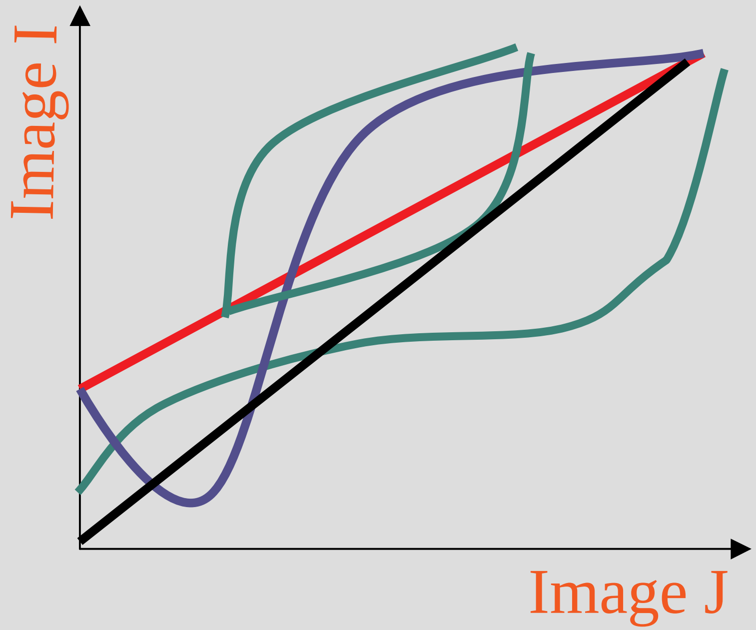

Roboscope : Quantify Brain Deformation during Neurosurgery

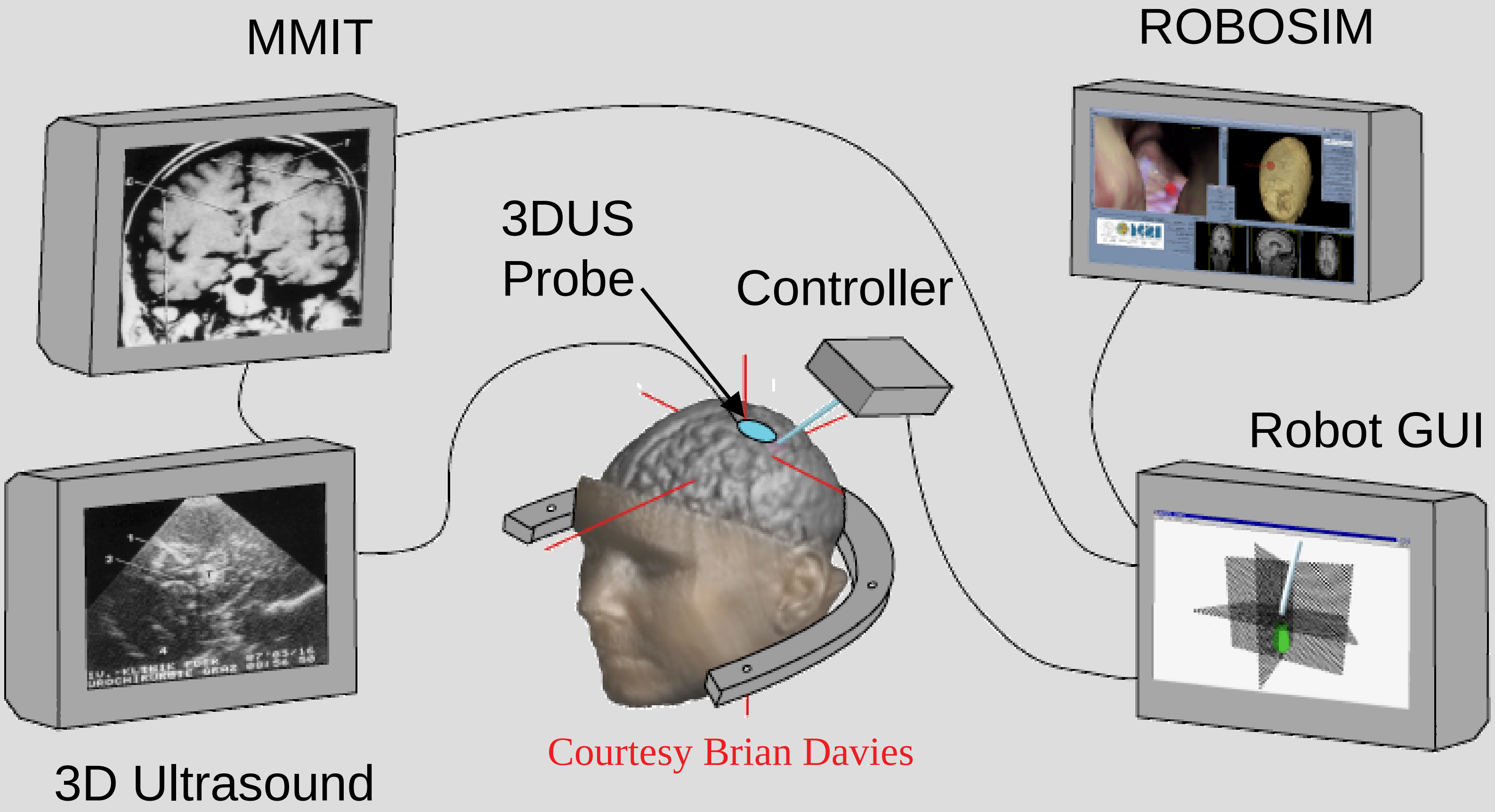

Courtesy Brian Davies

Image-Guided Manipulator-Assisted Neuro-Endoscopy

MR-US Images

Pre - Operative MR Image

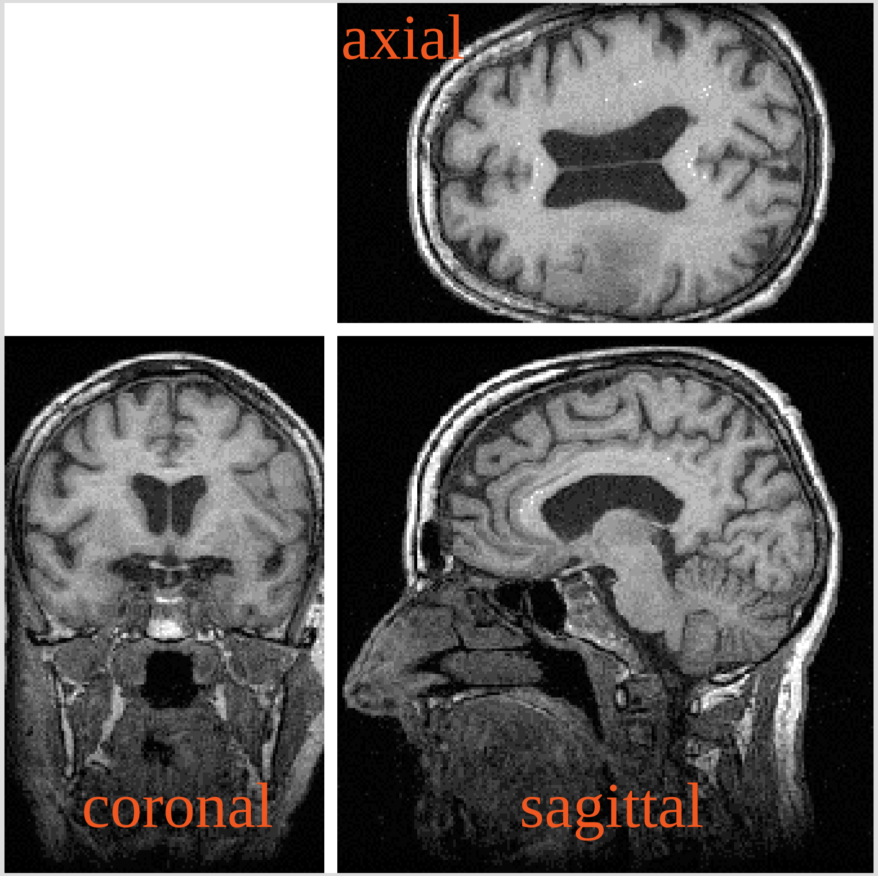

Per - Operative US Image

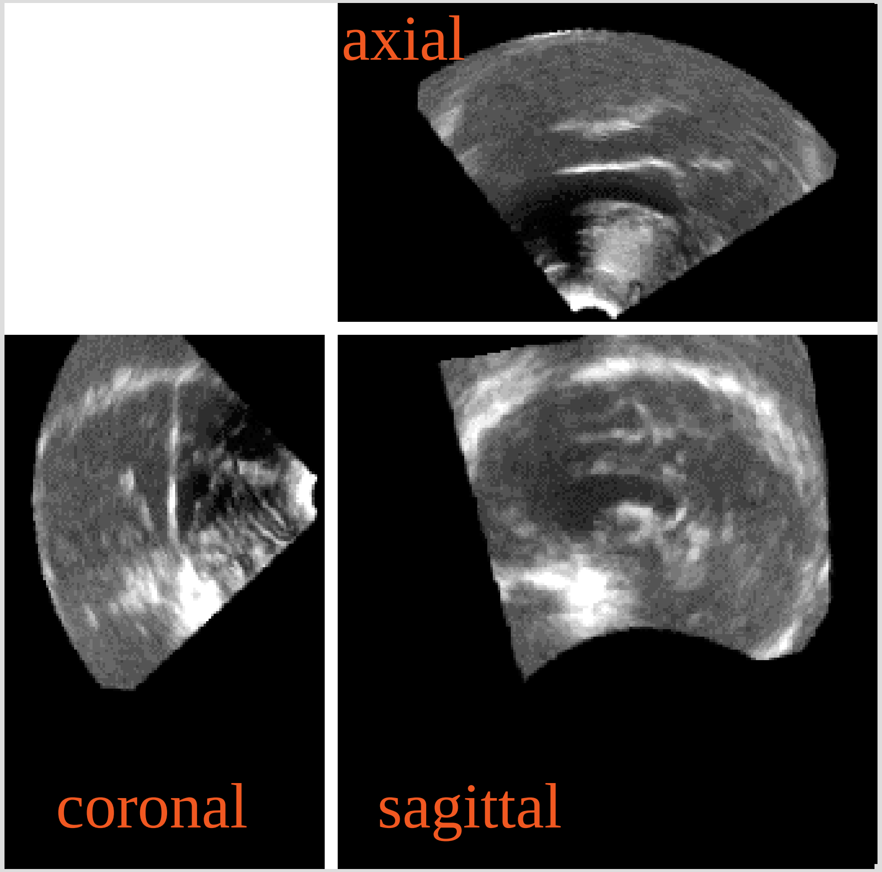

Acquisition of images : L. & D. Auer, M. Rudolf

Physics

- Physics of ultrasound and MRI show that as a first approximation, it is reasonable to assume a dependence of the US signal as a function of MR intensity and gradient.

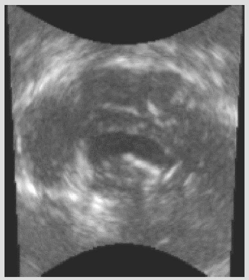 = function (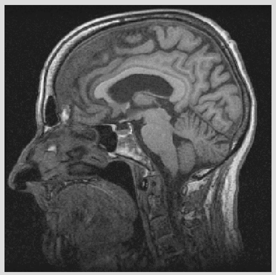 , 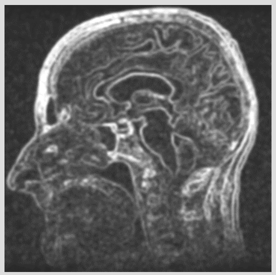)

Bivariate Correlation Ratio

- I function of 2 variables

$$I = f(J, |\nabla J|)$$

- 2 iterated stages
  - Robust polyn. approx. of f
  - Estimation of T:

$$\boxed{\hat{T} = \operatorname*{argmin}_{T} \sum_{k} \left(I(x_k) - \hat{f}\left(J(T(x_k)), \left|\nabla J(T(x_k))\right|\right) \right)^2}$$

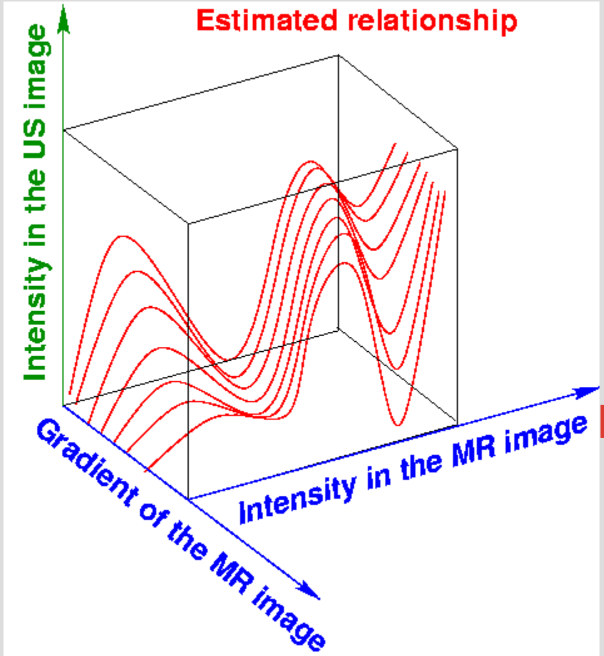

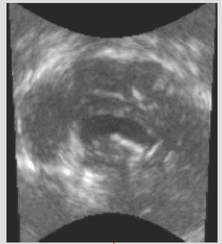

Dependency Hypothesis

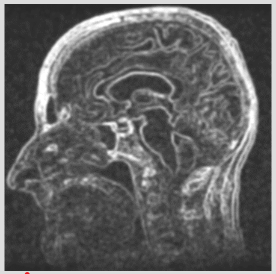

A. Roche, X. Pennec, G. Malandain, and N. Ayache
Rigid Registration of 3D Ultrasound with MR Images:
a New Approach Combining Intensity and Gradient Information.
IEEE Transactions on Medical Imaging, 20(10):1038--1049, October 2001.

Typical Registration Result with Bivariate Correlation Ratio

Pre - Operative MR Image

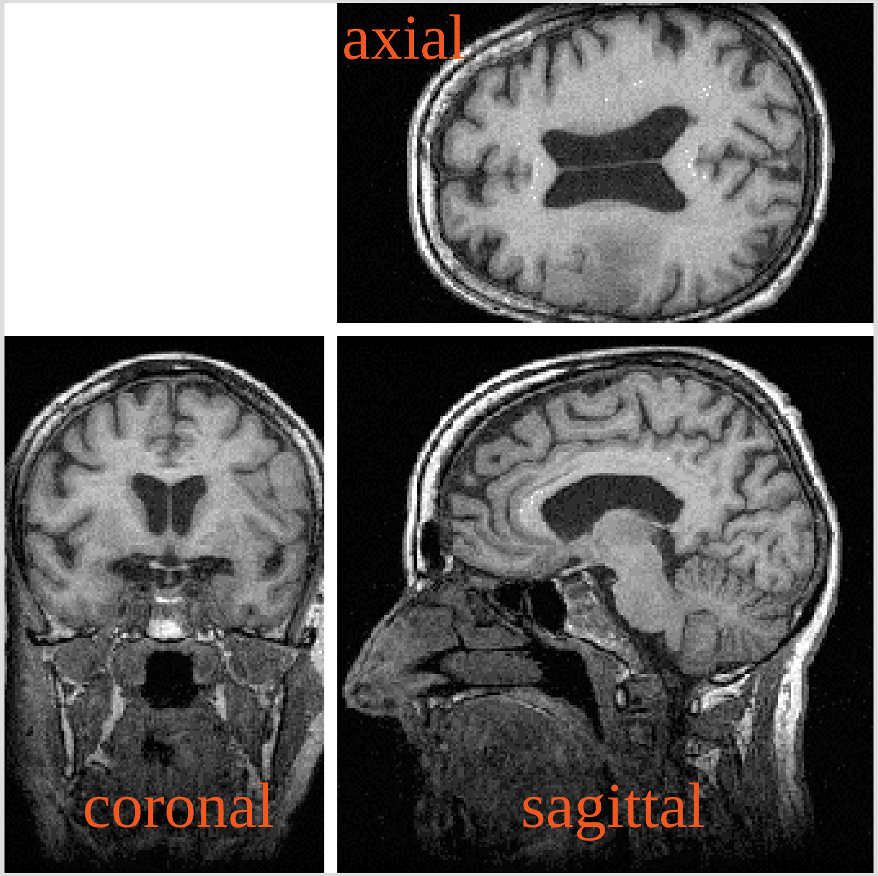

Per - Operative US Image

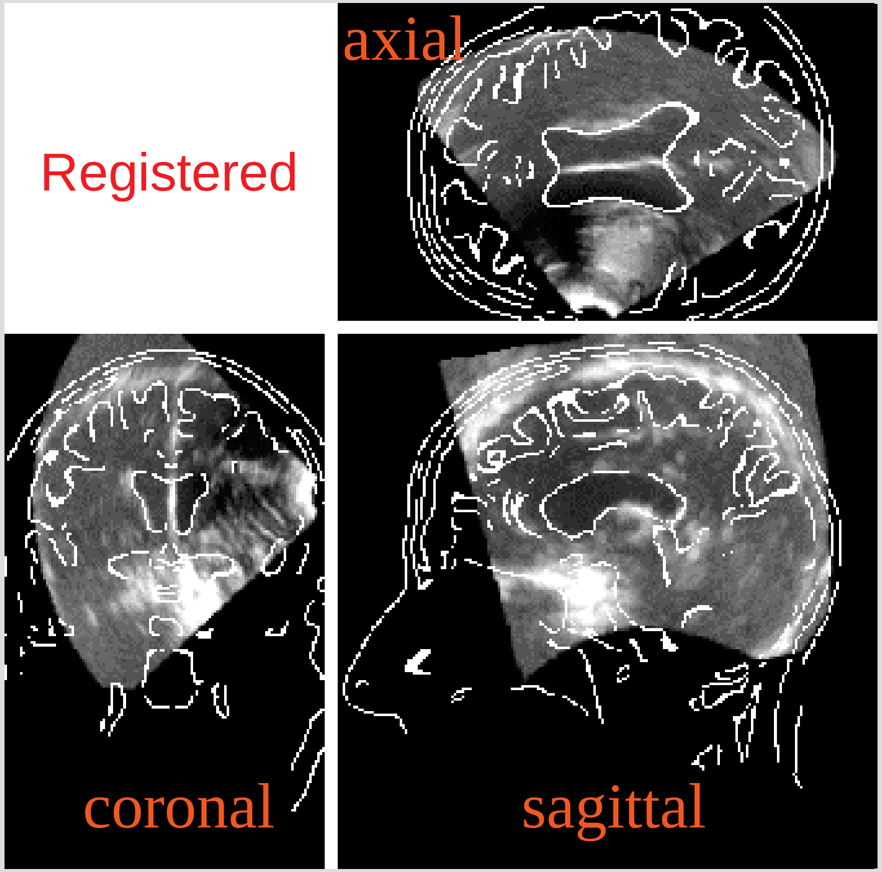

Acquisition of images : L. & D. Auer, M. Rudolf

Accuracy/Robustness

Sensitivity to initialization

200 registration with

- 15 deg random rotation
- 20 mm random translation

Bronze standard

- registration loops

	Failures	Mean accuracy
Biv. CR	6%	0.9 mm / 0.9 deg
Corr. ratio	12%	0.9 mm / 0.7 deg
Mutual info.	28%	1.4 mm / 0.8 deg

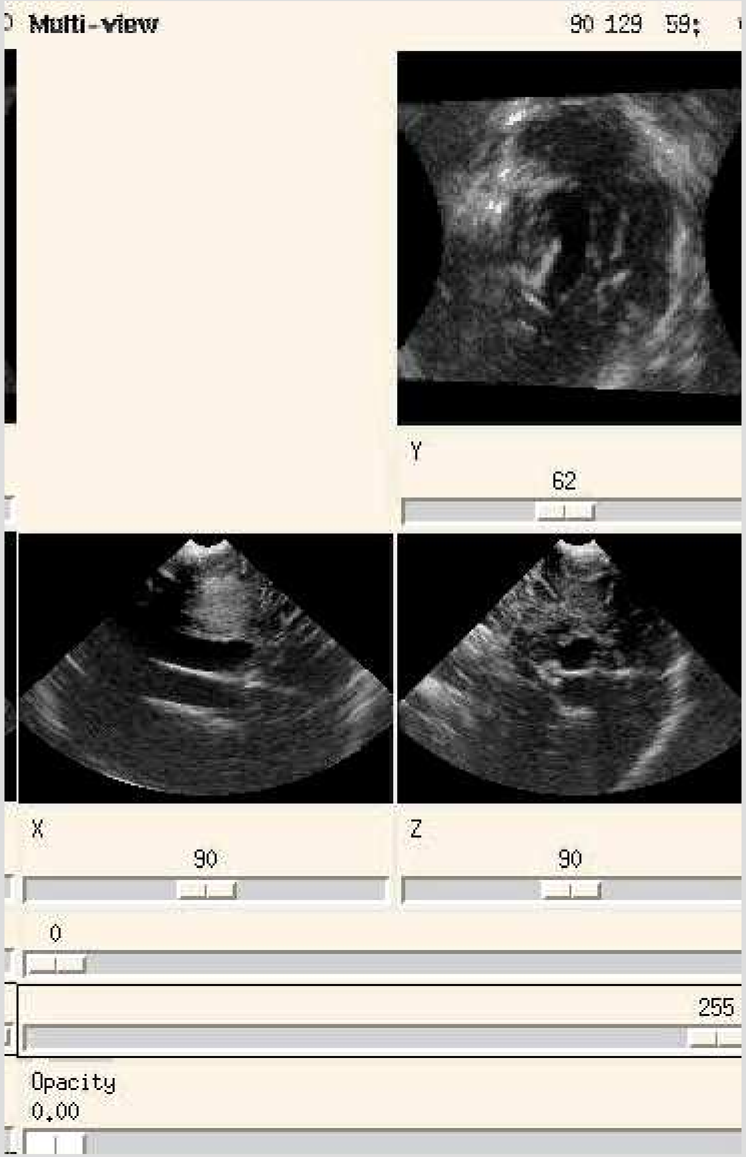

[Roche, Pennec, Malandain, Ayache, IEEE TMI 20(10), 1038-1049, Oct. 2001]

Tracking US Images

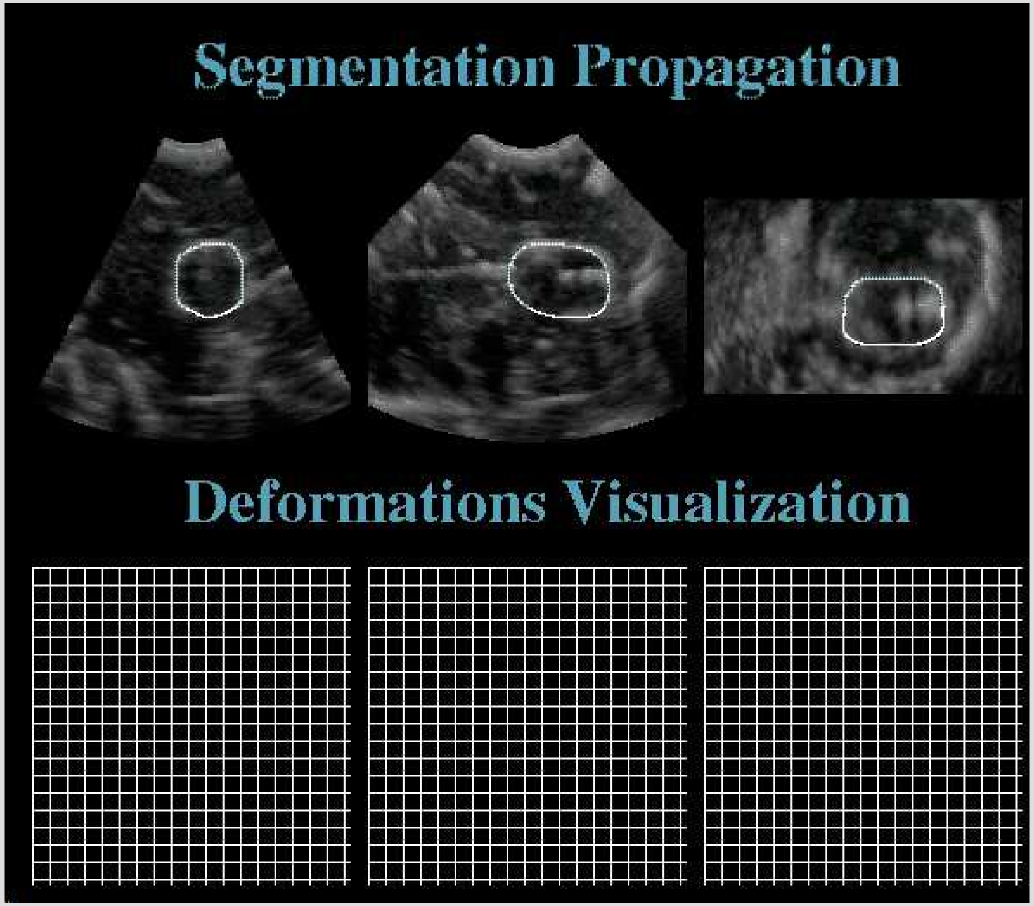

Pig Brain

- Parallel version of Pasha

R. Stefanescu, X. Pennec, and N. Ayache. Grid-Enabled Non-Rigid Registration of Medical Images. Parallel Processing Letters, In Press, 2004.

Metamorphosis

•

t=0

t=0,5

t=1

Metamorphosis

-

Interpolation and Extrapolation

t=0
neutral

t=0,5
attenuated expression

t=1
expression (smile)

t=1,5
exagerated expression

Interpolation of 2 images

- **Slow down motion in video sequences**

Original sequence of 7 images

Slow down 10 times, 61 images

Content

- Geometric
- Iconic (Monomodal, Multimodal)
- Hybrid
  - Geometric&Iconic;
  - Bloc Matching:
  - Piecewise parametric

Geometric-Iconic-Semantic

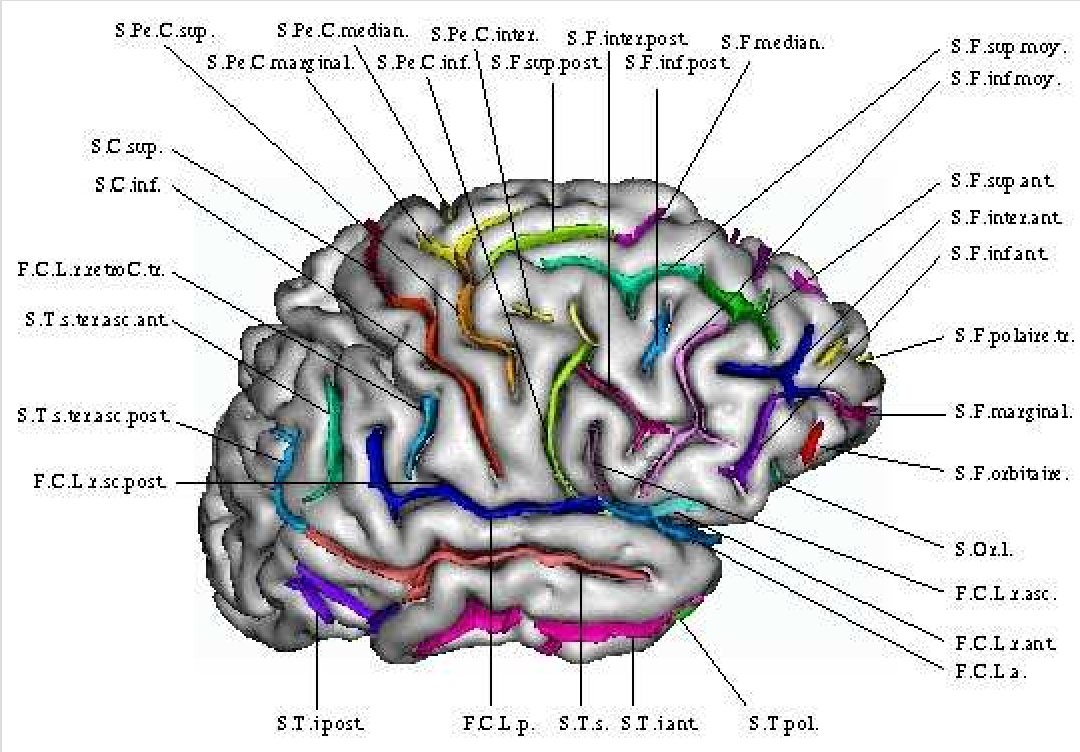

JF. Mangin, D. Rivière, SHFJ-CEA

Concerted action : CEA-Epidaure-Robotvis-Salpêtrière-Vista

Intersubject Brain Registration

- Geometric approach to match homologous sulci
- Iconic approach otherwise

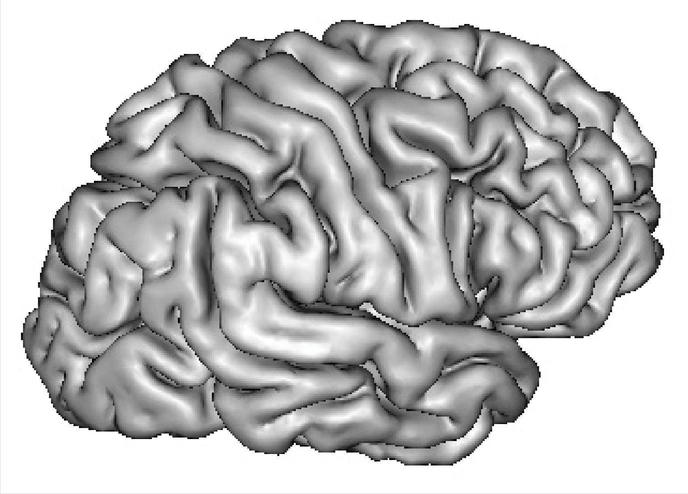

Cortex 1

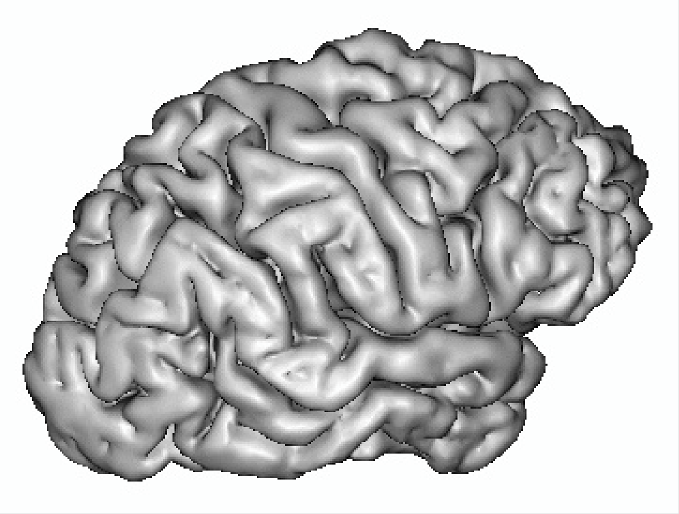

Cortex 2

Extension of Pasha Algorithm

- Add geometrical constraints C_2 between homologous sulci

$$E(C_1, C_2, U) = E_S(I, J, C_1) + \sigma_1 \int \| C_1 - U \|^2 + \sigma_2 \int \| C_2 - U \|^2 + \lambda \int \| \nabla U \|^2$$

[P. Cachier et al, MICCAI 2001]

Min. C_1 : gradient descent
Min. C_2 : closest point
Min. U : explicit solution (convolution+spline)

Three Sulcal Lines

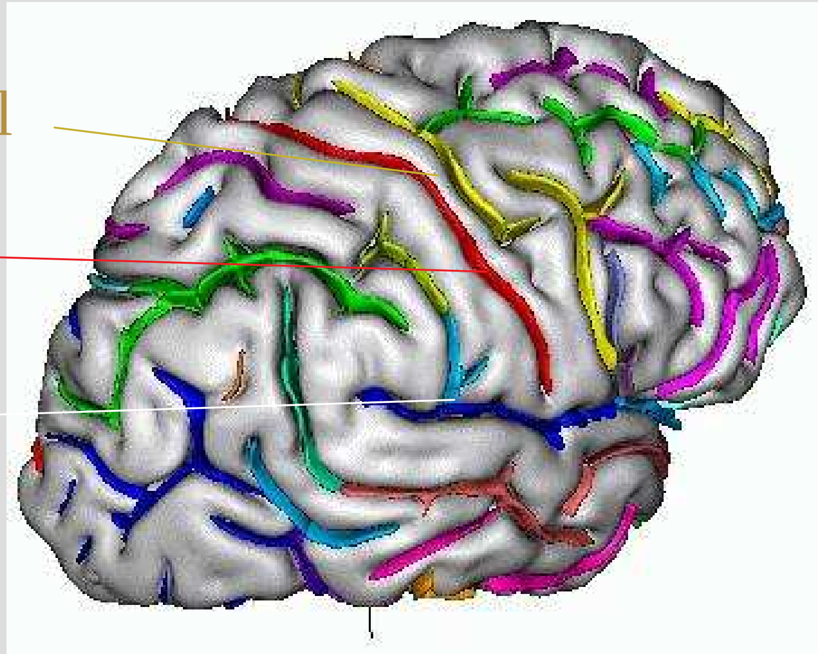

[Rivière *et al.*00]

Results with 5 subjects

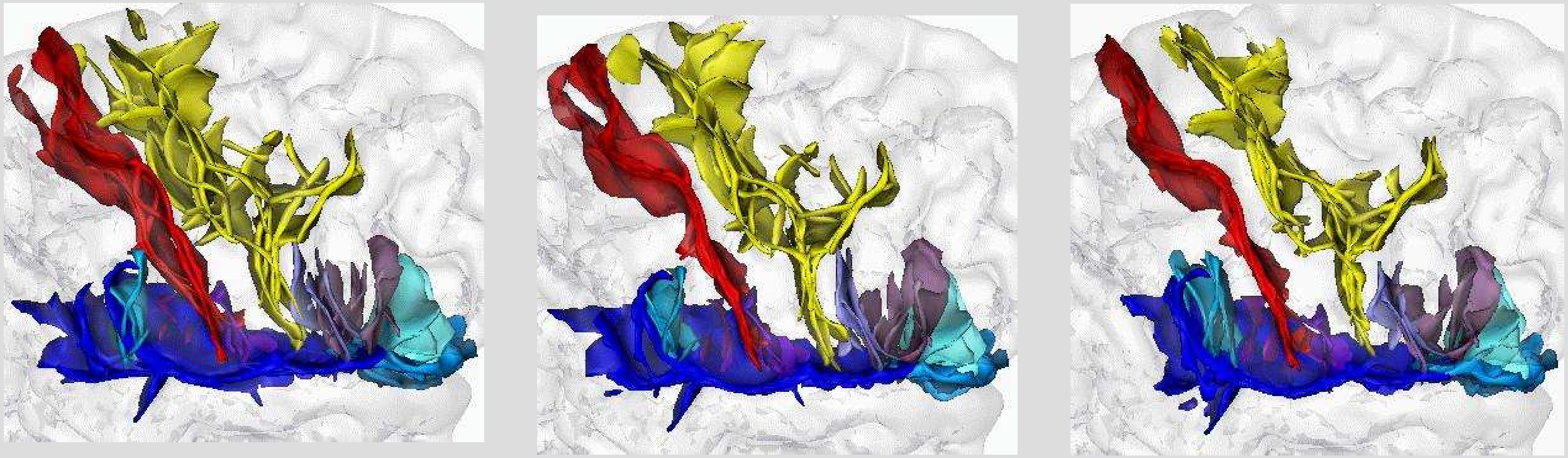

Affine Initialization Iconic Iconic + Geometric

P. Cachier, J.-F. Mangin, X. Pennec, D. Rivière, D. Papadopoulos, J. Régis, N. Ayache
Multisubject Non-Rigid Registration of Brain MRI using Intensity and Geometric Features.
MICCAI'01, LNCS vol 2208, 734-742, 2001.

Results with 5 subjects

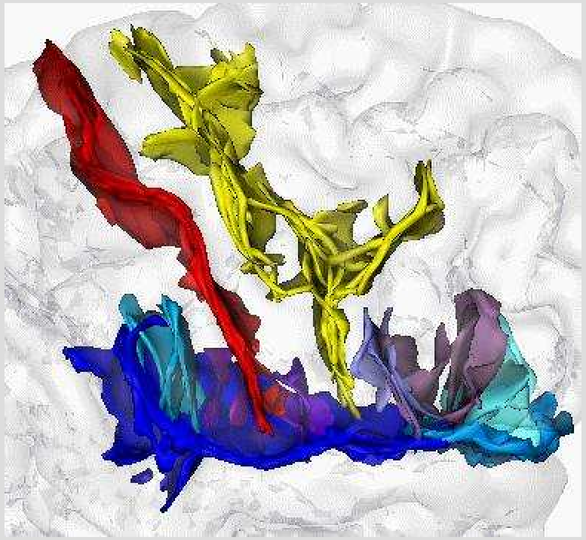

A Iconic + Geometric

P. Cachier, J.-F. Mangin, X. Pennec, D. Rivière, D. Papadopoulos, J. Régis, N. Ayache
Multisubject Non-Rigid Registration of Brain MRI using Intensity and Geometric Features.
MICCAI'01, LNCS vol 2208, 734-742, 2001.

Results with 5 subjects

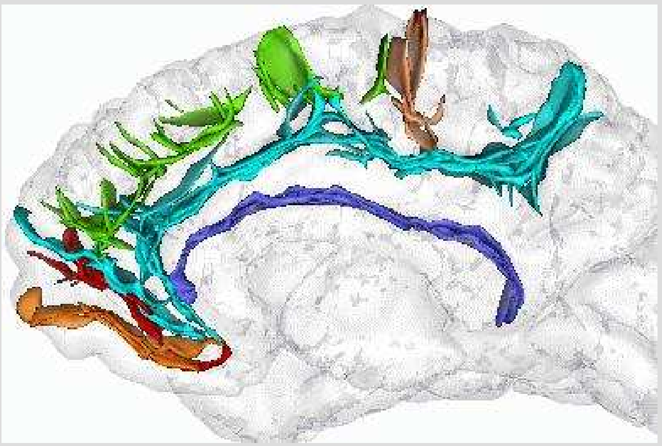

Iconic + Geometric

P. Cachier, J.-F. Mangin, X. Pennec, D. Rivière, D. Papadopoulos, J. Régis, N. Ayache
Multisubject Non-Rigid Registration of Brain MRI using Intensity and Geometric Features.
MICCAI'01, LNCS vol 2208, 734-742, 2001.

Content

- Geometric
- Iconic (Monomodal, Multimodal)
- Hybrid
  - Geometric&Iconic;
  - Bloc Matching:
  - Piecewise parametric

Histological Atlases

- Built from histological 2-D cross-sections
  - microscopic, macroscopic optical images
  - autoradiographies
- Fusion with 3-D medical images
  - for localisation or validation purposes

S. Ourselin, A. Roche, G. Subsol, X. Pennec, and N. Ayache. Reconstructing a 3D Structure from Serial Histological Sections. Image and Vision Computing, 19(1-2):25--31, January 2001.

Mapawamo Project

- Objectives
  - Mapping visual cortical regions in awake, behaving monkey using functional MRI
  - Compare fMRI results with standard metabolic mapping (ground truth) : double label 2deoxyglucose - 2DG

- Coordinator: G. Orban (Louvain), partners involve Odyssée, Epidaure,...
- Work of S. Ourselin, E. Bardinet, G. Malandain (Epidaure/INRIA)

Two registration problems

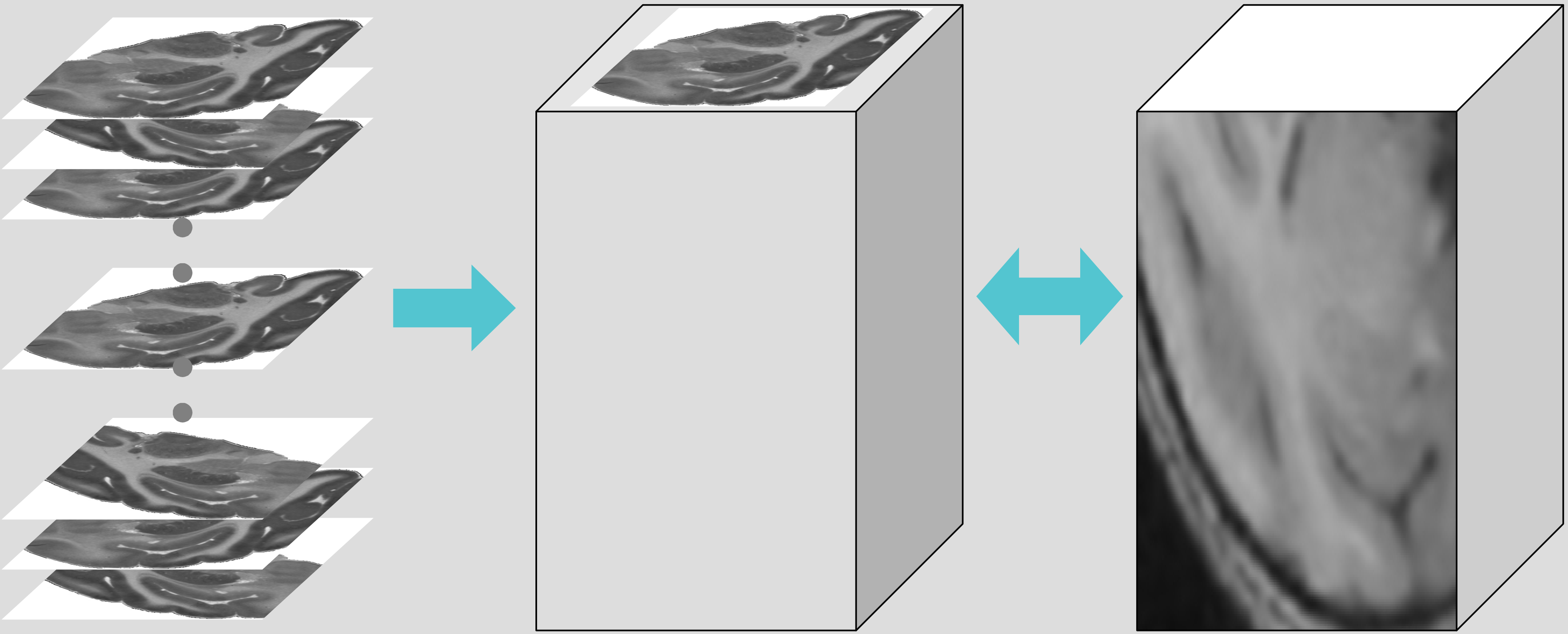

2-D -->3D
autoradiographies

3-D Autoradiographies &
3-D Anatomy Fusion

Registration by Block Matching

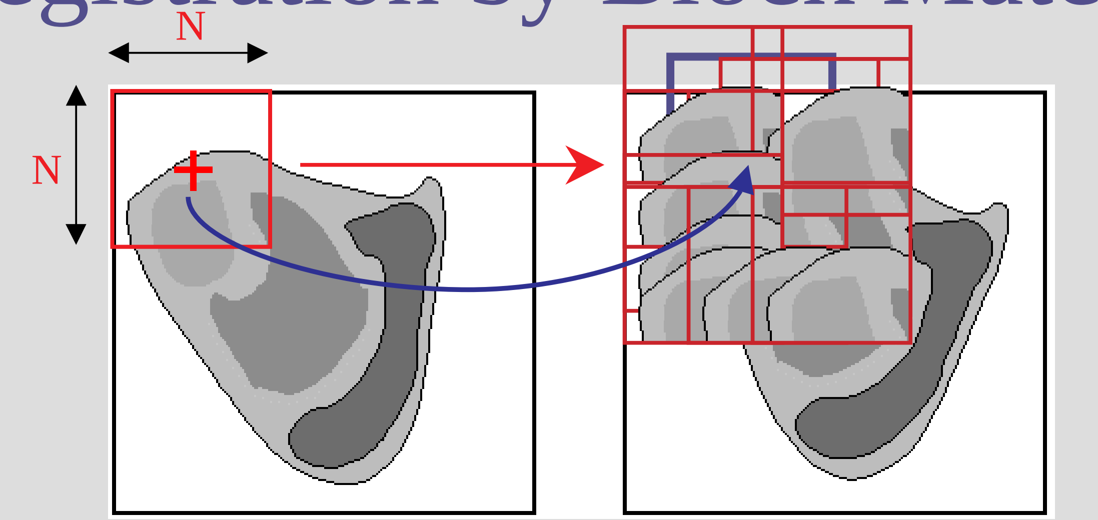

[

floating image I_1 *reference image I_2*

Sébastien Ourselin Thesis
Ourselin et al., IVC 2000

Following Z. Zhang et al.

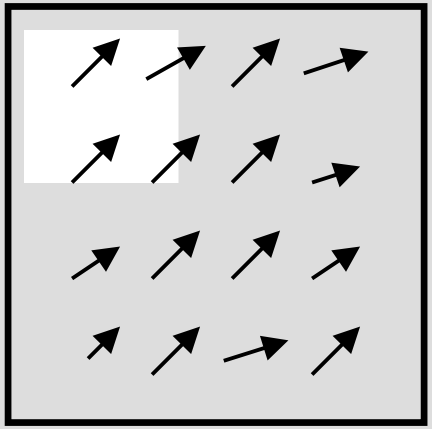

Displacement field

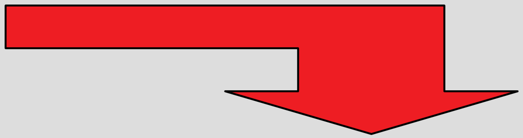

Robust & Multiscale Estimate of

Rigid /Affine **Global transformation**

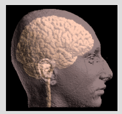

Alignment results

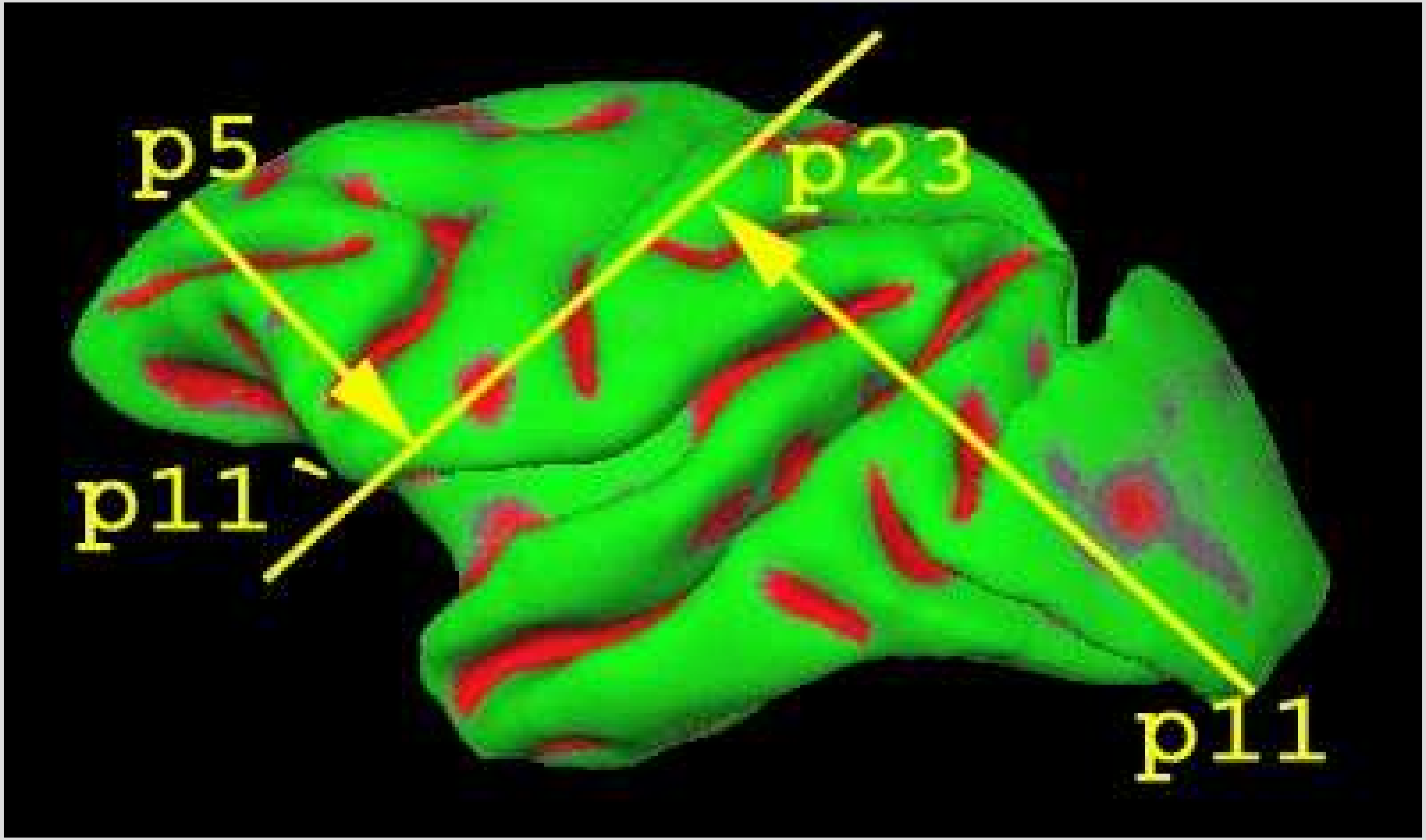

Posterior part

14C

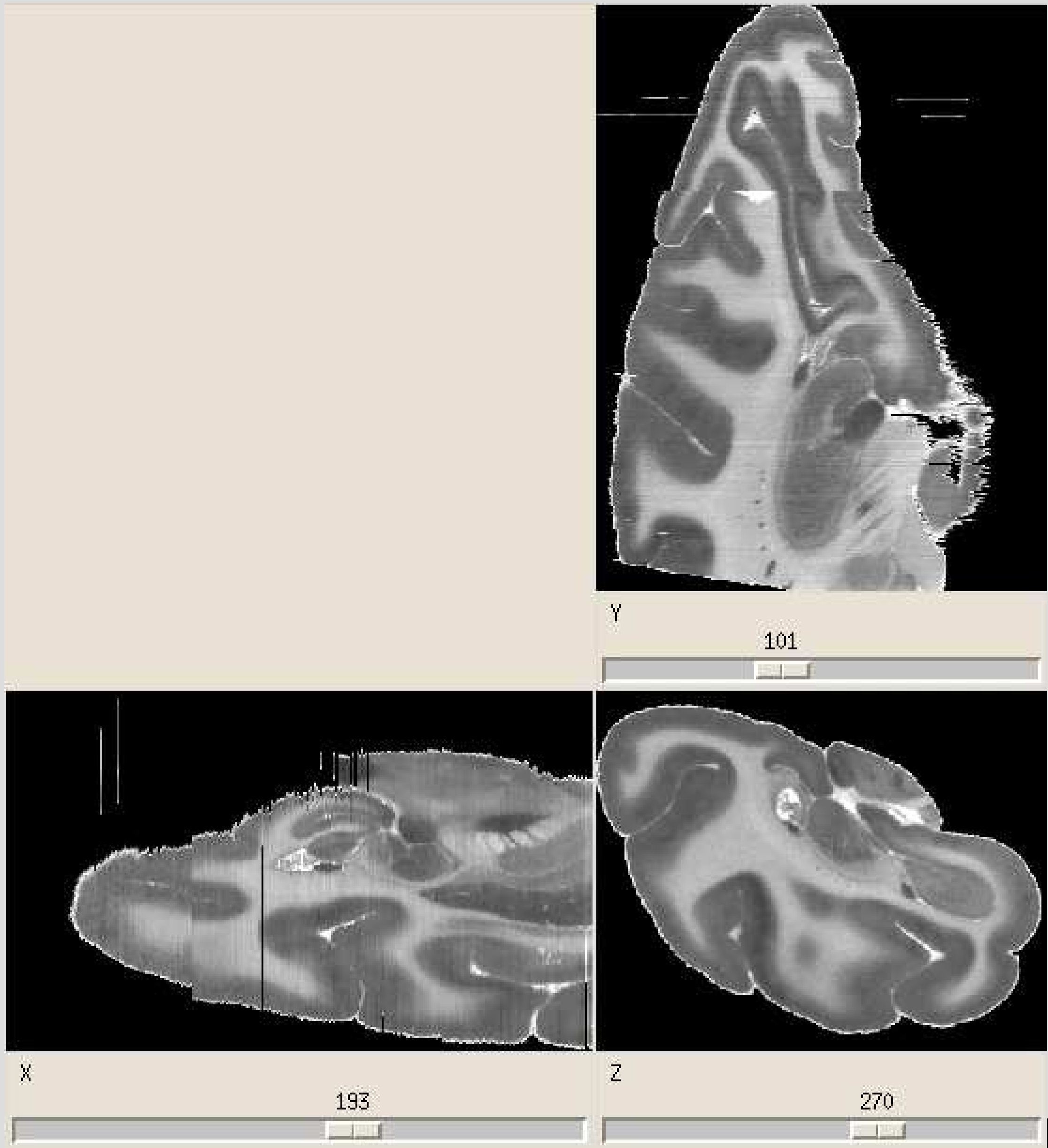

Anterior part

14C

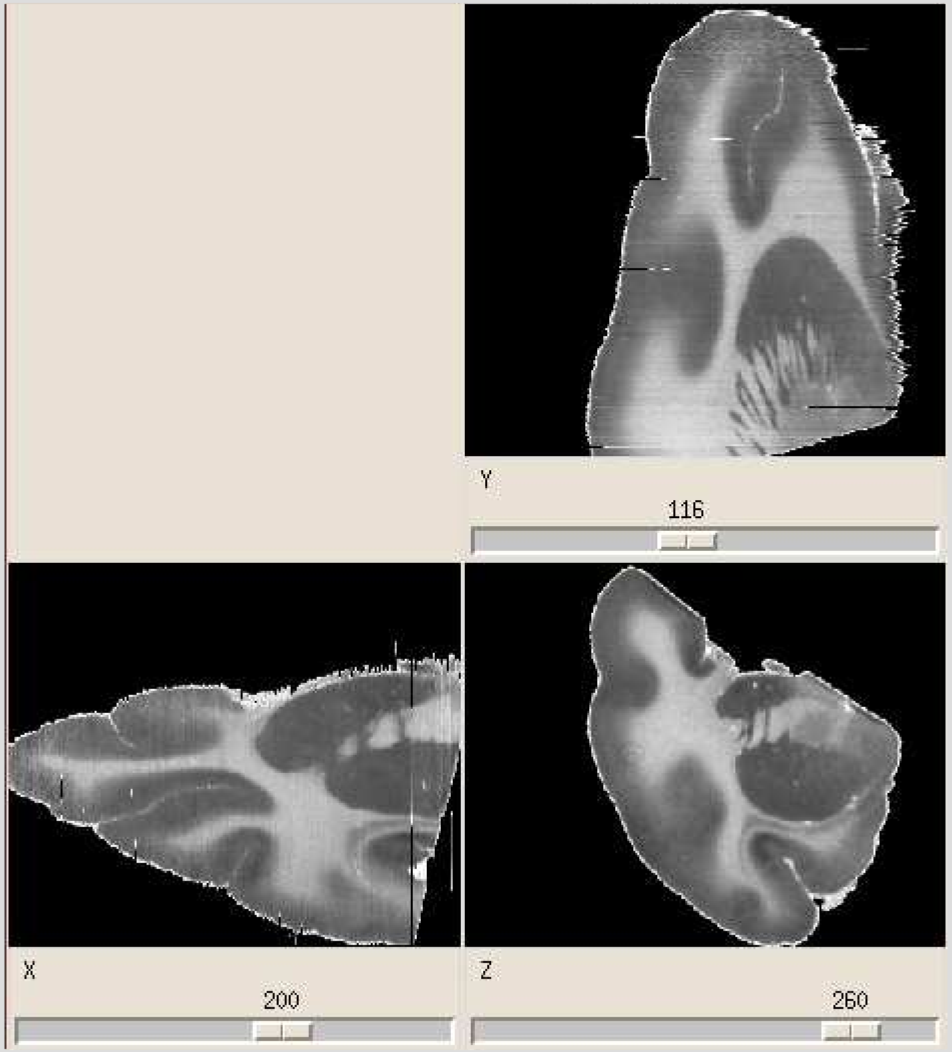

MRI / Autoradiography Registration

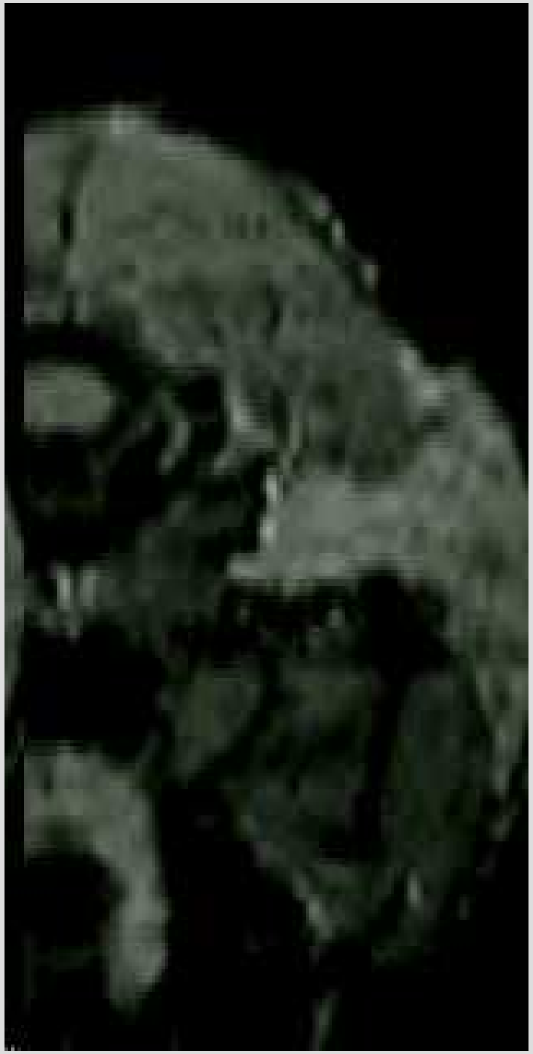

E. Bardinet, G. Malandain
Mapawamo Project

New Atlas of Deep Nuclei

- Built from histological cross-sections
- Fused with post-mortem MRI

(INRIA & Inserm U 289, Pitié-Salpêtrière)

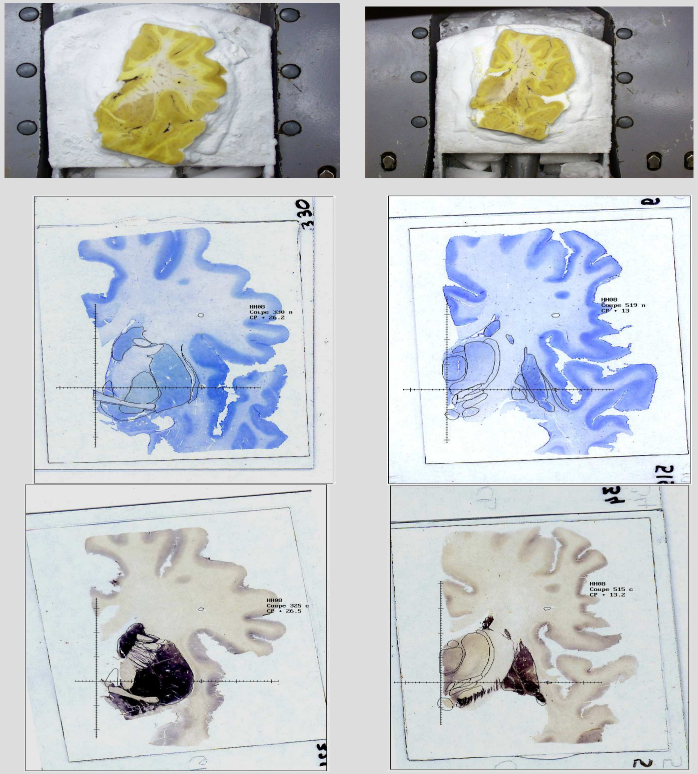

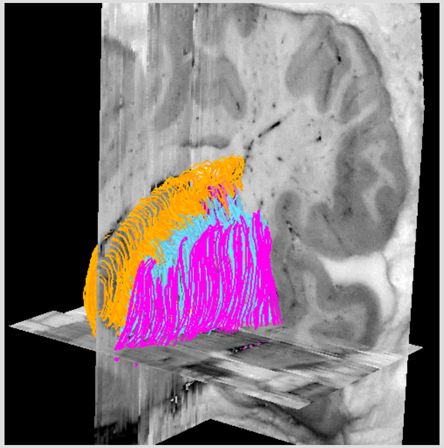

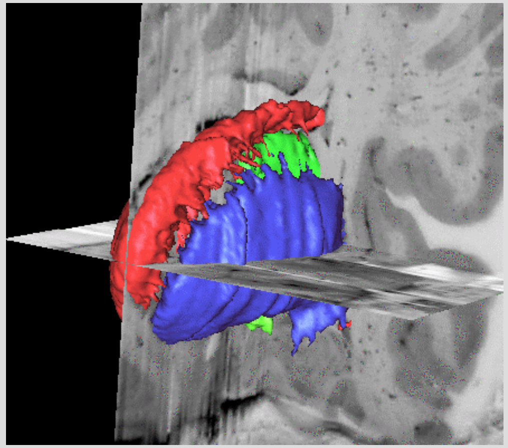

S.Ourselin,E.Bardinet, J.Yelnik D.Dormont et al.,MICCAI’01

Content

- Geometric
- Iconic (Monomodal, Multimodal)
- Hybrid
  - Geometric&Iconic;
  - Bloc Matching:
  - Piecewise parametric

Piecewise Affine Registration

- Hierarchical Clustering
- …Not a diffeomorphism

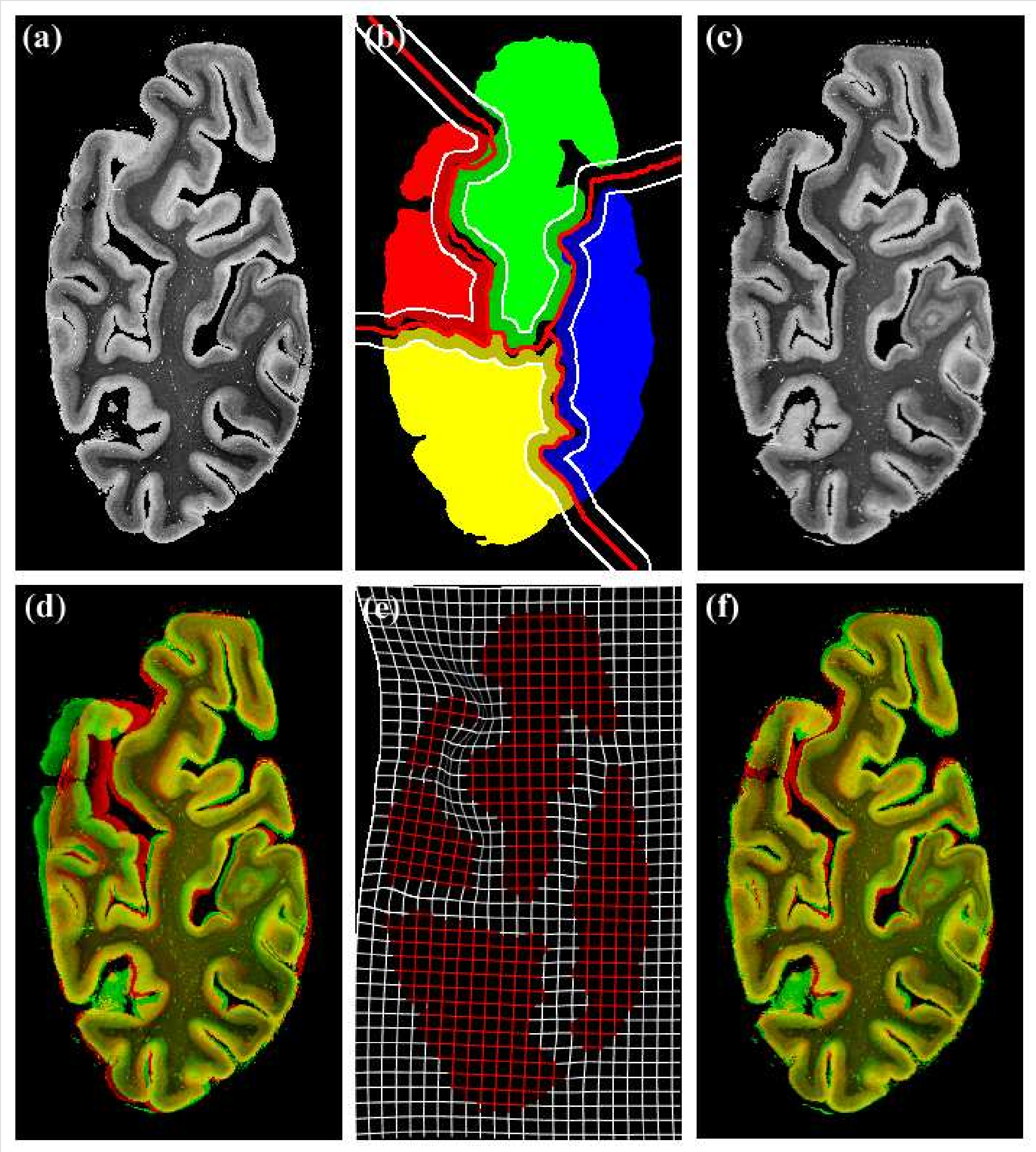

Pitiot, Bardinet
Thompson, Malandain
WBIR'03, Philadelphia

Polyrigid Transformations

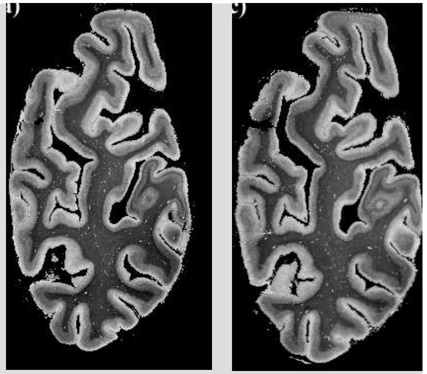

- N Components:
  - Local Rigid transformation : $T_i(x) = R_i.x + t_i$
  - Gaussian spatial influence
    - – anchor point : a_i
    - – local weight : p_i
    - – influence distance : σ_i

$$w_i(x) = p_i.G_{(a_i,\sigma_i)}(x)$$

- Direct averaging of transformations is not invertible

$$T(x) = \frac{\sum_i w_i(x) T_i(x)}{\sum_i w_i(x)}$$

V.Arsigny, X. Pennec, N. Ayache. *Polyrigid and Polyaffine Transformations: a New Class of Diffeomorphisms for Locally Rigid or Affine Registration.* MICCAI, LNCS 2879, 829--837, 2003

Polyrigid Transformations

- for each rigid component, the trajectory satisfies the following ODE ($A_i = \log(R_i)$):

$$\dot{x}(s) = V_i(x, s) = t_i + A_i(x - s\,t_i) \text{ for } s \in [0, 1]$$

- Idea : averaging *speed vectors :*

$$\dot{x}(s) = V(x, s) = \frac{\sum_i w_i(x) V_i(x, s)}{\sum_i w_i(x)}$$

- Global transformation found by integration :
  - diffeomorphism regular with respect to each parameter

Polyrigid Transformations

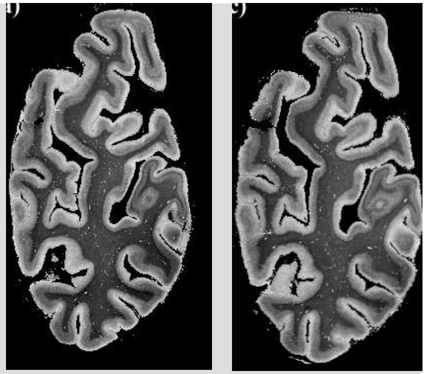

- 4 Rigid Components
- Optimized by Gradient Descent (ITK)

Difference images

Rigid registration

Affine registration

vs.

PRT registration

PRT deformed grid

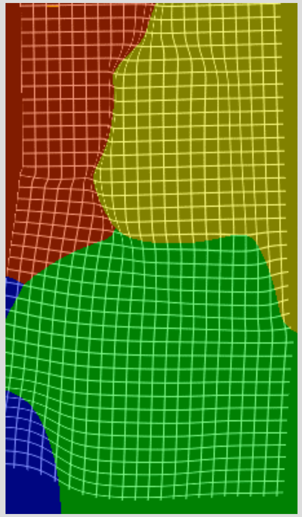

V.Arsigny, X. Pennec, N. Ayache. *Polyrigid and Polyaffine Transformations: a New Class of Diffeomorphisms for Locally Rigid or Affine Registration.* MICCAI, LNCS 2879, 829--837, 2003
Special Issue of Medical Image Analysis Journal on ITK, 2005

Content

- Geometric
- Iconic (Monomodal, Multimodal)
- Hybrid
- Shape Statistics
  - Revisiting Regularization
  - Statistics on Sulcal Lines

Revisiting Regularization

$$E(C,U,\dot{U}) = E_S(I,J,C) + \sigma\int \| C - U \|^2$$

$$\boxed{+\lambda\int \| \nabla U \|^2 + \mu\int \left\| \nabla \dot{U} \right\|^2}$$

- Modulate regularization as a function of
  - 1- local information (presence of texture/edges)
  - 2- local variability (statistics on anatomy)

R. Stefanescu, X. Pennec , N. Ayache, *Grid Powered Nonlinear Image Registration with Locally Adaptive Regularization*, Medical Image Analysis, Sept 2004 (also MICCAI'03)

1.Non Stationary *Fluid* Regularization

Inspired from non-stationary image diffusion

• Weickert 1997, 2000

$$\frac{\partial \dot{U}}{\partial t} = (1-k)\Delta \dot{U}$$

Confidence in the correction field

• k ~ 1 for edges (driving forces)

• k ~ 0 for uniform regions (interpolation)

0,05

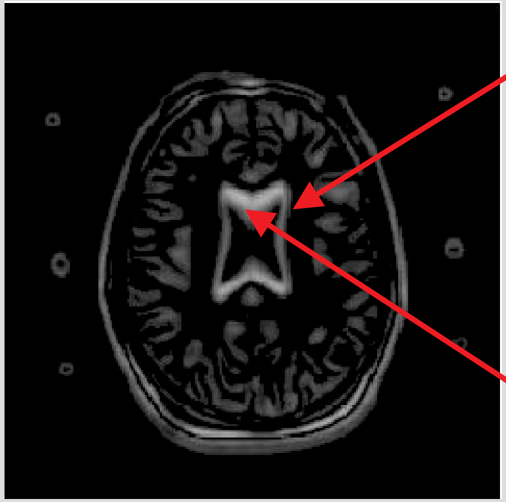

0,65

•Used to model pathologies (e.g. tumors)

Patient with Pathology

Fuzzy segmentation of the resection

Confidence

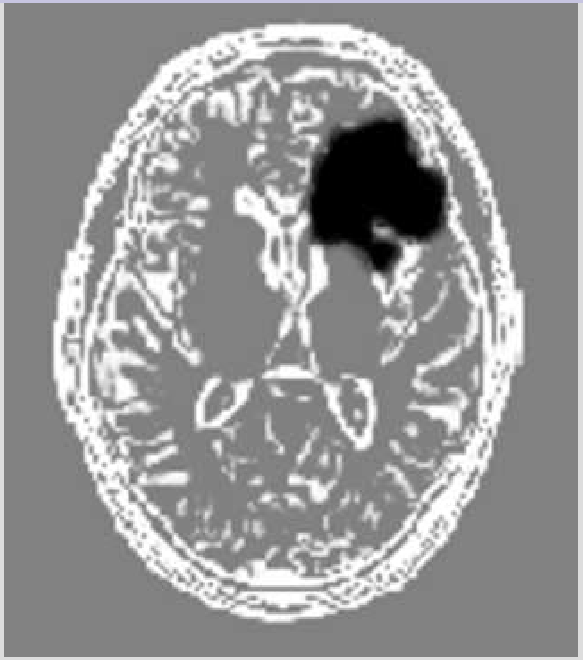

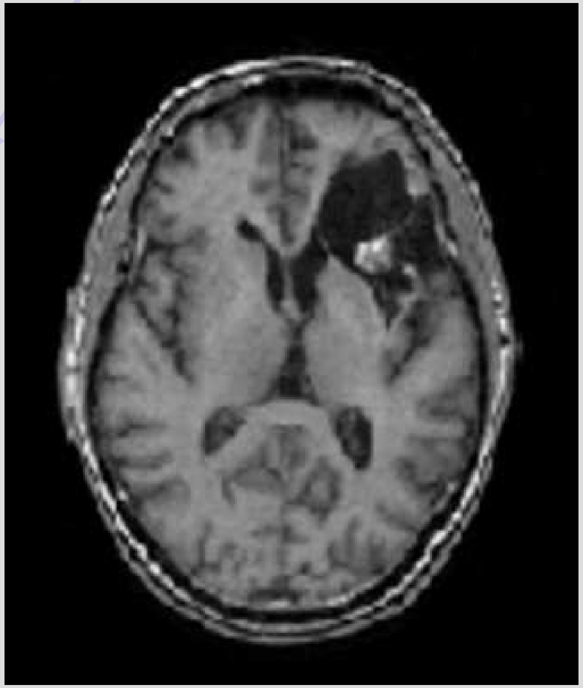

Low confidence values in the resection region

Patient T1-MRI

Atlas and Patient with Pathology

Initialization: affine registration maximizing the correlation ratio

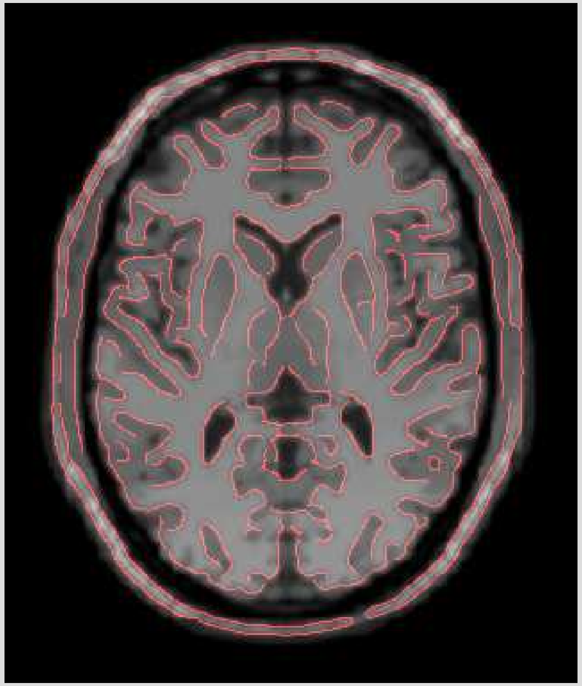

Atlas

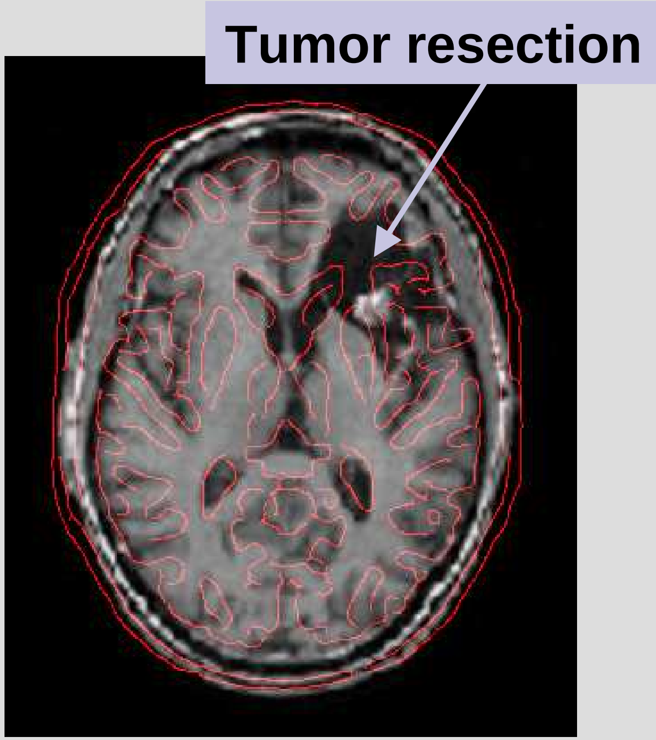

Patient T1-MRI

R. Stefanescu, O. Commowick, G. Malandain, P.-Y. Bondiau, N. Ayache, and X. Pennec. Non-Rigid Atlas to Subject Registration with Pathologies for Conformal Brain Radiotherapy. MICCAI'04, 2004.

Data courtesy of Dr. Pierre-Yves Bondiau, M.D., Centre Antoine Lacassagne, Nice, France

Registration Result

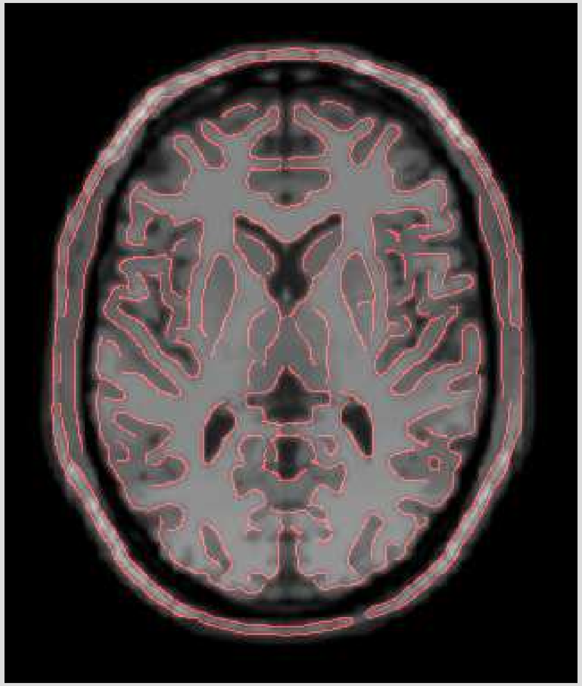

Atlas

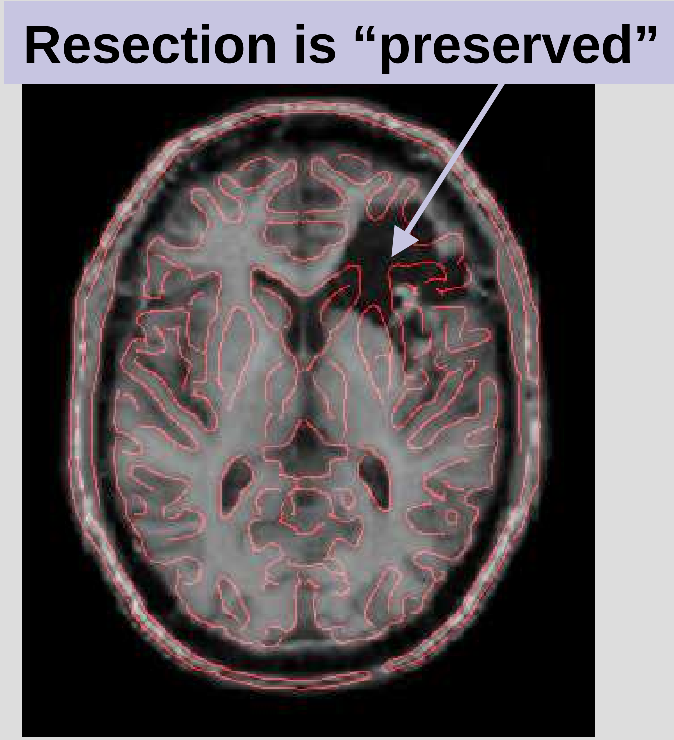

Patient T1-MRI

R. Stefanescu, O. Commowick, G. Malandain, P.-Y. Bondiau, N. Ayache, and X. Pennec. Non-Rigid Atlas to Subject Registration with Pathologies for Conformal Brain Radiotherapy. MICCAI’04, 2004.

Data courtesy of Dr. Pierre-Yves Bondiau, M.D., Centre Antoine Lacassagne, Nice, France

Classical (wrong) Registration

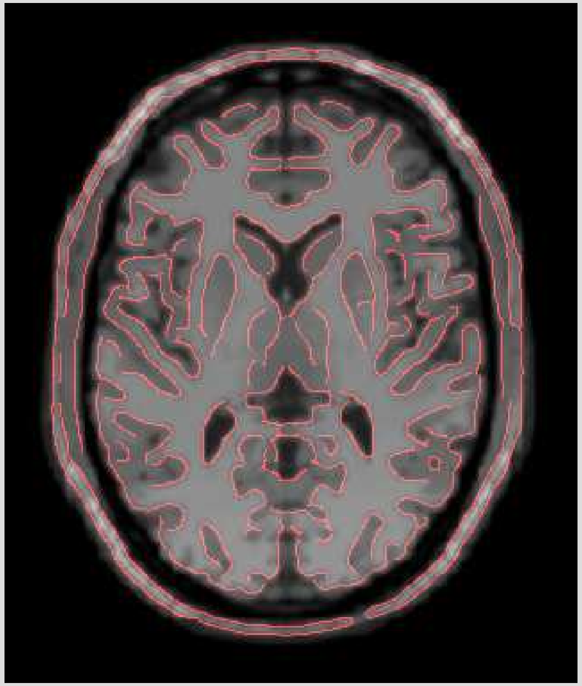

Atlas

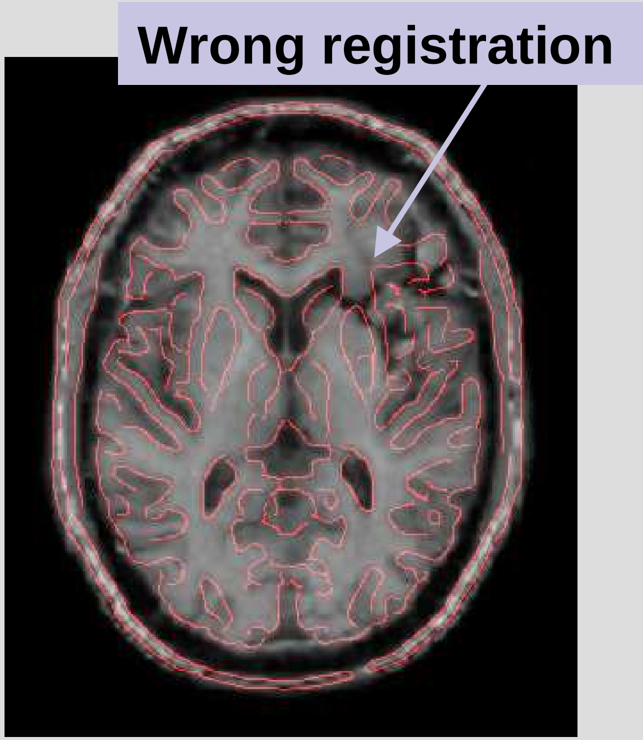

Patient T1-MRI

R. Stefanescu, O. Commowick, G. Malandain, P.-Y. Bondiau, N. Ayache, and X. Pennec. Non-Rigid Atlas to Subject Registration with Pathologies for Conformal Brain Radiotherapy. MICCAI'04, 2004.

Data courtesy of Dr. Pierre-Yves Bondiau, M.D., Centre Antoine Lacassagne, Nice, France

2- Non Stationary *Elastic* Regularization

$$\frac{\partial U}{\partial t} = div(D \nabla (U))$$

D encodes a priori variability

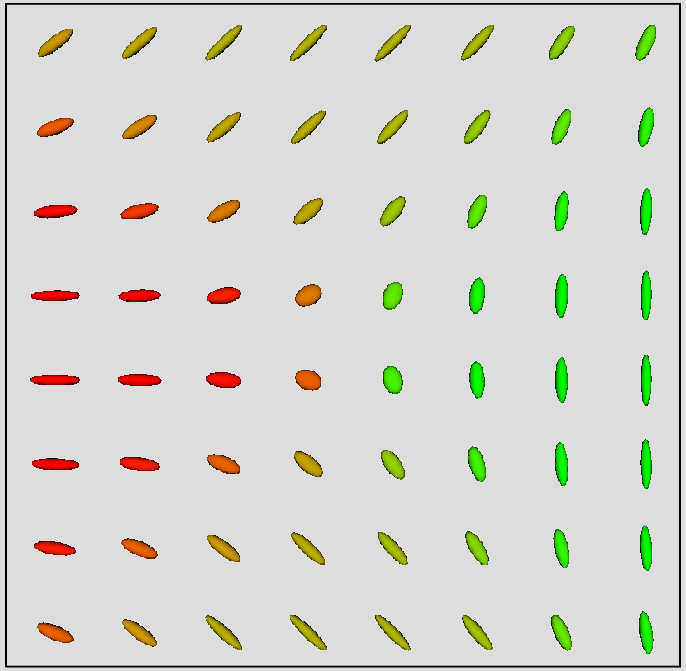

Algorithm Complexity

- Parallel implementation on cluster of PC's
  - Efficient parallel AOS scheme for diffusion PDEs:
  - Image size: 256x256x124
  - 15 PC's: 2GHz, Pentium IV processors
  - Execution time: 5 minutes

R. Stefanescu, X. Pennec, and N. Ayache. A Grid Service for the Interactive Use of a Parallel Non-Rigid Registration Algorithm of Medical Images. Methods of Information in Medicine, In Press, 2004

Content

- Geometric
- Iconic (Monomodal, Multimodal)
- Hybrid
- Shape Statistics
  - Revisiting Regularization
  - Statistics on Sulcal Lines

Statistics on Sucal Lines

- Goal:
  - Learn local brain variability from sulci
  - Better constrain inter-subject registration
  - Correlate this variability with age, pathologies

Collaborative work between Epidaure (INRIA) and LONI (UCLA)
V. Arsigny, N. Ayache, P. Fillard, X. Pennec and P. Thompson

Computation of Average Sulci

- Alternate minimization of global variance
  - Dynamic programming to match the mean to instances
  - Gradient descent to compute the mean curve position

Arsigny et al. 2004, to appear

red : mean curve
green et yellow : ~80 instances of 72 sulci

Sylvius Fissure

Covariance Tensors

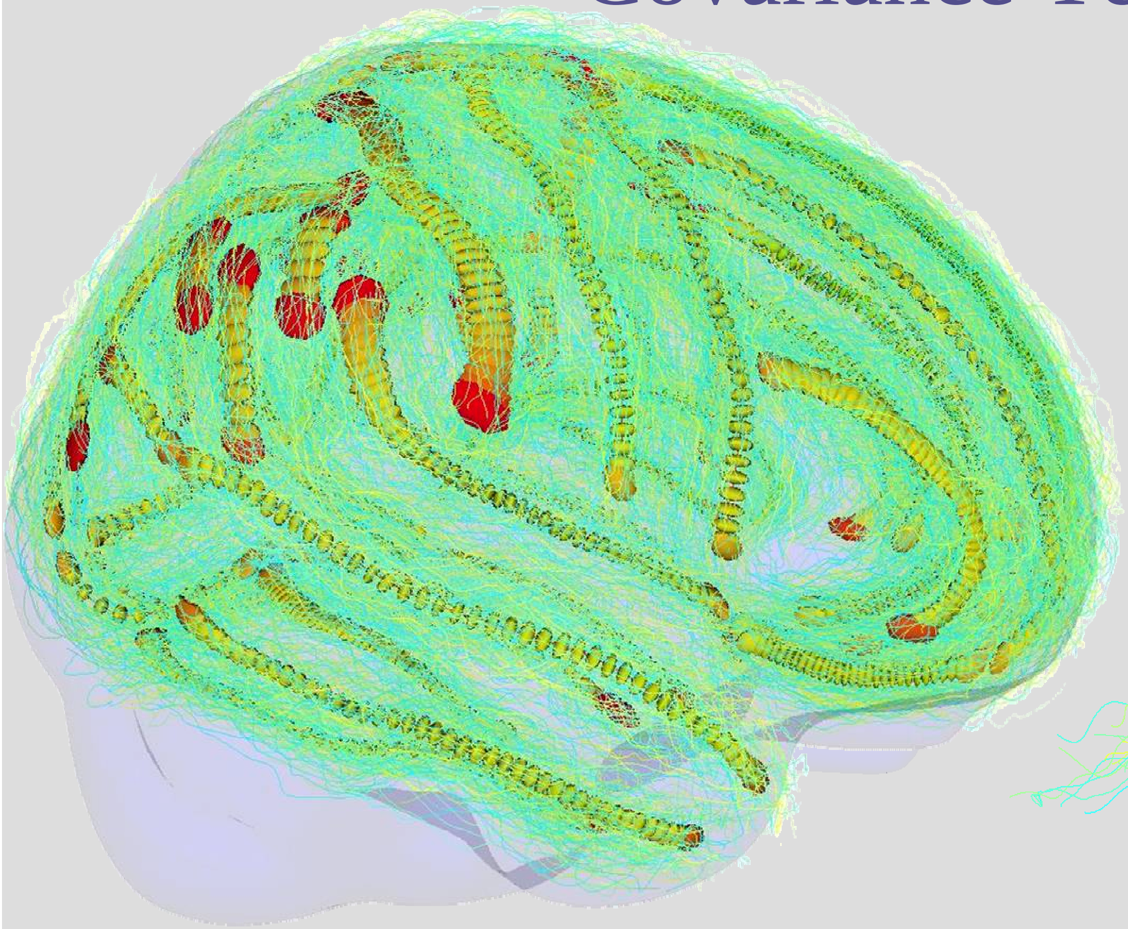

Color codes Trace

Currently:

80 instances of 72 sulci

About 1250 tensors

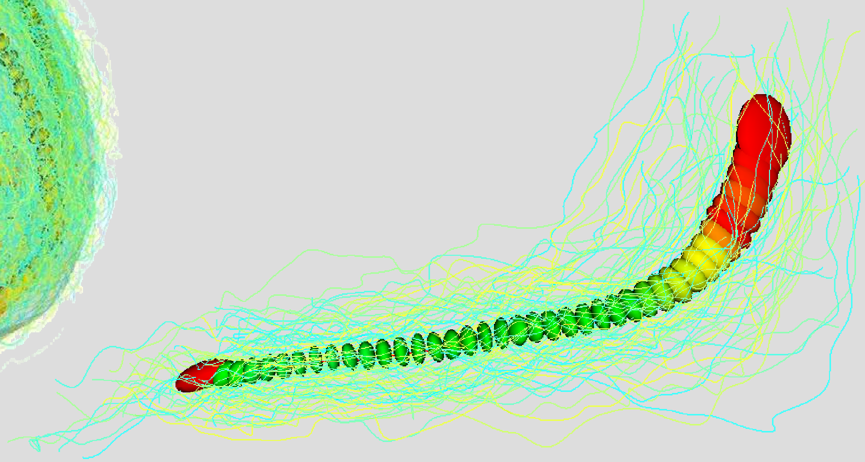

Covariance Tensors along Sylvius Fissure

Fillard, Pennec, Ayache, Thompson, 2004, to appear

Tensor Computing

- Tensors = Symmetric Definite Positive Matrices
- Various operations
  - regularization, interpolation, compression, extrapolation
  - statistical comparisons
- Previous work includes Statistics on Manifolds and Tensor Computations
  - Skovgaard84, Pennec96&99&04, Pennec-Ayache98, Forstner-Moonen99, Poupon00, Alexander01, Tschumperlé02, Chefd'hotel02&04, Lenglet04, Coulon04, Fletcher-Joshi04, etc.

Affine Invariant Metric

- Action of Linear Group GL_n

$$\forall A \in GL_n,\ A * \Sigma = A \Sigma A^T$$

- Affine Invariant Distance

$$dist(A * \Sigma_1, A * \Sigma_2) = dist(\Sigma_1, \Sigma_2), \forall A \in GL_n$$

Scalar product on $\boldsymbol{T_{Id}M}$:

$$\langle W_1 \mid W_2 \rangle_{Id} \stackrel{def}{=} Tr\left(W_1^T W_2\right) = Tr\left(W_1 W_2\right)$$

$$W_1, W_2 \in T_{Id} M$$

on $\boldsymbol{T_\Sigma M}$:

$$\langle W_1 \mid W_2 \rangle_\Sigma \stackrel{def}{=} \left\langle \Sigma^{-1/2} * W_1, \Sigma^{-1/2} * W_2 \right\rangle_{Id}$$

X Pennec,P.Fillard,N.Ayache:A Riemannian Framework for Tensor Computing, Research Report 5255, INRIA, July 2004

Exponential and Logarithmic Maps

- Geodesics $\Gamma_{Id,W}(t) = \exp(tW)$

  - Exponential Map :

$$\exp_\Sigma(\overrightarrow{\Sigma\Psi}) = \Sigma^{1/2} \exp(\Sigma^{-1/2}.\overrightarrow{\Sigma\Psi}.\Sigma^{-1/2})\Sigma^{1/2}$$

  - Logarithmic Map :

$$\log_\Sigma(\Psi) = \Sigma^{1/2} \log(\Sigma^{-1/2}.\Psi.\Sigma^{-1/2})\Sigma^{1/2}$$

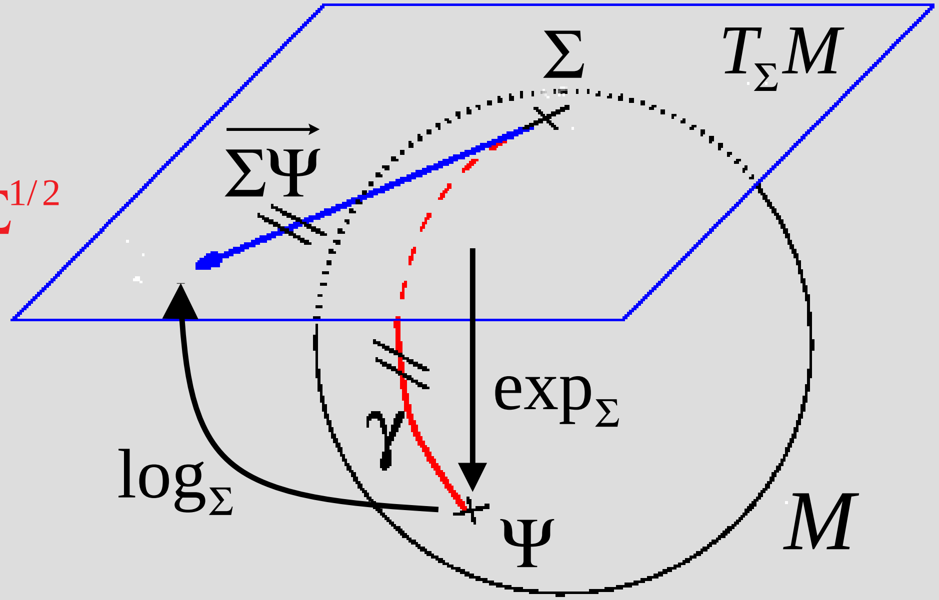

$$\boxed{dist(\Sigma,\Psi)^2 = \left\langle \overrightarrow{\Sigma\Psi} \mid \overrightarrow{\Sigma\Psi} \right\rangle_\Sigma = \left\| \log(\Sigma^{-1/2}.\Psi.\Sigma^{-1/2}) \right\|_{L_2}^2}$$

Linear vs. Riemannian Interpolation

Interpolation of the coefficients:

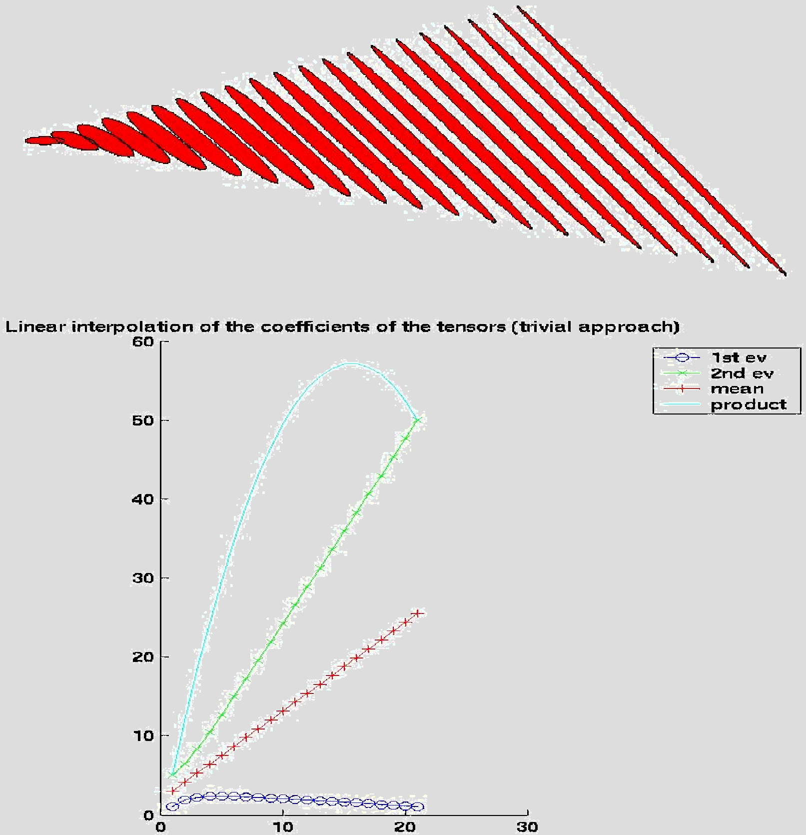

Interpolation achieved with the Riemannian metric:

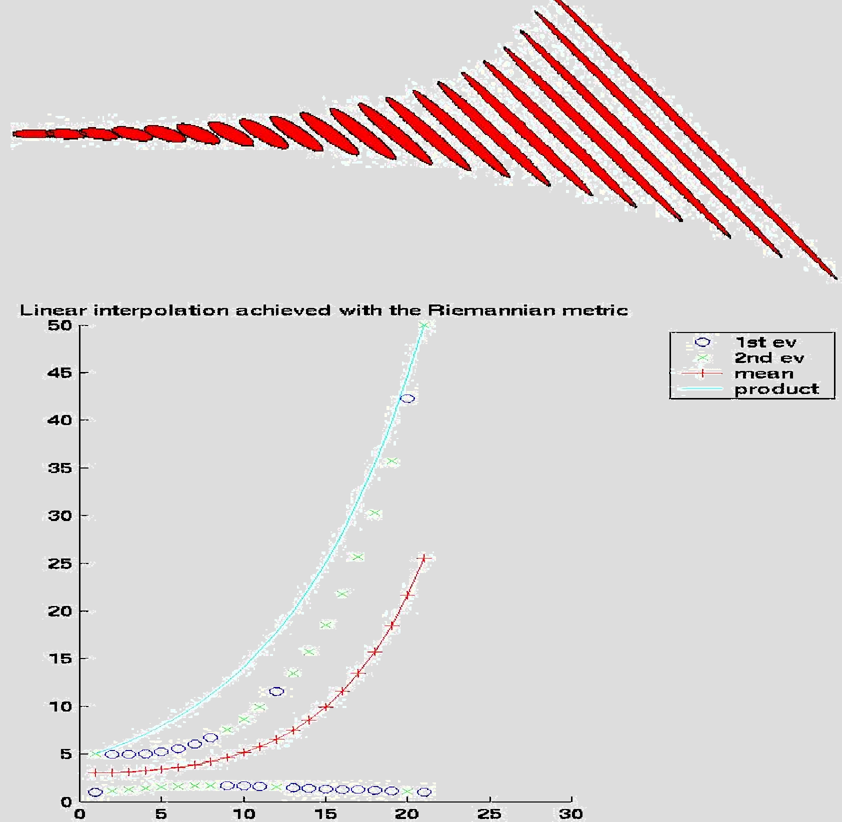

Epidaure

Compressed Tensor Representation

- Mean sulcal line + 4 covariance matrices
  - optimize for the 4 most representative tensors
  - Interpolation in-between, extrapolation outside (removes outliers)

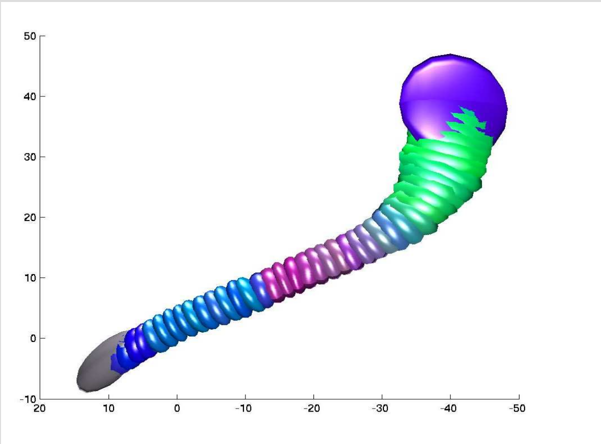

Raw estimation

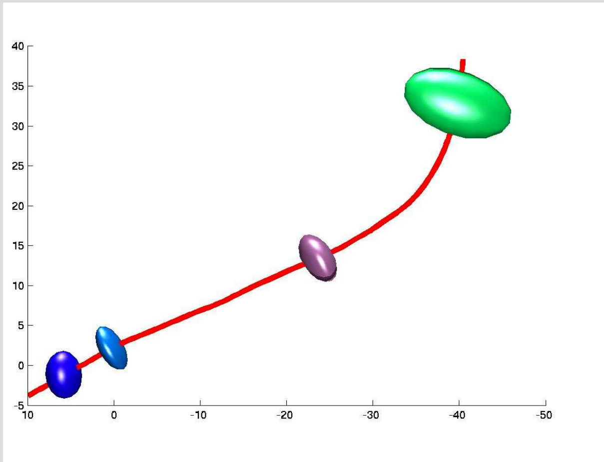

The 4 most representative tensors.

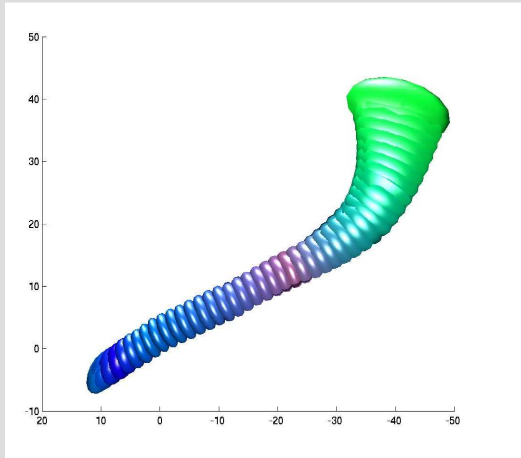

Interpolation from the 4 tensors.

Sylvian fissure

Compressed Tensor Representation

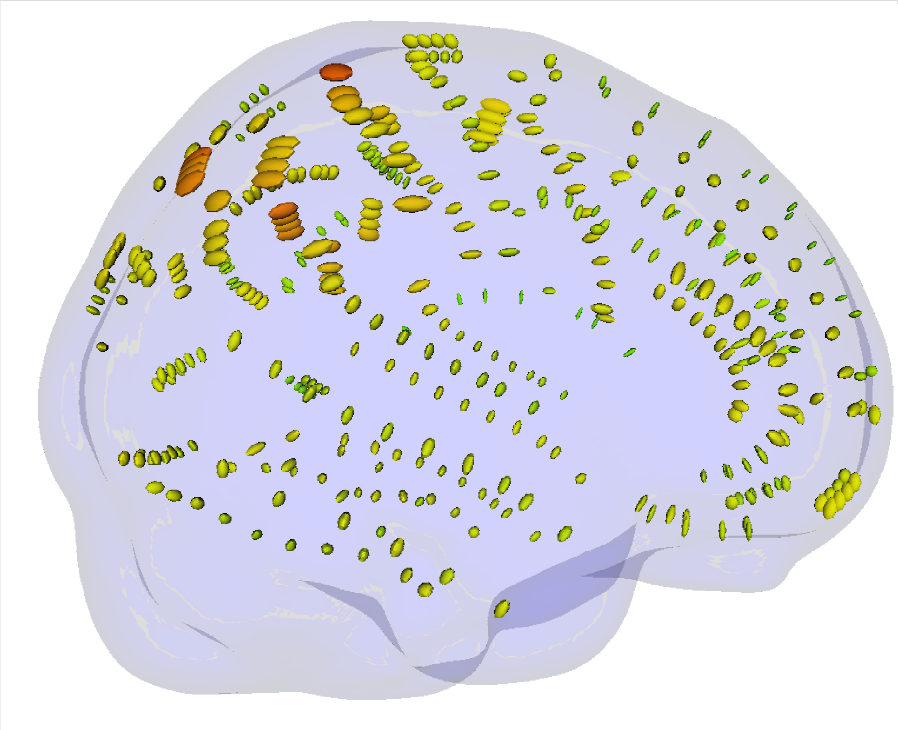

Representative Tensors (250)

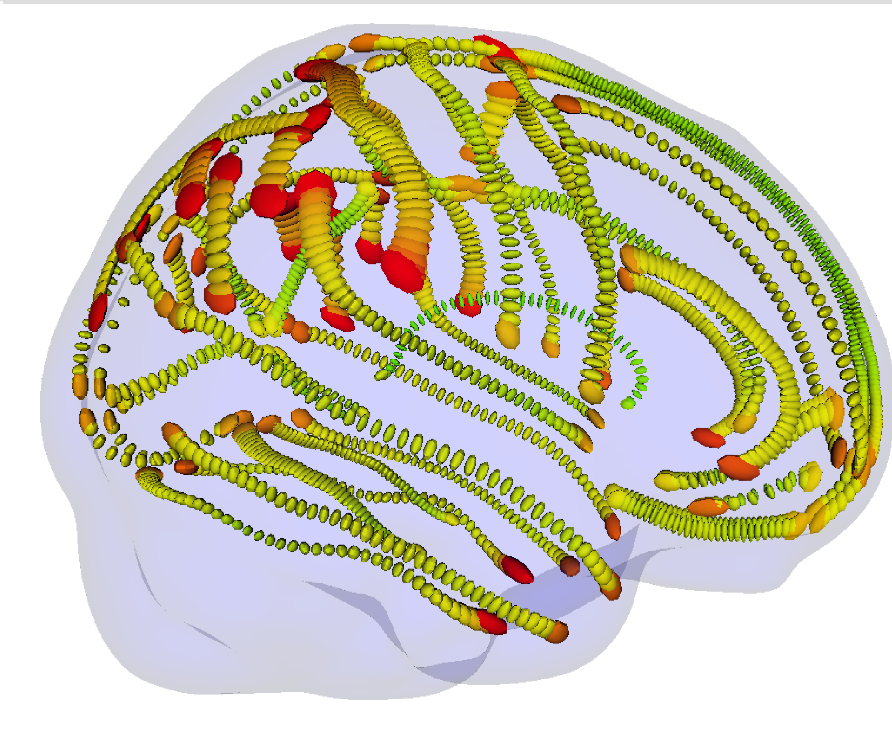

Reconstructed Tensors (1250)
(Riemannian Interpolation)

Fillard-Pennec-Thompson-Ayache 2004, to appear

Variability Tensors

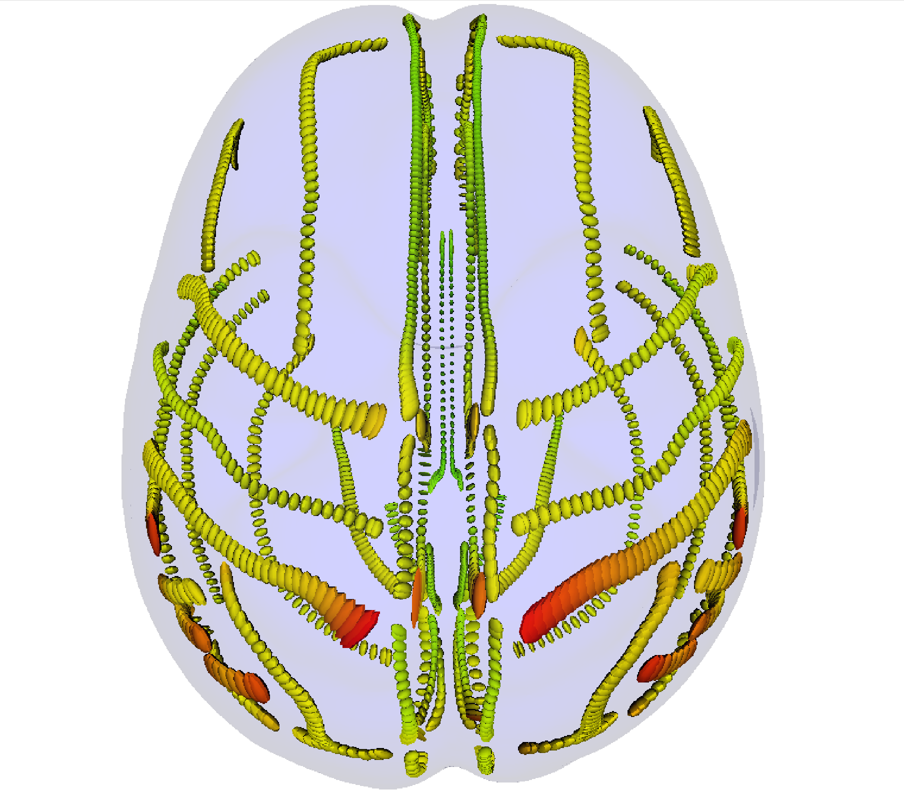

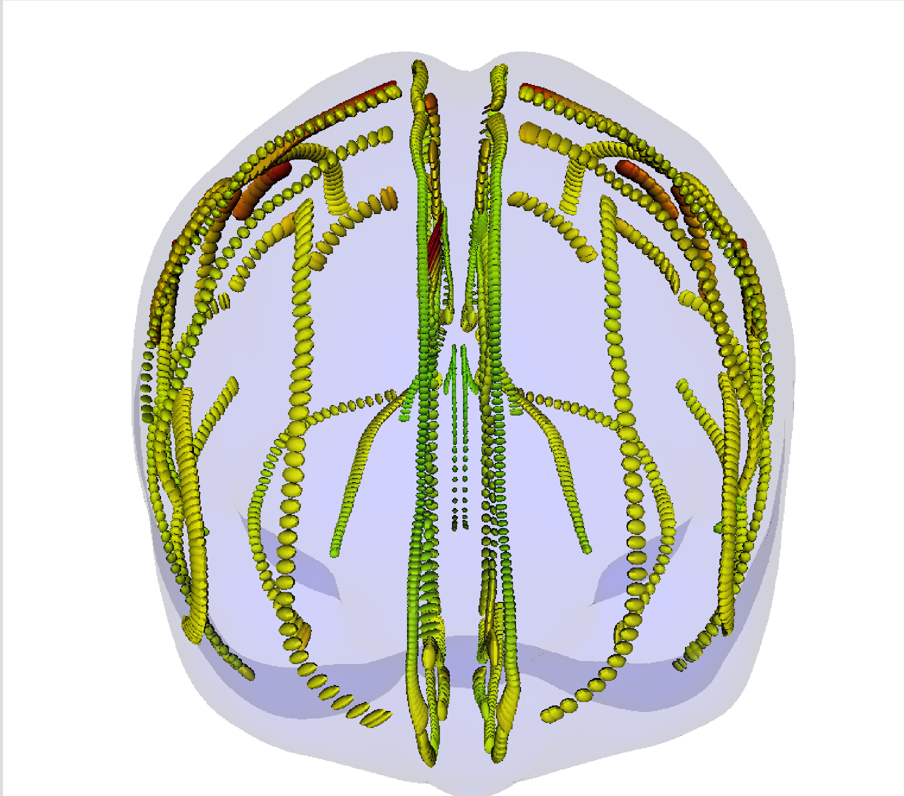

Color codes tensor trace

Fillard-Pennec-Thompson-Ayache 2004, to appear

Asymmetry Measure

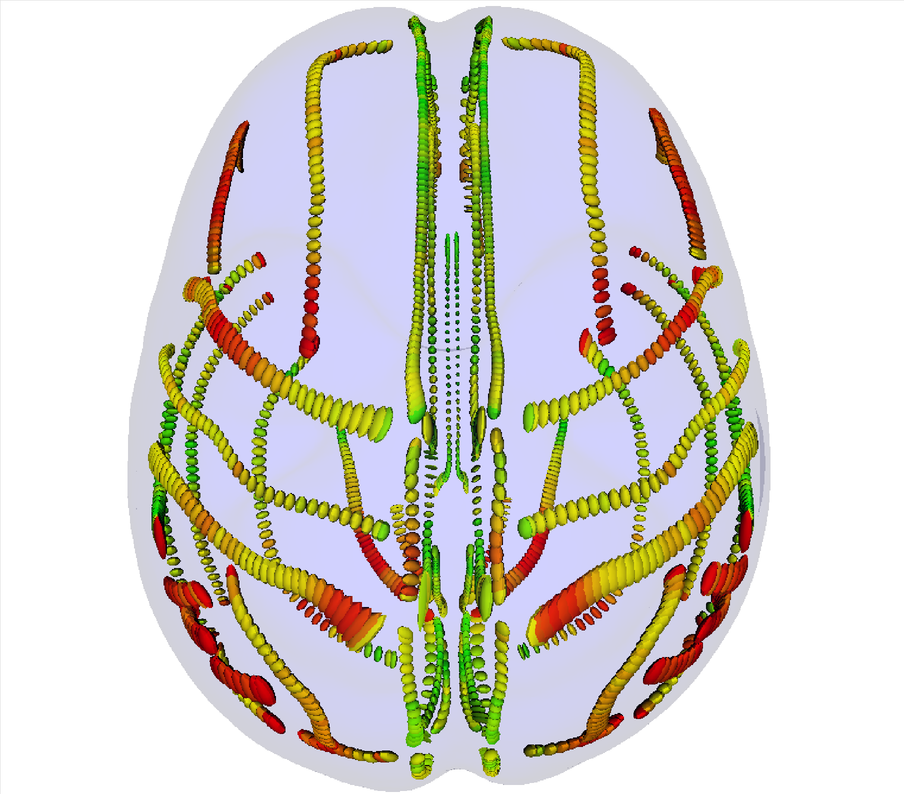

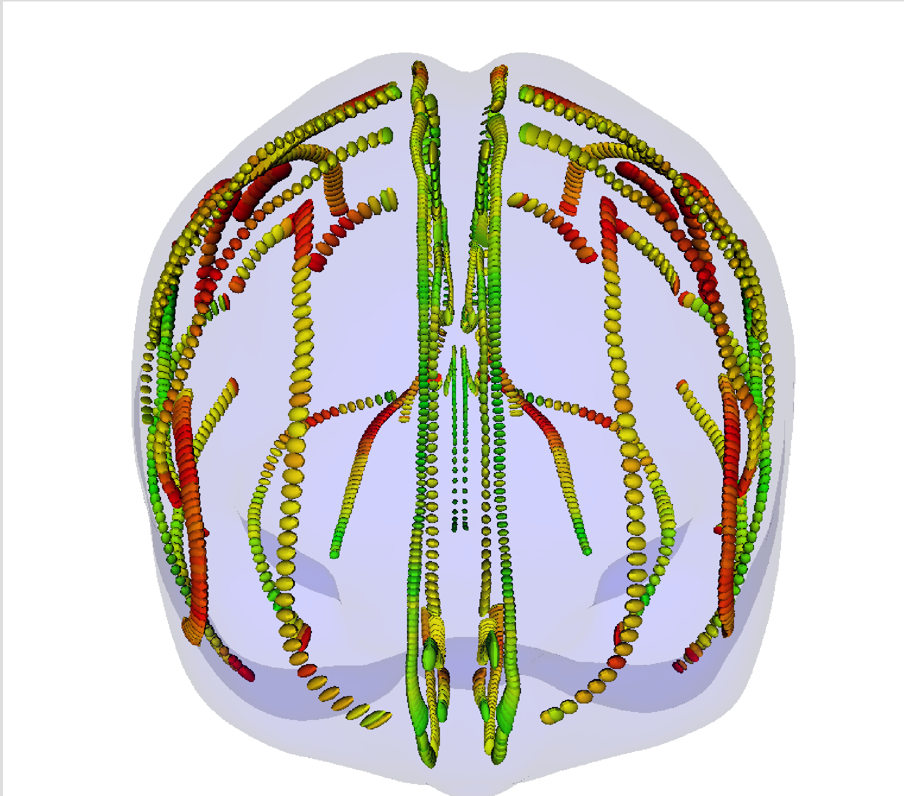

Color Codes Distance between "symmetric" tensors

$$\boxed{dist(\Sigma,\Sigma')^2 = \left\langle \overrightarrow{\Sigma\Sigma'} \mid \overrightarrow{\Sigma\Sigma'} \right\rangle_{\Sigma} = \left\| \log(\Sigma^{-1/2}.\Sigma'.\Sigma^{-1/2}) \right\|_{L_2}^{2}}$$

Extrapolation by Diffusion

- sources = tensors at given positions
- smooth extrapolation

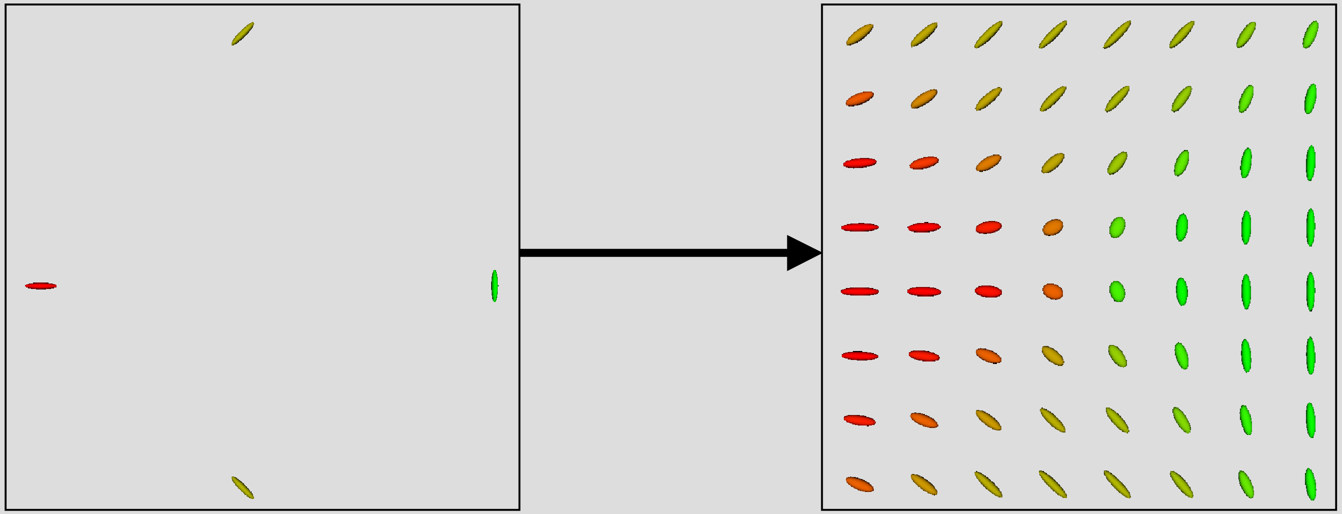

Extrapolation by Diffusion

- Minimize

$$C(\Sigma) = C_A(\Sigma) + C_D(\Sigma)$$

$$= \frac{1}{2}\int_\Omega \sum_{i=1}^{n} G_\sigma(x - x_i)\, dist(\Sigma(x), \Sigma_i)^2\, dx + \frac{\lambda}{2}\int_\Omega \|\nabla\Sigma\|^2$$

- Evolution Equation : $\Sigma_{t+1}(x) = \exp_{\Sigma_t(x)}\left(-\varepsilon \nabla C(\Sigma)(x)\right)$

$$\nabla C(\Sigma)(x) = -\sum_{i=1}^{n} G_\sigma(x - x_i)\overrightarrow{\Sigma(x)\Sigma_i} - \lambda(\Delta\Sigma)(x)$$

Extrapolation by Diffusion

$$C(\Sigma) = \frac{1}{2}\int_{\Omega} \sum_{i=1}^{n} G_{\sigma}(x-x_i)\,dist(\Sigma(x),\Sigma_i)^2\,dx + \frac{\lambda}{2}\int_{\Omega} \|\nabla\Sigma\|^2$$

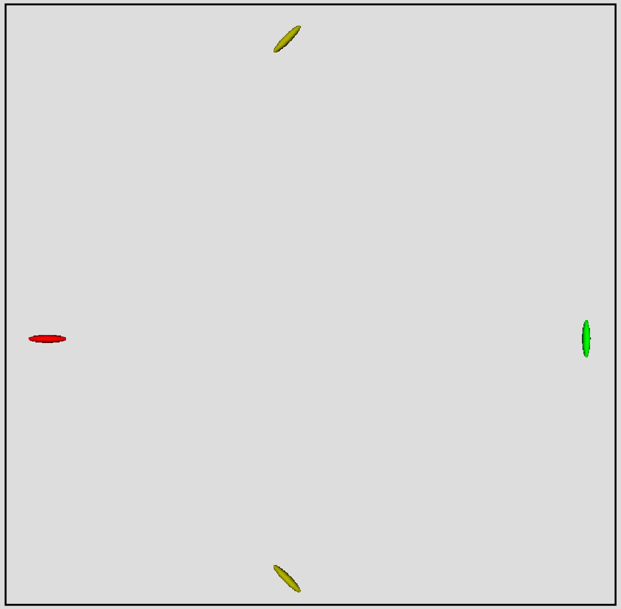

Original Tensor Data

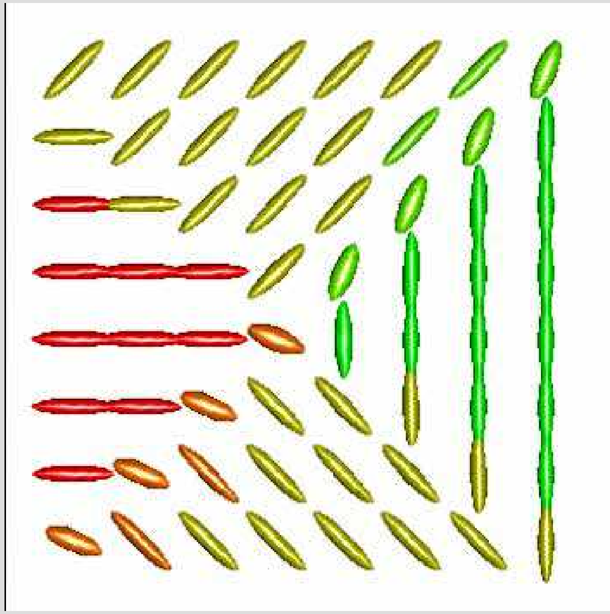

Diffusion Without data attachement

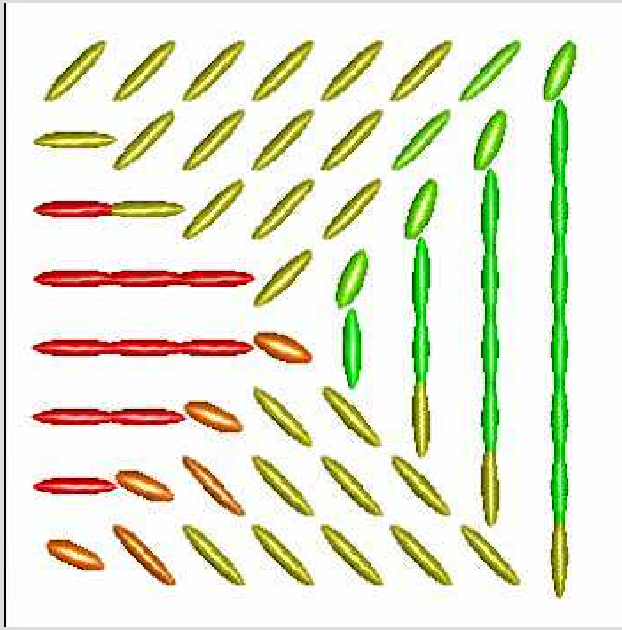

Diffusion with data attachement

Full Brain Interpolation

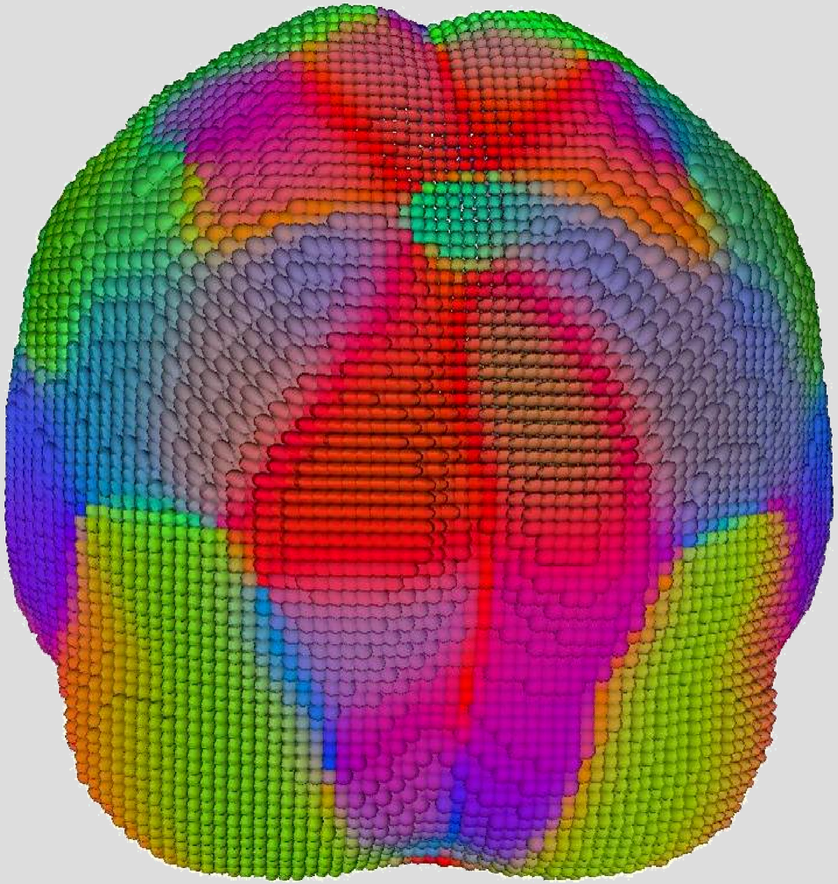

Color code: Principal Eigenvector
red: left-right, green: posterior-anterior,
blue: inferior-superior

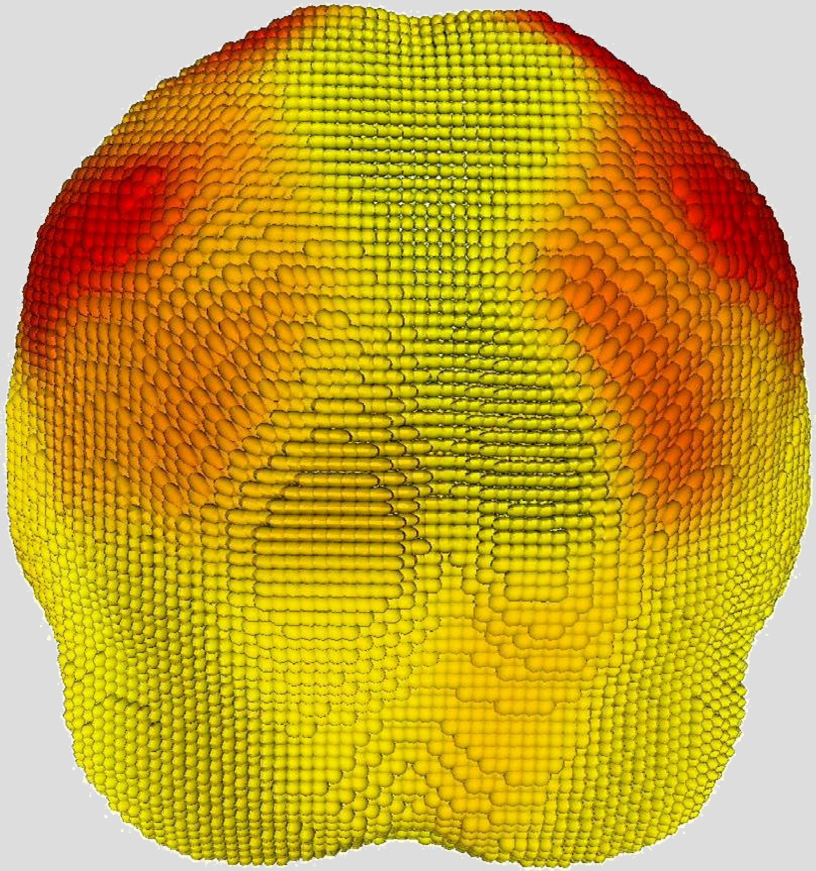

Color Code: Trace

Fillard-Pennec-Thompson- Ayache 2004, to appear

Anterior view

Full Brain Interpolation

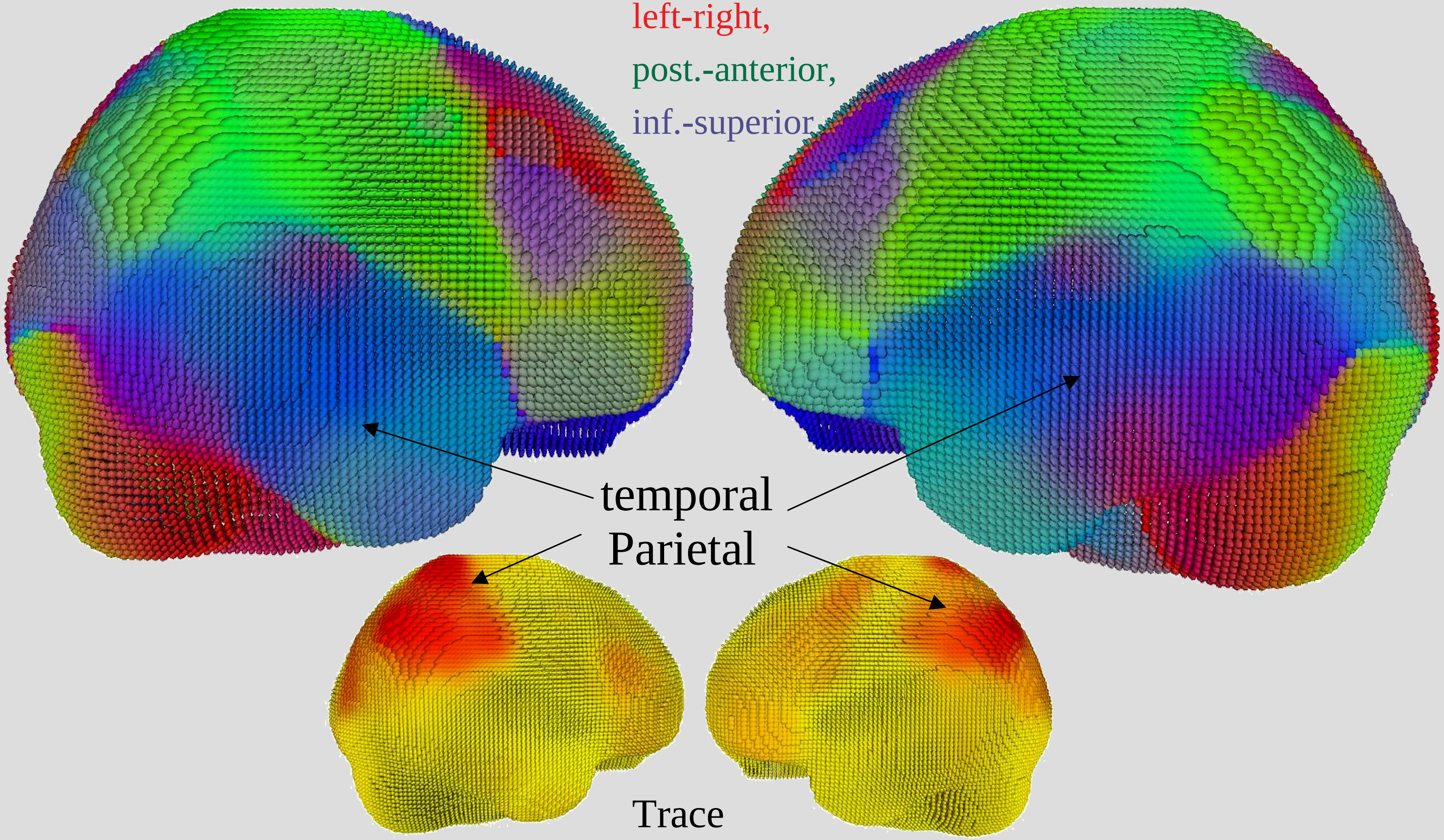

Full Brain Interpolation

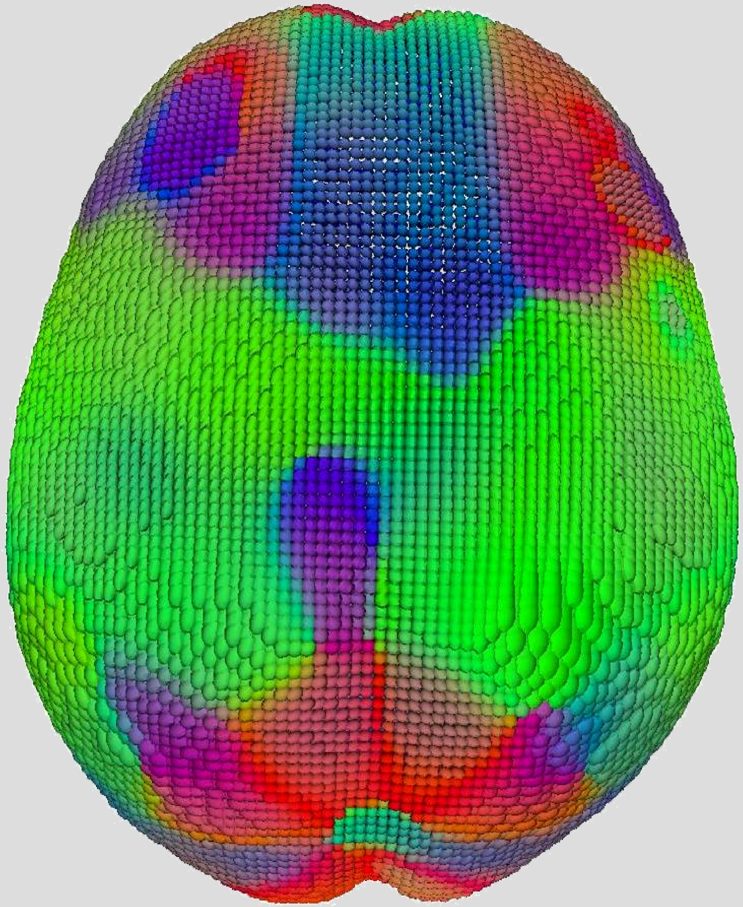

Principal Eigenvector

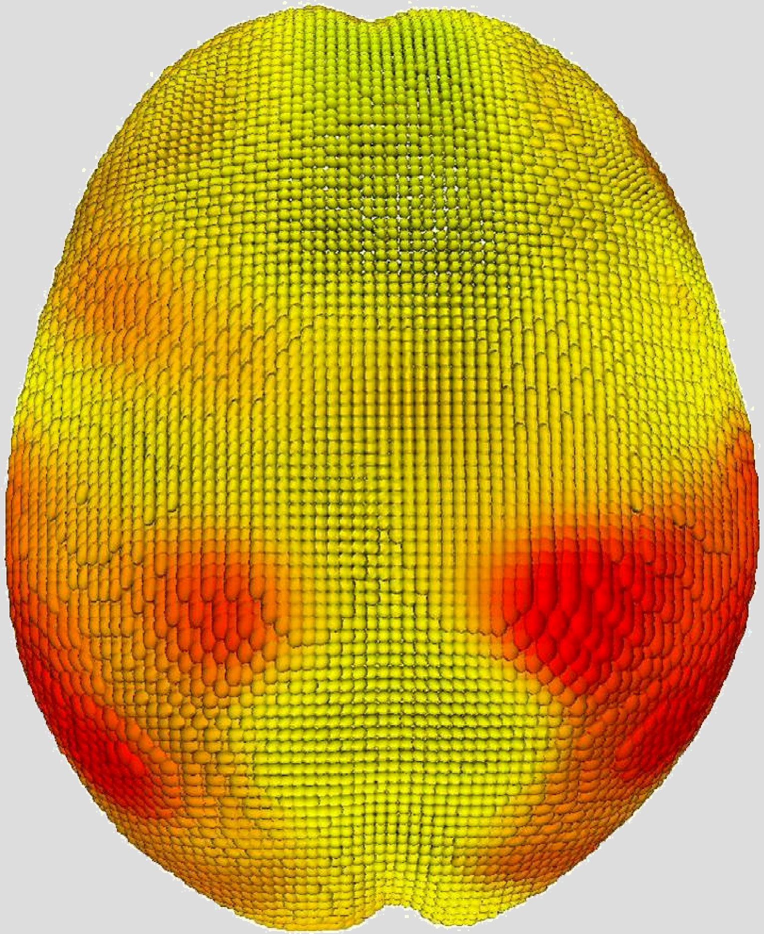

Trace

Fillard-Pennec-Thompson- Ayache 2004, to appear

Superior view

Anisotropic Filtering

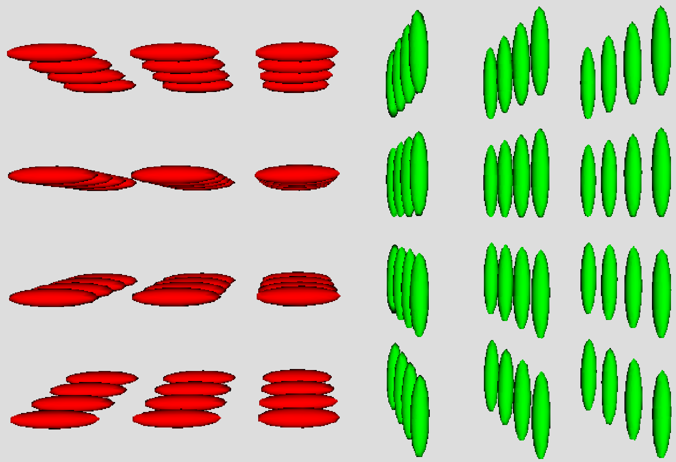

Original Tensor
Field

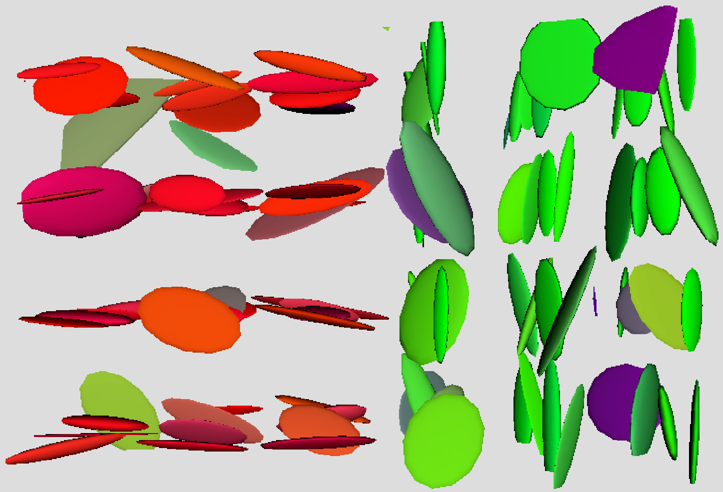

Noisy Tensor
Field

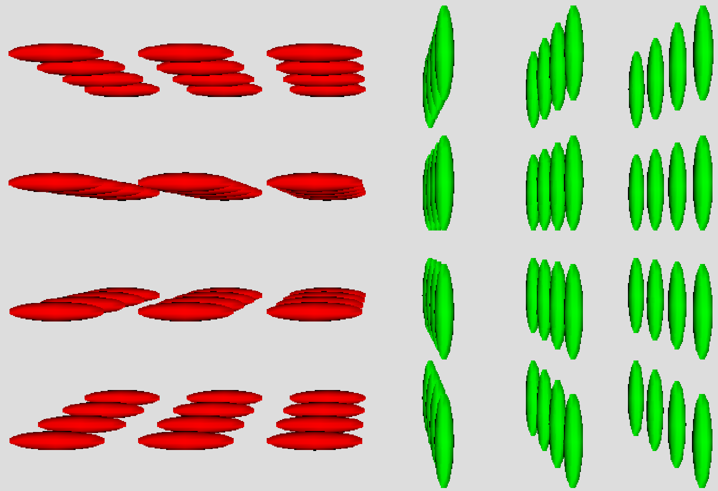

Filtered Tensor
Field

Anisotropic Filtering

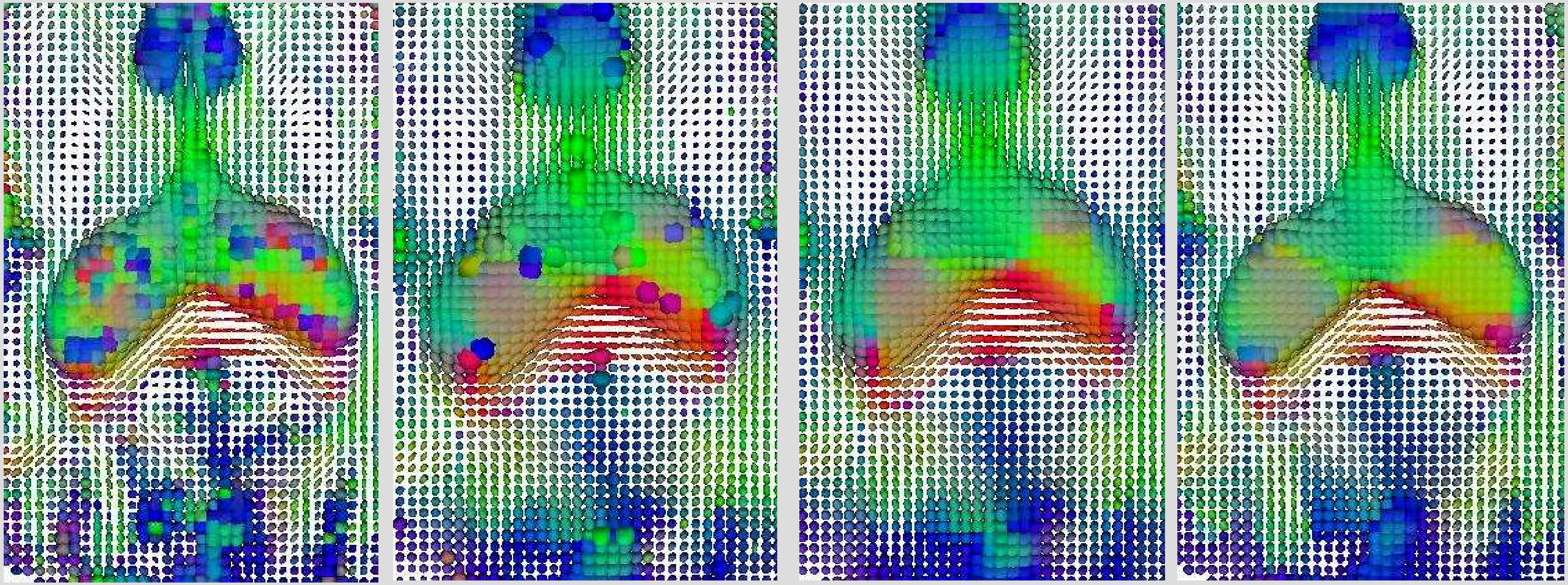

Raw tensors	Gaussian Flat Metric	Gaussian Riemann Metric	Anistropic Riemann Metric

Next Stages

- Learn Variability from Large Group Studies
- Statistical Comparisons between Groups
- Exploit Learned Variability to Improve Inter-Subject Registration

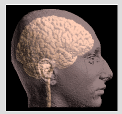

Content

- Geometric
- Iconic (Monomodal, Multimodal)
- Hybrid
- Shape Statistics
- Perspectives

Registration and Shape Variations

- Registration tools, based on geometrical and/or physical models
- Differential operators on deformation fields to detect and quantify local shape variations
- Tensor fields to encode local variability and adapted tensor metric to compare tensors
- Possibility to learn variability and improve non-rigid registration

Some Remaining Challenges

- Shape Statistics : Avoid any registration?
- Validating non-rigid registration
  - intra-subject : e.g. Truth Cube at Harvard,
  - inter-subject : e.g. Bronze Standard (Pennec et al.)
- Microscopic imaging:
  - Detect shape variations at microscopic level
  - Correlate with macroscopic changes

In Vivo “Endoscopic” Observations of Rat Bladder

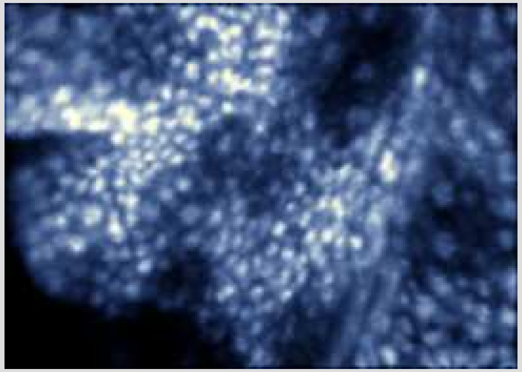

200 microns

• 1 mm probe introduced via catheter

• real-time dynamic images of tissue surface with cellular resolution (cf. movie below)

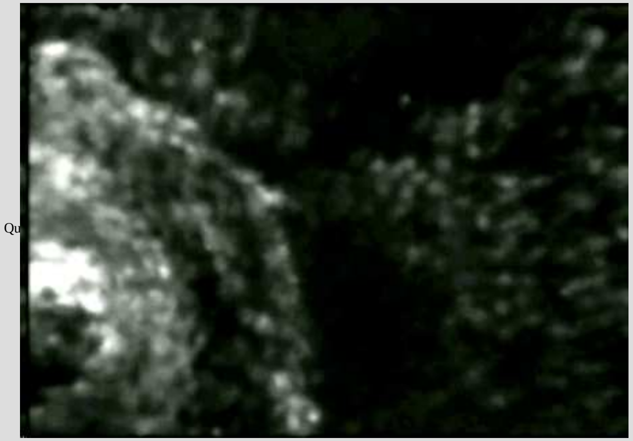

200 microns

Images obtained with the team of Prof. Guillemin at the Centre Alexis Vautrin, National Cancer Center in Nancy, France

http://www.maunakeatech.com/

Neurobiology

Transgenic mice expressing EGFP in neurons and dendrites

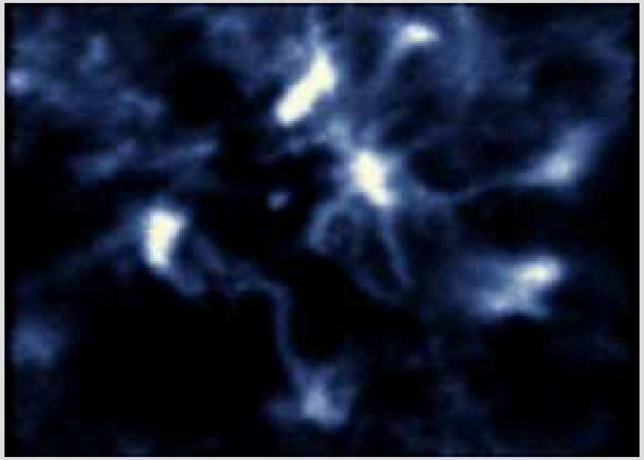

Field : 400 x 280 µm
Proflex diameter:
800µm

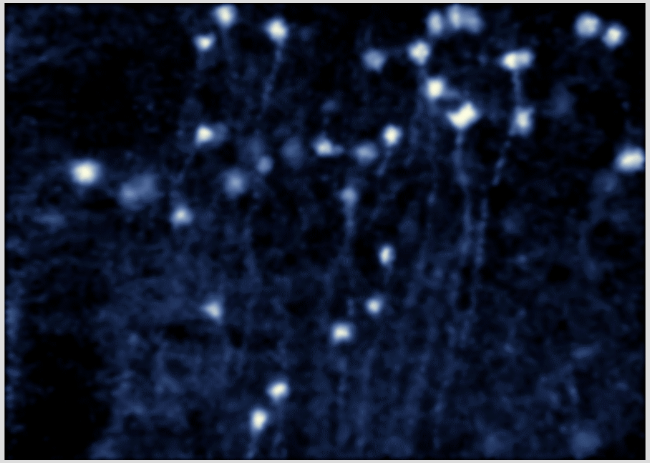

In VITRO visualization of lateral dendrites
from the basal pyramidal neuron layer

http://www.maunakeatech.com/

Images obtained by Mauna Kea Technology with the team of Prof. Changeux at Institut Pasteur, Paris.

Micro-circulation

http://www.maunakeatech.com/

- Live images of micro-vessels

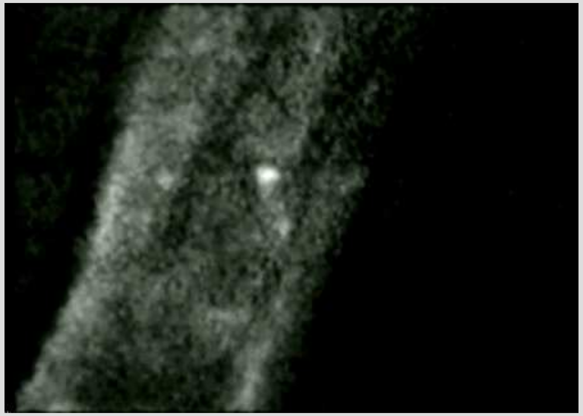

Leukocytes :
Size =7-11 microns

180 microns

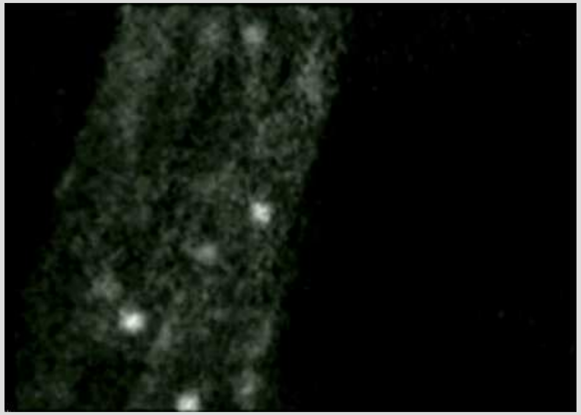

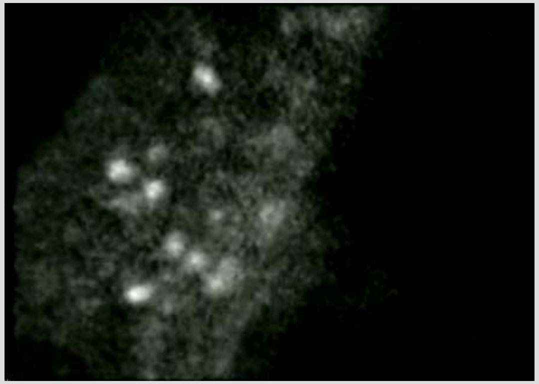

Study of

- **Angiogenesis,**
- **drug delivery**
- **cardiovascular diseases**
- **etc.**

Images obtained by Mauna Kea Technology with the team of Prof. Eric Vicaut at Hôpital Lariboisière, Paris.

Dynamic images of microcirculation

- **Live images of micro-vessels**

- **Angiogenesis, drug delivery, cardiovascular disease management.**

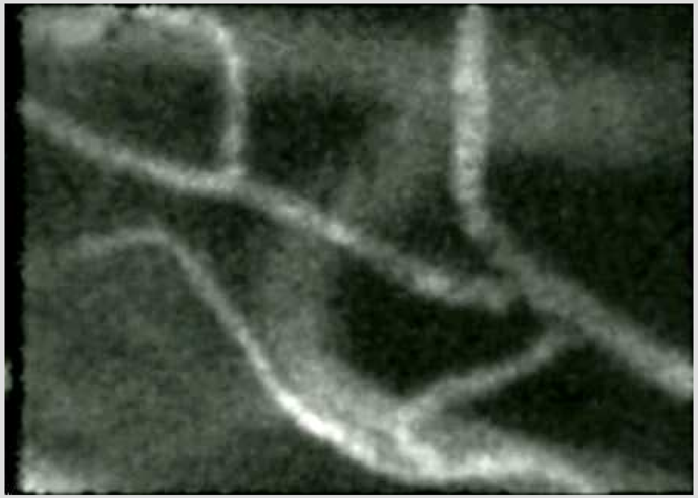

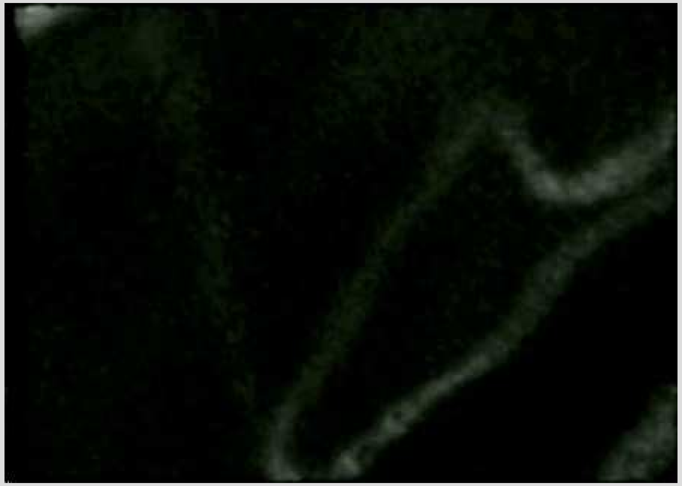

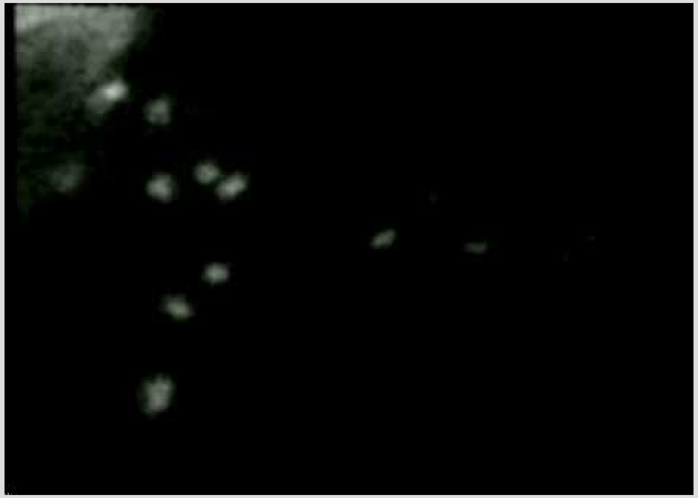

200 microns

Images obtained with the team of Prof. Eric Vicaut at Hôpital Lariboisière, Paris.

http://www.maunakeatech.com/

Real-Time Blood Flow Measurement

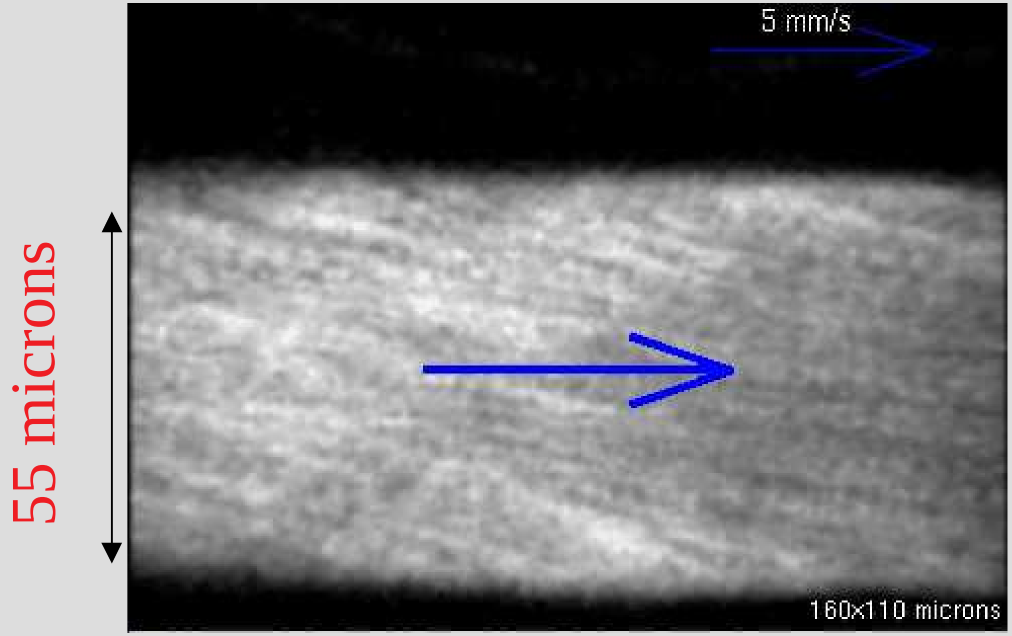

- Average speed: 7.18 mm/s; Std Deviation: 0.7 mm/s

N. Savoire, G. Le Goualher, A. Perchant, F. Lacombe, G. Malandain, and N. Ayache. Measuring Blood Cells Velocity In Microvessels From a Single Image: Application To In Vivo and In Situ Confocal Microscopy. ISBI, 2004

Brain Deformation & Tumor Growth

- Coupling physiological model of tumor growth with geometrical and physical (biomechanical) models

- In Vivo Cellular Imaging to Calibrate the model

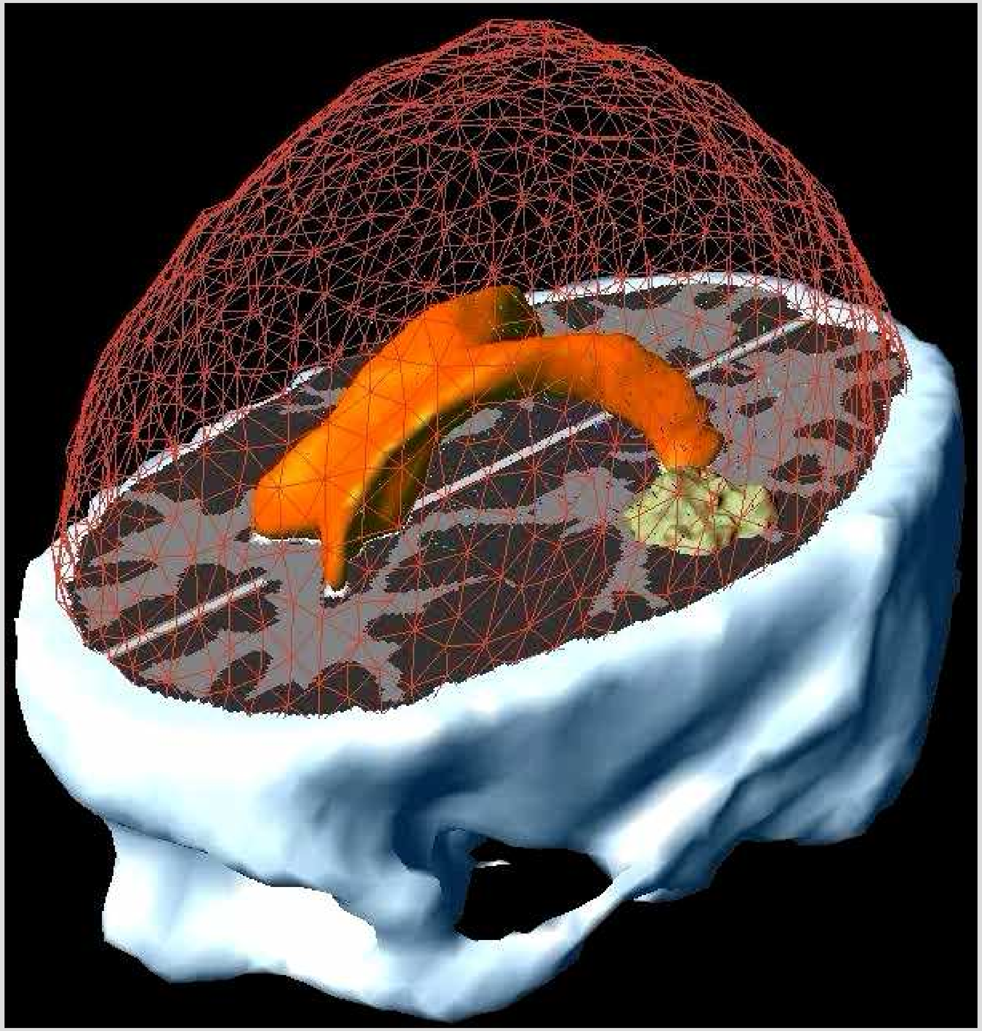

O. Clatz, P.Y. Bondiau, H. Delingette, M. Sermesant, S. K.Warfield, G. Malandain, N. Ayache. Brain Tumor Growth Simulation. Research report 5187, INRIA, 2004.

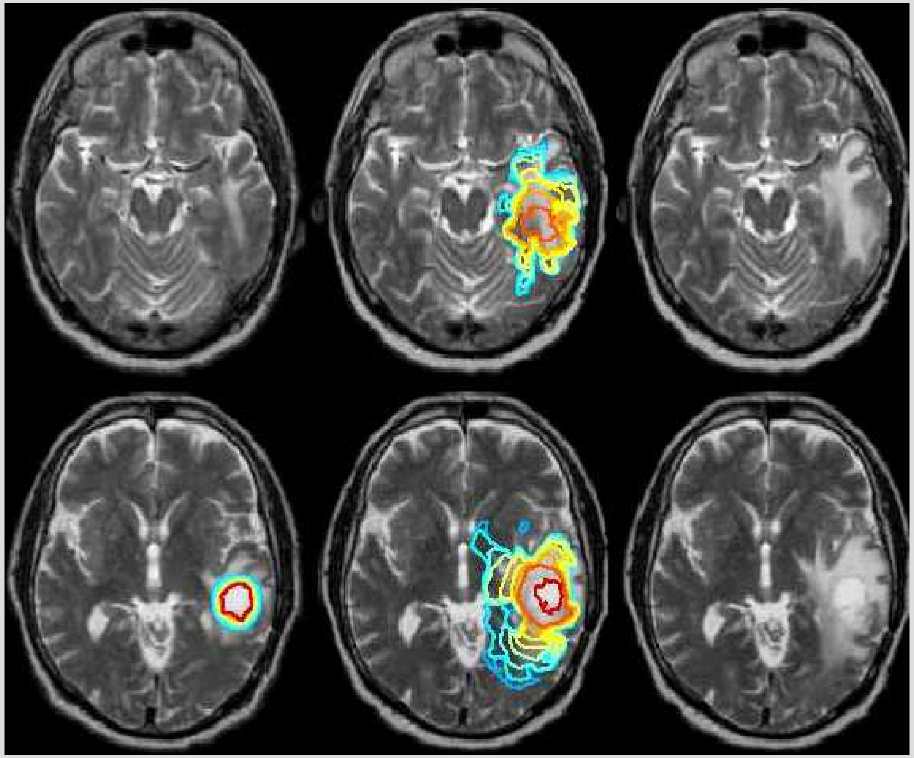

March	September	September
	Simulation

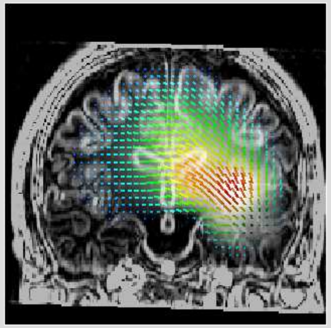

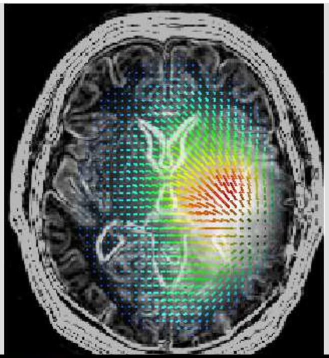

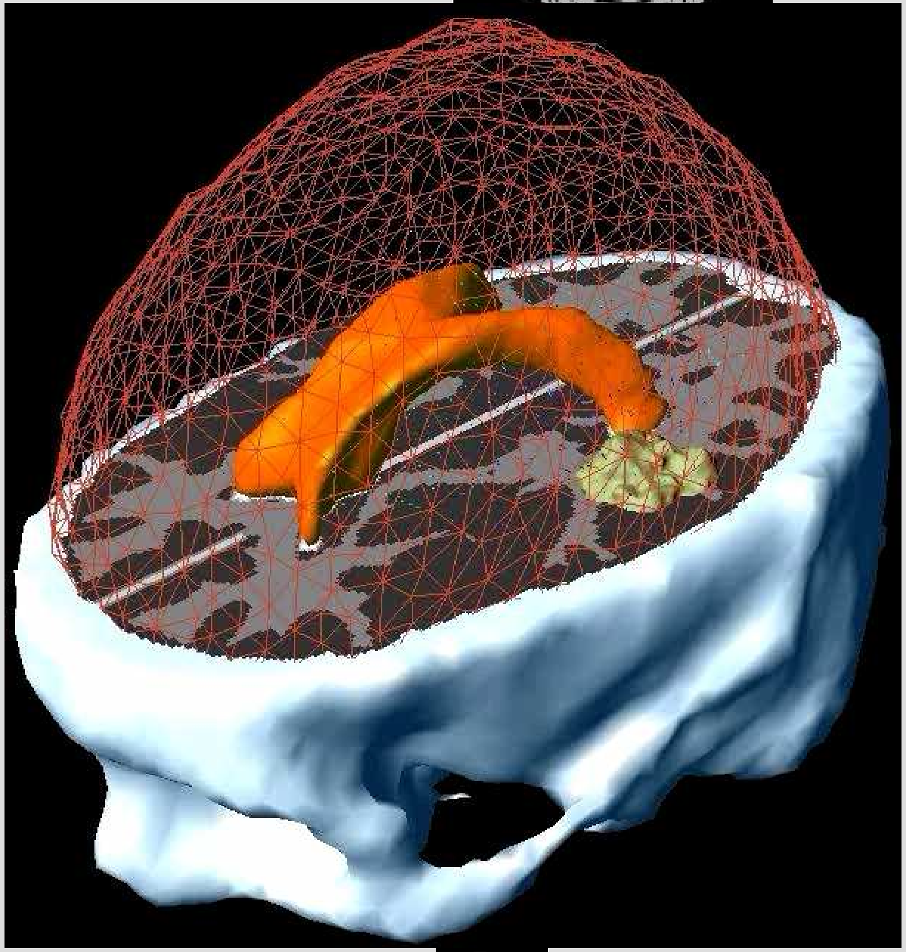

O. Clatz, P.Y. Bondiau, H. Delingette,
M. Sermesant, S. K.Warfield,
G. Malandain, N. Ayache.
Brain Tumor Growth Simulation.
Research report 5187, INRIA, 2004.

Credits

- Epidaure Team *past/current members*
  - V. Arsigny, E. Bardinet, P. Cachier, O. Clatz, H. Delingette, P. Fillard, G. Malandain, S. Ourselin, X. Pennec, A. Pitiot, S. Prima, G. Subsol, D. Rey, A. Roche, R. Stefanescu, J.P. Thirion, etc.
- Academic & Clinical partners
  - L. Auer, D. Dormont, R. Kikinis, C. Lebrun, J.F. Mangin, D. Rivière, P. Thompson, J. Yelnik, S. Warfield etc.

Thank You

Publications available on line http://wwwsop.inria.fr/epidaure/